UNIVERSITY OF CALIFORNIA
SANTA CRUZ

IMPROVEMENTS TO A GP120 BASED SUBUNIT VACCINE FOR HIV

A dissertation submitted in partial satisfaction of the requirements for the degree of

DOCTOR OF PHILOSOPHY in

Molecular Cellular Developmental Biology

by

Rachel C. Doran

September 2018

The Dissertation of Rachel C. Doran is approved:

_____
Professor Phillip W. Berman, chair

_____
Professor Rebecca M. Dubois

_____
Professor Martha Zúñiga

_____
Lori Kletzer
Vice Provost and Dean of Graduate Studies

Table of Contents

List of Figures

List of Tables

Abstract

IMPROVEMENTS TO A GP120 BASED SUBUNIT VACCINE FOR HIV

Rachel C Doran

Over three decades have passed since Human Immunodeficiency Virus (HIV) was identified as the causative agent of AIDS. With committed distribution and use of antiretroviral therapy, the AIDS crisis ebbed to a point where it is no longer a major concern for a majority in first world countries. However, for the select regions in the world where the disease endures as a major public health concern, there remains considerable incentive to develop a safe, effective vaccine against HIV. The RV144 HIV vaccine clinical trial completed in 2009 has been the only study to show protection against HIV infection. However, the modest efficacy (31.2%, P=0.04) indicated that the vaccine design used in the trial would need to be improved for higher efficacy before widespread use. Since the results of the RV144 clinical trial, various lines of research have elucidated methods that could be explored to improve vaccine efficacy. Follow-up studies of the RV144 trial indicated that an antibody response against regions in the HIV envelope protein (gp120) variable domains (V1V2 and V3) inversely correlated to infection. The identification of broadly neutralizing antibodies (bNAbs) against gp120 was a welcome discovery providing evidence that a human antibody response could effectively neutralize a vast majority of HIV strains. Perhaps most surprising was the observation that multiple families of bNAbs targeting regions in the V1V2 and V3 domains bound oligo-mannose N-linked glycans on gp120. This observation was particularly relevant, as the original gp120 immunogens of the RV144 trial displayed predominantly sialic acid-

terminal N-linked glycans. The work in this dissertation describes three major lines of research that converge upon improving upon the efficacy of gp120 based HIV vaccines. First, the identification of a monoclonal antibody that binds a glycan-dependent antibody within the V1V2 domain suggests that antibodies to such epitopes can be raised by immunization with gp120 molecules, providing further support for the viability of a gp120 based vaccine design. Secondly, we show that the addition of key, conserved glycosylation sites to the A244 and MN rgp120 vaccine immunogens of the RV144 clinical trial, in conjunction with modification of the incorporated glycoform, results in new binding by multiple families of bNAbs previously thought not to bind monomeric gp120 proteins. We further built upon the development of glycan-optimized gp120 immunogens by showing that a CHO-derived cell line, in which the Mannosyl (Alpha-1,3-)-Glycoprotein Beta-1,2-N-Acetylglucosaminyltransferase had been inactivated, could be stably transfected to produce glycan-modified clade C rgp120 immunogen. The resulting immunogen would be more amenable for translation to large-scale production, thereby making relevant gp120 based immunogens more accessible for widespread investigation. Finally, we investigated the potential for glycosylated V1V2 and V3 based gp120 protein fragments to improve the magnitude of the antibody response to regions associated with protection in the RV144 trial. Cumulatively, these studies contribute both potential reagents for, as well as a deeper understanding of, a second-generation of gp120 based vaccines for use in clinical trials.

Dedication

To Mom and Dad

For always encouraging me to be curious,

fearless, and persevering

And to G

For your endless support and patience

++

Acknowledgements

This work would not have been possible without the support and mentorship of my advisor, Professor Phil Berman. I would like extend my deepest gratitude to Phil, for all your advice, encouragement, and optimism. That optimism, in particular, came in handy as I faced the multitude of ups (and downs) PhD students inevitably face as they stumble through their graduate career. I cannot count the times I would walk away from one our meetings with a sense of renewed excitement and enthusiasm for my projects. Such positivity, particularly if in the context of negative results or failed gels, goes a long way. I would also like to thank my committee members, Professor Martha Zúñiga and Professor Rebecca M. Dubois for their guidance and support throughout my time at UCSC. Thank you to Martha in particular, for inspiring (and slightly intimidating) me with your tenacity, wit, and encyclopedic knowledge of immunology. Every conversation I had the pleasure of sharing with you endowed me with lessons on life and science that I will carry with me throughout my career.

I am indebted to the past and present members of the Berman lab – Richard Theolis, Trevor Morin, Javier Morales, Bin Yu, Lucy Yin, David Alexander, Sara O'Rourke, Meredith Wright, Briana To, Gerardo Perez, Jennie Richardson, Sophia Li, Gabriel Byrne, Gwen Tatsuno, and Kate Mesa. Thank you in particular to Kate, whose passion for science and comprehensive knowledge on every reagent in the lab greased the wheels for everyday labwork. Your cheerful greetings in the mornings were always appreciated.

I would also like to thank Nik Sgourakis for his insightful discussions and computer genius, and Teel Lopez, who was invaluable in helping me navigate through my graduate career. Finally, I would like to thank my colleagues and friends at UCSC, who helped make my time at UCSC particularly memorable and enjoyable.

Introduction

When old approaches don't work: challenges for HIV vaccine design

A brief history of vaccine strategies

The development of vaccines is arguably one of the greatest scientific achievements of mankind. While the oldest known instances of vaccination date before the 18th century in East Asia, the concept was catapulted into the western world when Edward Jenner published the western world's cornerstone text on variolation in 1798 (1). Just under a century later, Pasteur and colleagues reported immunological resistance against rabies in rabbits and later, humans(2). Pasteur's initial success inadvertently relied on the concept of attenuation, in which a pathogen, as an etiologic agent of a disease, could be attenuated, or weakened, to reduce virulence and introduced to train the immune system without causing mortality. The method of chemically or biologically attenuating a pathogen was later successfully used to develop vaccines against yellow fever (3) polio (4), measles (5), mumps (6), rubella (7), and varicella (8), amongst others. Inactivated vaccines use a similar approach to vaccinate using a whole pathogen that has been killed or inactivated using chemical or heat treatment. This approach was later successfully used to develop vaccines against multiple pathogens, including (9), pertussis (10), diphtheria (11), polio (12), and hepatitis A (13), amongst others. However, whole inactivated or attenuated vaccines were associated with reactogenicity and febrile illness (14-16), and additionally, posed the risk of causing infection in the case of pathogen survival of an inactivation step, or reversion from an attenuated form. For these reasons, whole or attenuated vaccine strategies are slowly losing favor to subunit-based vaccines that do not incorporate whole pathogens (17) (18). This approach is particularly

attractive for the creation of multivalent vaccines against pathogens, such as HIV, that exhibit multiple immunotypes.

Genetic engineering ushered in a new age of recombinant vaccines that could be made without the growth or purification of infectious virions (19). The concept of a recombinant vaccine, in which a gene for an antigen is inserted into a vector and expressed in a host cell, supported development for efficient, pure, and large-scale production of vaccines. The use of recombinant and subunit vaccines could reduce localized reactions associated with immunization (17) (18),and additionally eliminate safety concerns of possible vaccine reversion in attenuated or inactivated vaccines. Today, vaccines can use a combination of antigens across varying subtypes to overcome genetic diversity in certain pathogens, though such approaches have only shown success in pathogens that present relatively low degrees of genetic variation (19-22). The gp120 vaccine immunogens used in the RV144 trial are based on a recombinant subunit vaccine approach and will be described in detail later in the chapter.

HIV: A challenge to Modern Vaccine Design

Despite the aforementioned success in vaccines to prevent multiple diseases and millions of deaths worldwide, a safe and effective vaccine for Human Immunodeficiency Virus (HIV) remains elusive. HIV poses challenges for modern vaccine design in no small part due to its unique biology, which contributes to confounding factors for vaccine design. Some important factors that have provided significant obstacles to HIV immunogen design and/or manufacture are listed below:

1. High mutation rate: The high mutation rate of HIV (23) introduces an abnormally high risk in the potential use of live-attenuated or whole killed HIV vaccine that has led many in the

field to dismiss the potential of such approaches (24). In addition, the high mutation rate of HIV gives rise to tremendous antigenic variation (25) resulting in an increased incentive to find and target rare or immunologically recessive conserved epitopes on the virus.

2. Integration into the host genome and viral latency. The integration of HIV into host cells provides a latent viral reservoir that makes natural resolution of infection improbable, if not impossible (26). This characteristic of HIV has contributed to the dearth of representative models for successful clearance of infection. The potential incomplete inactivation of a whole killed HIV vaccine could therefore theoretically result in HIV infection, and provides an argument against an inactivated vaccine concept for HIV.

3. HIV envelope proteins are sparsely presented on the virion surface. Cryoelectron microscopy tomography has shown that HIV displays comparatively few antigens (as few as 14 trimeric spikes per virion) on its outer membrane (27). The sparseness of viral epitopes that can be recognized by the immune response may contribute to its challenge as a vaccine target.

4. The lack of a good model of infection and viral clearance: The success of early vaccines for other diseases relied on animal and human models of protective immune responses. Animal models were important in identifying correlates of protection; i.e., components of the immune response that contribute to immunity. From successful animal models, assays were set up that informed minimal antibody titers for neutralization, aggregation, or inactivation. HIV uses the receptor CD4 and co-receptors CC-chemokine receptor 5 (CCR5) or CXC-chemokine receptor 4 (CXCR4) for viral entry into a host cell. In addition, HIV relies on various other host proteins for successful target cell entry and self-

replication (28). This unique, multifaceted manipulation of host-specific proteins for effective infection has limited commonly used animal models (29, 30).

The closest animal model of natural control of HIV is the control of the Simian Immunodeficiency Virus (SIV) in sooty mangabees and African green monkeys. Discouragingly, control of infection in this context appears to rely on a short, robust tinnate immune response, rather than adaptive immunity (reviewed in thoroughly in reference (31)). The SHIV model to test HIV vaccines, in which an SIV has been engineered to express HIV-1 envelope glycoproteins, has been used in non-human primate studies of vaccine. However, success in this model has yet to translate to HIV protection in humans (28).

5. gp120 is heavily glycosylated. The functional unit of the envelope protein gp120 is a trimer of heterodimers. The heterodimer consists of the gp120 surface subunit that is linked to the transmembrane gp41 subunit. The envelope protein of HIV consists of the glycoprotein 120 (gp120) and the gp41 transmembrane domain. Together, these protein components are the only accessible viral epitopes on the intact HIV virion. Both the gp120 and gp41 display an extraordinarily high amount of glycosylation; the gp120 protein contains up to 25 potential N-linked glycosylation sites. Glycans comprise up to 50% of the molecular weight of gp120 and have a dominant effect on the epitope landscape of gp120. The uncommonly high density of N-linked glycosylation sites results in incomplete processing of the N-linked glycans by glycosidases resulting in predominantly oligomannose glycoforms on gp120 trimer (32). This dense cover of glycans on gp120 forms a glycan “shield”, occluding neutralization sensitive protein epitopes both on the gp120 core as well as the variable domains (33-38). This unique glycosylation has implications on immunogen production in addition to immune

recognition. The host cell expression system can profoundly alter the occupancy (how often a glycan structure is added to the N-X-S/T motif) and glycoform of glycan structures incorporated onto recombinant gp120 base immunogens (39). Indeed, many of the major vaccine clinical trials to date used gp120 antigens produced in CHO cells, which incorporate predominantly complex, sialic acid terminal that significantly differ from the oligomanose terminal glycans found on virion associated gp120 (40). A current challenge facing the HIV vaccine field is thus a robust method to faithfully and consistently produce immunogens displaying glycosylation patterns of infectious virions.

6. Proteolytic cleavage has historically been an issue for protein production. The original rgp120 immunogens in immunogenicity studies displayed high degrees of cleavage from CHO cell-derived serine proteases. The major sites of gp120 proteolysis occurs in the crown of the immuno-dominant V3 loop of gp120. This proteolysis site coincides with a major epitope recognized by virus neutralizing antibodies. Thus, production of recombinant gp120 necessitated added purification and quality control steps by affinity chromatography that selected for un-cleaved, intact gp120 immunogen(41). This characteristic presents challenges for gp120 production even today, as steps necessary to purify gp120 based immunogens further reduce total yield of usable immunogen product. Additionally, proteolysis has recently been implicated in cleavage of conserved and potentially immunologically accessible or functional epitopes, such as amino acid motifs commonly recognized by neutralizing antibodies, integrin binding sites, or preferentially used in cross-presentation pathways (42, 43).

HIV correlates of protection and their application for vaccine design

As discussed above, knowledge of which components of the immune response confer protection against a pathogen is useful, and sometimes, imperative, in vaccine design. Until recently, there existed no such known targets that successfully translated to a human model of HIV protection. Within the last decade, studies of long-term non-progressors and elite neutralizers of HIV as well as correlates of protection in the RV144 clinical trial have offered potential correlates.

The RV144 HIV vaccine trial and follow up correlates of protection studies

The Thai RV144 vaccine efficacy trial (ClinicalTrials.gov number, NCT00223080) was a trial of a “prime-boost” vaccine concept (44). The four priming immunizations were comprised of a canarypox vector, with the final two injections administered in conjunction with the bivalent gp120 subunit vaccine (41, 44). The canarypox vector prime (ALVAC-HIV [vCP1521]) is a recombinant canarypox virus expressing the gag and pol genes of the clade B LAI strain and a clade CRF01 A/E gp120 linked to the transmembane domain (gp41) of the clade B LAI strain of HIV. Canarypox-infected cells produce noninfectious, virus-like particles capable of entering mammalian cells and inducing host immune responses against HIV gene products and non-protein epitopes (45). The bivalent gp120 subunit vaccine, AIDSVAX B/E contained the clade B (MN) and clade CRFO1 A/E (A244) recombinant gp120 immunogens co-formulated with alum adjuvant. The bivalent AIDSVAX B/E vaccine was tested independently of the canarypox prime in the VAX003 and VAX004 clinical trials. Interestingly, neither the ALVAC-HIV [vCP1521]) nor the AIDSVAX B/E showed vaccine efficacy when administered individually. However, the RV144 prime-boost regimen, in which both components were tested together, resulted in a modest, yet statistically significant vaccine

efficacy of 31.2% over 42 months, with up to 60% efficacy within the first year after vaccination (44, 46).

Follow-up correlates of protection studies found that risk of infection inversely correlated with levels non-neutralizing antibodies binding to a V1V2 fragment of gp120. A second correlate found was with high levels of antibody-dependent cellular cytotoxicity (ADCC) in the absence of a high IgA titer (46, 47). This observation was supported by the additional finding that antibody titers against a peptide within the V2 domain inversely correlated with infection (48, 49).

There is a growing appreciation for the role of ADCC in a protective immune response. Protection conferred by most existing vaccines relies on antibodies that block initial or systemic infection. However, the immune response has evolved to be redundant, and it should not be surprising that other facets of the immune response contribute to protection (50, 51). Indeed, anti-gp120 ADCC was identified to correlate inversely with risk of infection (46, 52) and HIV progression (53). Interestingly, a comparison of the specificity and functionalities of the antibody response elicited by the RV144 and VAX003/VAX004 protocols found that the VAX003 and VAX004 elicited antibodies with higher prevalence of IgG4 isotype, while the RV144 induced higher levels of IgG1 and IgG3 isotypes, which have been found to display higher affinity for Fc-receptors. (54) (55). Thus, immunogens capable of preferentially eliciting subsets of antibodies with ADCC functionalities could be ideal candidates for an HIV vaccine.

Long Term Non-Progressors, Elite Neutralizers, and Broadly Neutralizing Antibodies

HIV infected individuals classified as Long term Non-progressors (LTNPs) and Elite neutralizers of HIV provide models for correlates of protection of HIV infection in humans.

The term “Long Term Non-progressors” refers to individuals who are able to maintain low-to undetectable viremia (as few as <50 copies/mL) and normal CD4 T-cell counts (>500 cells/mL) over long periods without the use of antiviral therapies (56). Multiple host factors have been associated with LTNPs. LNTP phenotypes are correlated with reduced inflammation, chemokine expression levels (that compete for binding to CCR5 or CXCR4) and different HLA-haplotypes (57). Over the past decade, viral factors identified with LTNPs, such as decreased viral fitness (reviewed in (58)), have limited application in immunogen design.

Elite neutralizers of HIV are a subset of individuals who possess serum antibodies capable of potently neutralizing in in vitro neutralization assays two or more pseudoviruses across four subtype groups at an IC(50) titer of 300 or more (59). In most instances broad neutralization is conferred by the presence of antibodies that target a variety of different epitopes (60-62). However, monoclonal antibodies capable of recapitulating the neutralization breadth and potency of some Elite Neutralizer sera have been identified (63-67). These antibodies, known as broadly neutralizing antibodies (bNAbs or bNAbs) isolated from different donors were found to target epitopes that fit into one of five general categories (reviewed in (68) and discussed in detail in Chapter 3). Passive transfer studies of bNAbs in SHIV challenge models have successfully protected against SHIV challenge. These preliminary results suggest that an bNAb-like antibody prior to HIV exposure may prevent HIV infection in humans (69, 70). Thus, a potential concept for HIV vaccine design would be to design a vaccine that can elicit a bNAb-type polyclonal response. However, as scientifically exciting this concept is, the challenges to successfully pursuing this strategy are daunting.

A major obstacle to eliciting bNAb-type antibodies is that they display uncommonly high degrees of somatic hypermutation (67, 71-74) and are substantially divergent from putative germline genes from which they arose (72, 75). Researchers have created “designer

antigens" to direct affinity maturation of B-cell-receptors with bNAb characteristics (76-79). Work in this area has focused on the VRC01 class of bNAbs, for which the putative CDR regions are not as rare as other classes of bNAbs (78). Passive transfer studies have shown that bNAb families targeting a minimum of two diverse epitopes may be necessary to prevent viral immune escape (70, 80, 81). Although eliciting the VRC01-like class of bNAbs in humans would be a technically impressive feat, it would not be sufficient to induce protection without elicitation of additional, more technically challenging bNAb families that incorporate rare germline genes.

Although this dissertation focuses on the design of a protein immunogen, it is impossible to consider vaccine design, particularly using a subunit approach, without addressing adjuvants. The adjuvant choice for an HIV vaccine may ultimately be decisive on whether the vaccine is efficacious or not. A major downfall for recombinant vaccines is the fact that, while effective in eliciting antibody ant CD4+ T-cell responses, they were ineffective in eliciting CD8+ restricted cytotoxic lymphocyte (CTL) responses. The fact that subunit vaccines are often extremely pure (and in the case of RV144, monomeric) proteins is an advantage for production and purification of an immunogen, but a bane for elicitation of a robust cell mediated immune response. To overcome this limitation, co-immunization with viral vectors (e.g. pox viruses or adenoviruses) have been utilized to stimulate robust cell mediated immune responses. However, the anti-gp120 antibody response that correlated with protection in the RV144 trial was short lived, and that a drop in titers against gp120 correlated with an observed decrease of protective efficacy of the vaccine over time (82-84) suggests that additional adjuvant formulations or immunization regimens may be required. Ultimately, an adjuvant that can provide robust, durable antibody response against HIV may be just as, if not more, important that the optimization of the immunogen itself.

A roadmap for improvement

It is unknown what it takes to consistently induce a protective antibody response to HIV in humans. However, the identification of bNAbs in addition to the correlates of protection observed in RV144 can guide immunogen design on multiple levels. The various families of bNAbs that have been identified cover a variety of regions on the envelope protein, and their dependence on diverse structural and glycan components provides a roadmap to better emulate the epitopes presented by the infectious virion. The observed correlation of protection with antibodies, ADCC that targets in the V1V2 and V3 domains additionally provides a direction for vaccine immunogen improvement. Immunogens that promote the magnitude and ADCC activity of antibodies, particularly to regions that correlate with protection, may improve the efficacy observed in RV144. This dissertation contains preliminary sets of experiments to ask how glycan modifications to gp120 antigens might improve antigenicity and immunogenicity of bNAb and RV144 relevant epitopes. Finally, it asks how such modified gp120 immunogens might be produced in a manner amenable to real world application and use in future clinical trials.

Chapter 1

Characterization of a monoclonal antibody to a glycan-dependent epitope in the V1V2 domain of the HIV-1 envelope protein gp120

1.1 Foreword

This chapter contains text and figures from the following manuscript:

> Doran, R. C., Morales, J. F., To, B., Morin, T. J., Theolis, R., Jr., O'Rourke, S. M., Yu. B., Mesa K. A., Berman, P. W. (2014). Characterization of a monoclonal antibody to a novel glycan-dependent epitope in the V1/V2 domain of the HIV-1 envelope protein, gp120. Mol Immunol, 62(1), 219-226.

The work was completed as a collaboration amongst all authors, JFM performed immunizations, RCD, JFM, RT, BT, cloned hybridomas, RCD and BT screened clones, RCD performed characterization assays, RCD, SMO, and KAM contributed to antigen production, BY performed protein purification. PWB was responsible for conceptualization, oversight, and attaining funding.

Recent studies have described several broadly neutralizing monoclonal antibodies (bNAbs) that recognize glycan-dependent epitopes (GDEs) in the HIV-1 envelope protein, gp120. These were recovered from HIV-1 infected subjects, and several (e.g., PG9, PG16, CH01, CH03) target glycans in the first and second variable (V1/V2) domain of gp120. The V1/V2 domain is thought to play an important role in conformational masking, and antibodies to the V1/V2 domain were recently identified as the only immune response that correlated with protection in the RV144 HIV-1 vaccine trial. While the importance of antibodies to polymeric glycans is well established for vaccines targeting bacterial diseases, the

importance of antibodies to glycans in vaccines targeting HIV has only recently been recognized. Antibodies to GDEs may be particularly significant in HIV vaccines based on gp120, where 50% of the molecular mass of the envelope protein is contributed by N-linked carbohydrate. However, few studies have reported antibodies to GDEs in humans or animals immunized with candidate HIV-1 vaccines. In this report, we describe the isolation of a mouse mAb, 4B6, after immunization with the extracellular domain of the HIV-1 envelope protein, gp140. Epitope mapping using glycopeptide fragments and in vitro mutagenesis showed that binding of this antibody depends on N-linked glycosylation at asparagine N130 (HXB2 numbering) in the gp120 V1/V2 domain. Our results demonstrate that, in addition to natural HIV-1 infection, immunization with recombinant proteins can elicit antibodies to the GDEs in the V1/V2 domain of gp120. Although little is known regarding conditions that favor antibody responses to GDEs, our studies demonstrate that these antibodies can arise from a short-term immunization regimen. Our results suggest that antibodies to GDEs are more common than previously suspected, and that further analysis of antibody responses to the HIV-1 envelope protein will lead to the discovery of additional antibodies to GDEs.

1.2 Introduction

Recombinant forms of the HIV-1 envelope (Env) protein have long been studied as HIV vaccine immunogens (85, 86). The Env protein is synthesized as a 160 kDa precursor, gp160, which then undergoes maturational cleavage to yield gp41, a membrane-bound protein that mediates virus fusion, and gp120, a peripheral membrane protein that is responsible for CD4 and chemokine receptor binding and virus tropism. In virus particles, the envelope proteins gp120 and gp41 are associated by non-covalent interactions and form a trimeric spike structure. Both gp120 and gp41 are highly glycosylated, with approximately 50% of their molecular mass attributed to N-linked glycosylation. Since both gp120 and gp41 possess epitopes recognized by neutralizing antibodies, multiple vaccine development efforts have investigated the immunogenicity of these proteins. However, after more than 30 years of effort, none of the candidate vaccines described to date has been effective in eliciting broadly neutralizing antibodies (bNAbs). For many years, the inability to elicit bNAbs has been attributed to the inability to accurately emulate the trimeric structure of the Env protein found on the surface of viruses or virus-infected cells. However, the recent discovery of (bNAbs to glycan-dependent epitopes (GDEs) on monomeric HIV-1 (87-91) has raised the possibility that the inability to elicit bNAbs was due to: 1) the inability to accurately emulate the specific glycan structure of envelope proteins on the surface of viruses and virus-infected cells and 2) our inability to direct antibody responses to GDEs. Indeed, little is known about immunization regimens or adjuvant formulations that favor the formation of antibodies to GDEs.

Of particular interest is the GDE landscape within the first and second variable (V1/V2) domain of gp120. Although the V1/V2 domain is known as a “variable” region (92), numerous glycosylation sites within the V1/V2 domain exhibit a high degree of conservation (93, 94). Previously, it was thought that glycans on gp120 were poorly immunogenic. This

characteristic, in addition to the unusually large number of glycosylation sites on gp120, was thought to be a major mechanism, glycan shielding, responsible for immune escape (95-100). However, the recent discovery of bNAbs to GDEs suggests that these epitopes are more immunogenic than previously imagined and that a vaccine targeting GDEs might help to overcome the problem of virus variation. Thus, we have begun to investigate the magnitude, specificity, and frequency of antibodies to GDEs resulting from immunization with recombinant Env proteins.

At this early stage of investigation, all antibodies to GDEs of the HIV-1 envelope protein are informative; however, antibodies to the V1/V2 domain of gp120 are of particular interest. First, the V1/V2 domain contains the GDEs recognized by several bNAbs (e.g., PG9, PG16, CH01-4, PGT145) (66, 67, 87, 88, 90, 101, 102). Secondly, non-neutralizing antibodies to the V1/V2 domain represent the only antibody response found to correlate with protection in the RV144 HIV vaccine trial, which included immunization with the ALVAC-HIV canarypox vector vaccine (vCP1521) and the AIDSVAX B/E recombinant gp120 subunit vaccine (41, 44, 46, 103). The lack of correlation between neutralizing antibodies and protection in the RV144 trial caused investigators to consider numerous ways by which non-neutralizing antibodies against the V1/V2 domain may confer protection against infection (104). Such methods may involve viral inactivation through antibody-dependent cell-mediated virus inhibition, virion aggregation, or inhibition of virion mobility and transport across mucosal surfaces (104). Therefore, GDEs in the V1/V2 domain recognized by both neutralizing and non-neutralizing antibodies represent intriguing targets for candidate vaccines to prevent HIV-1 infection.

1.3 Materials and Methods

Production of HIV envelope proteins gp120, gp140, and gp120 fragments

Recombinant gp140 was prepared as described previously (86, 105) from the 108060_Q655R clinical isolate (106). From this sequence, the extracellular domain of gp160 (gp140), full length gp120, and nine overlapping fragments of 108060_Q655R were created and expressed as previously described (107). All proteins contained a flag epitope from herpes simplex virus glycoprotein D (gD) fused to the amino terminus as described previously (85, 108). All proteins were purified by immunoaffinity chromatography using an immunosorbant prepared with 34.1, a mAb to the gD flag epitope. Point mutations N130H or T132A were introduced into a V1/V2 fragment of gp120 from the MN strain of HIV-1 by site-directed mutagenesis, using a QuikChange Lightning kit (Agilent, Santa Clara, CA). The resulting construct was verified by confirmatory sequencing. Plasmids for protein expression were transfected into FreeStyle™ 293-F cells (Invitrogen, Carlsbad, CA).

Deglycosylation studies

Digestion with the enzyme peptide-N-glycosidase F (PNGase F) was used to remove N-linked glycans on HIV gp120 proteins or fragments of gp120. The enzyme with its respective buffers was obtained from New England Biolabs (Ipswich, Mass) and used per manufacturer's instructions. Briefly, 200 µg of recombinant gp120 or V1/V2 fragment was denatured in 10x denaturation buffer. Samples were boiled at 100°C for 10 min, then mixed with 10x reaction buffer and 5,000 units of PNGase F. Digests were carried out at 37°C for 12 hr. To confirm digest completion, the digest product was analyzed by polyacrylamide gel electrophoresis (PAGE) using precast polyacrylamide gels (4-12% Bis-Tris) in MOPS running buffer (NuPAGE®, Invitrogen). Proteins were transferred to nitrocellulose paper (Novex, Life

Technologies, Carlsbad, CA). The 4B6 mAb was used as the primary antibody, and the goat anti-mouse IgG/M conjugated to HRP (American Qualex Antibodies, San Clemente, CA) was used as the secondary antibody. The anti-gD antibody, 34.1, was used as a control, as its binding to gp120 constructs was not affected by deglycosylation treatment.

Immunizations

BALB/c mice from Charles River (Hollister, CA) were initially immunized with 5μg of 108060_Q655R gp140 incorporated in Freund's Complete Adjuvant, and then boosted multiple times over a four-week period with 5 μg of immunogen incorporated in Freund's Incomplete Adjuvant.

Monoclonal antibody production

Splenocytes were harvested from immunized mice, and fused to the mouse sp2/0 cell line to create immortalized hybridoma cell lines using standard procedures (109). To identify antibodies that bound the gp120 region, hybridomas were selected using HAT media, and hybridoma subclones were screened for secreted antibody reactivity against gD-tagged 108060_Q655R-rgp120. Hybridoma supernatants that tested positive for reactivity against 108060_Q655R-rgp120 in an enzyme-linked immunosorbent assay (ELISA) were subcloned, and the secreted mAbs were further characterized by ELISA. These assays were carried out in flat bottomed 96 well microtiter plates (Nunc Maxisorp®, Affymetrix, Santa Clara, CA) and coated with 2 μg/mL of protein in PBS, overnight at 4°C. After 12 hr, plates were blocked with PBS containing 1% BSA and 0.02% sodium azide for 1 hr at room temperature. After 1 hr, PBS solution was removed, and plates were washed four times. For initial screening, 60 μL of hybridoma supernatant obtained directly from the 96 well culture plate was added to the gp120-coated plates. Plates were incubated with gentle agitation for 1 hr at room

temperature, washed four times in PBS, and incubated for 1 hr at room temperature with goat-anti-mouse, or goat-anti-human, HRP-conjugated antibodies (Jackson ImmunoResearch Laboratories, West Grove, PA). Plates were then washed four times in TBST. Plates were developed with OPD solution and stopped with 50 µl of 3M H_2SO_4. Absorbance was read at 492nm. The isotype of mAb 4B6 was determined using the Pierce Rapid ELISA Mouse Antibody Isotyping kit (Thermo Fisher Scientific Inc., Rockford, IL).

Immunoassays

ELISAs were used to detect antibody binding to gp120s from clade B, C, and CRF01_AE isolates and to overlapping fragments of 108060_Q655R-rgp120. The gp120s and V1/V2 fragments used in these studies were similar to those described previously (107, 110). Epitopes were further mapped using a library of overlapping peptides 15 amino acids in length derived from the MN sequence (NIH AIDS Reagent Program, Germantown, MD; catalog number 6541). Peptide ELISAs were performed with an initial coating of peptide at 5 µg/mL, and subsequent steps followed the ELISA described above. Antibody binding to peptide was tested in duplicate. The PG9 mAb used in competition assays was purchased from Polymun Scientific (Klosterneuburg, Austria).

Neutralization assays

A TZM-bl neutralization assay (111) was used to evaluate the neutralization potential of the mAbs described in this paper. The viruses used in this assay were from the clade C isolate MW693, and from clade B isolates MN, 108060_Q655R, QHO692, PV04, and JR-FL. Plasmids for the construction of all pseudoviruses with the exception of 108060_Q655R were kindly provided by Dr. David Montefiori (Duke University, Durham, NC). A positive control, consisting of a mixture of the monoclonal Abs (IgG1b12, 2G12, and 2F5) was used.

Sequence alignments and amino acid numbering

The sequences of gp120s compared in this study were aligned using MAFFT (112). The numbering of the amino acids described in this paper is provided using the HXB2 standard reference sequence (Los Alamos National Laboratories, HIV Sequence Compendium, Los Alamos, NM, hiv.lanl.gov/content/sequence/HIV/compendium.html).

1.4 Results

Immunization with 108060_Q655R _rgp140 and initial mAb screening

In previous studies, we characterized an envelope protein from the clade B clinical isolate 108060_Q655R (106). This isolate contains a point mutation in gp41 that appeared to increase neutralization sensitivity to broadly neutralizing, monoclonal and polyclonal antibodies by destabilizing the pre-hairpin fusion intermediate. We postulated that immunization with this envelope protein might provide access to epitopes in gp120 and gp41 (e.g., the membrane proximal external region, or MPER) that are normally concealed until the formation of the 6-helix coiled-coil structure is triggered by the engagement of the CD4 and chemokine receptors (106). Although immunization with gp140 prepared from the 108060_Q655R envelope protein did not result in antibodies with exceptional neutralizing activity, mouse hybridomas were isolated as reagents to investigate the antibody response against the unique structural features of this molecule. To map the epitopes recognized by mAbs secreted by these hybridomas, a series of glycopeptide fragments was prepared. These were designed to contain overlapping sequences of the 108060_Q655R-rgp140, similar to those previously described (107) (**FIGURE 1-1**; **SUPPLEMENTAL FIGURE 1-1**). Briefly, fragments of the 108060_Q655R-rgp140 sequence were designed to contain consecutive

domains of HIV. The smallest fragment contains only the V1/V2 domain (**SUPPLEMENTAL FIGURE 1-1**F), while the largest fragment includes from the V1/V2 domain through the C4 domain (**SUPPLEMENTAL FIGURE 1-1**B). Constructs were appended with an N-terminal gD tag for purification purposes and were expressed by transient transfection in FreeStyle™ 293-F cells. In order to maintain gross tertiary structure, the constructs were designed to contain endogenous cysteines to form disulfide bridges found in the full-length gp140. As described previously (107, 113), fragments of this type are typically glycosylated, and maintain the disulfide structures required for recognition by a variety of conformation-dependent antibodies. MAbs were tested for their binding to these scaffolds.

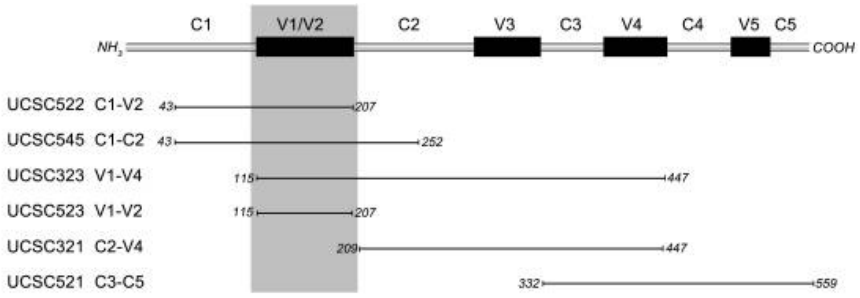

	Fragment of 108060-rgp120						
Reagent	C1-V1	C1-C2	V1-V4	V1-V2	C2-V4	C3-C5	full length
4B6	2.142	2.318	2.289	2.230	0.057	0.062	1.463
34.1	2.293	2.324	2.541	0.190	0.333	2.103	1.916
Mouse IgGκ	0.043	0.064	0.043	0.041	0.043	0.041	0.096

Figure 1-1 Mapping of the 4B6 epitope using gD-tagged fragments of 108060-rgp120. Binding of 4B6 to various fragments of the 108060 envelope protein was assayed by ELISA. All fragments were bound by the positive control antibody to the gD tag (34.1). A mouse IgGκ mAb served as a negative control. Values represent absorbance (492 nm) from single point ELISA using undiluted 4B6 cell culture supernatant. Shading indicates minimal length of epitope bound by the 4B6 antibody.

Isolation and characterization of mAb 4B6

Analysis of mAb binding to a panel of six different 108060_Q655R fragments (**FIGURE 1-1**; **SUPPLEMENTAL FIGURE 1-1**) led to the discovery of the hybridoma clone, 4B6. The mAb from this clone was found to bind to all 108060_Q655R fragments that contained the V1/V2 domain (UCSC522, UCSC545, UCSC323, and UCSC523), including the short fragment (UCSC523) that included only the V1/V2 domain (**FIGURE 1-1**; **SUPPLEMENTAL FIGURE 1-1**). In contrast, 4B6 did not bind to the two fragments (UCSC321 and UCSC521) that lacked the V1/V2 domain (**FIGURE 1-1**). These data suggested that 4B6 recognizes an epitope located within the V1/V2 domain of 108060_Q655R_rgp120. Isotype analysis of 4B6 revealed that it belonged to the IgG2a subclass (data not shown).

In order to further map the 4B6 epitope, we attempted to measure antibody binding to a series of overlapping of synthetic peptides, 15 amino acids in length, from the V1/V2 domain of the MN strain of HIV-1 (NIH AIDS Reagent Program). These synthetic peptides contained neither the glycosylation nor the disulfide structures present in the secreted fragments used for the initial screening. In contrast to rabbit antibodies to MN-rgp120 that bound to multiple peptides, 4B6 was unable to bind to any of the synthetic peptides in this panel (**SUPPLEMENTAL TABLE 1-1**). This result suggested that 4B6 might recognize a conformation-dependent epitope. To further investigate this possibility, we measured binding to the native and the reduced and carboxymethylated (RCM) forms of the V1/V2 domain of MN-rgp120 (**SUPPLEMENTAL FIGURE 1-1**, panel G). Surprisingly, we found that 4B6 bound to both the native and the RCM MN V1/V2 fragment (**FIGURE 1-2**). This result demonstrated that 4B6 recognized a conformation-independent epitope in the V1/V2 domain of both MN and 108060_Q655R gp120. The observation that 4B6 bound to the RCM form of MN V1/V2 but not to the synthetic peptides indicated that a factor other than conformation was required for 4B6 binding. We hypothesized that 4B6 binding may be dependent on the glycosylation

present in the V1/V2 fragment expressed in mammalian cells, but not in the synthetic peptides.

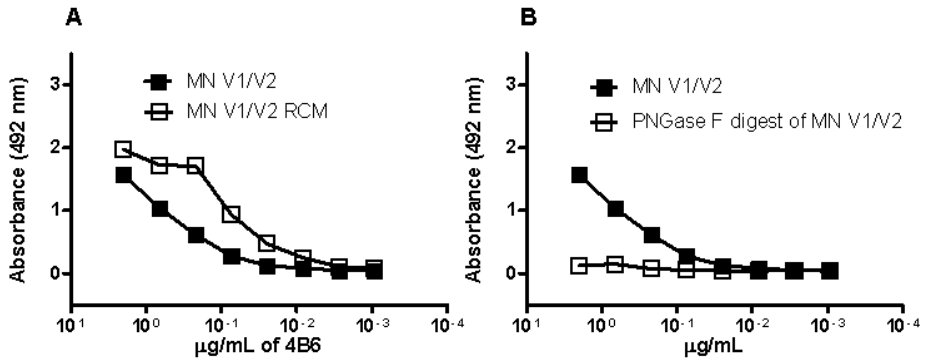

Figure 1-2 Effect of secondary structure and glycosylation on mAb 4B6 binding. A fragment corresponding to the V1/V2 domain of MN-rgp120 expressed in 293 HEK cells was treated by reduction and carboxymethylation (RCM) or PNGase digestion as described in Materials and Methods. The resulting proteins were coated onto microtiter plates and 4B6 binding was measured by ELISA. (A) the binding of 4B6 to RCM V1/V2 domain (open squares) and native V1/V2 domain (closed squares). (B) the binding of 4B6 to PNGase-treated V1/V2 domain (open squares) or mock digested V1/V2 domain (closed squares).

Sequence comparison and in vitro mutagenesis to localize the 4B6 epitope

To further localize the epitope recognized by 4B6, we evaluated its ability to bind to a panel of seventeen purified gp120s with diverse sequences expressed in mammalian cells (**FIGURE 1-3**). These included eleven clade B gp120s including MN, IIIB, SC422, TRO.11, JRFL, WITO (114), and five clinical isolates 108060_Q655R, UCSC101, UCSC109, UCSC127, and UCSC195. Additionally, we measured binding to five clade C gp120s described previously (CN97001, CN98005, IN98026, TZ97005, and ZA97010) (110) and to

the CRF01_AE A244-rgp120 (41). Of the gp120s tested, only eight of the clade B sequences were bound by the 4B6 antibody (**FIGURE 1-3**).

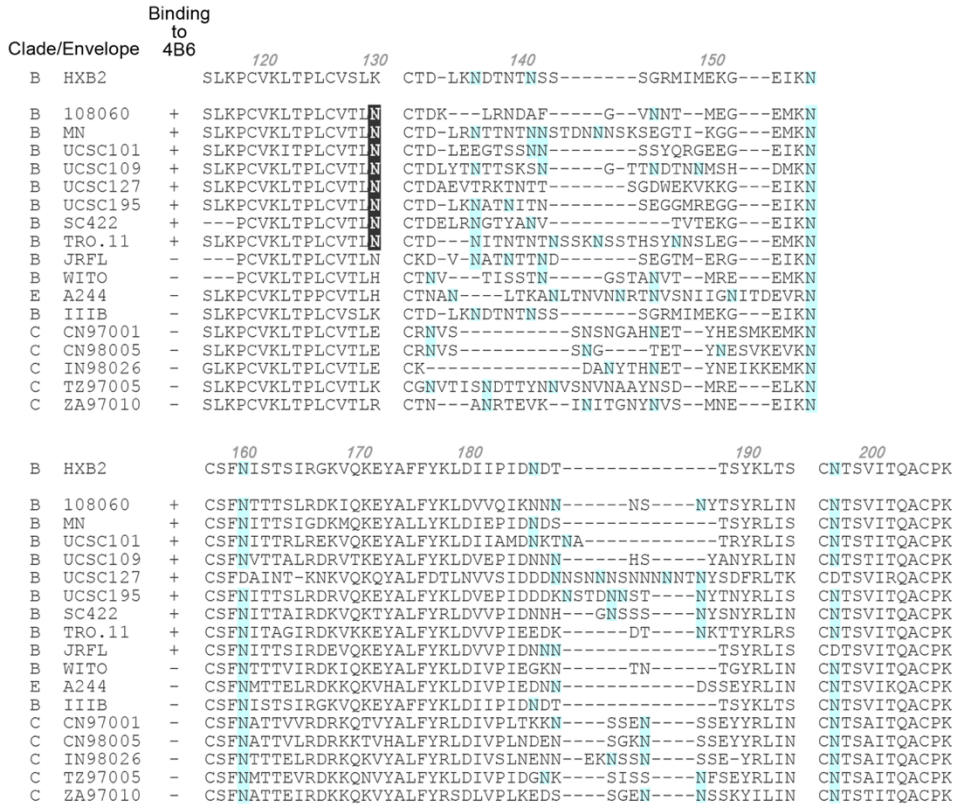

Figure 1-3 Amino acid sequence alignment of V1/V2 domains from gp120s used for 4B6 binding studies. The binding of 4B6 to gp120s from 17 different isolates was measured by ELISA. The gp120s able to bind 4B6 are indicated by plus signs (+) and those unable to bind are indicated by minus (-) signs). The sequences of all of the gp120s were aligned using MAFFT (112). The location of the N130 PNGSs that matched the pattern of 4B6 binding is indicated by white on black letters. The location of other predicted glycosylation sites that failed to match the pattern of 4B6 binding is indicated by black on blue letters. Numbering is provided with reference to the standard HXB2 numbering.

To localize the epitope recognized by 4B6, the sequences of the 4B6 binding and non-binding envelope proteins were aligned, and the amino acid sequences compared to identify polymorphisms that segregated with 4B6 binding (**FIGURE 1-3**). The sequence alignments implicated several predicted N-linked glycosylation sites (PNGSs) that were present in the gp120s that bound 4B6, and not present in gp120s unable to bind 4B6. The most promising site from this comparison was asparagine at position 130 (N130). Of note, while the clade B sequence JR-FL contains the N130 residue, it lacks the required the serine or threonine of the full N-X-S/T motif necessary for N-linked glycosylation. Without this full motif, a glycan binding to a N130 glycosylation site would not be expected to bind to JR-FL.

In vitro mutagenesis studies were then carried out to investigate the dependency of 4B6 binding on position 130. To prevent glycosylation at this position, we independently substituted either the N or the T of the canonical N-X-T/S N-linked glycosylation motif. First, we replaced N at position 130 with histidine (H). H was selected to replace N at position 156 because examination of multiple HIV sequence data sets revealed that histidine is the second most common amino acid at position 130 after N. The results of this study are shown in **FIGURE 1-4**. We found that replacement of N with H at position 130 completely abolished the binding of 4B6 to the V1/V2 fragment of MN-rgp120. To confirm this finding, we replaced threonine (T) at position 132 with alanine (A) in an independent construct. This substitution also disrupted the N130 PNGS and abolished the binding of 4B6 to the V1/V2 fragment of MN-rgp120 (**FIGURE 1-4**B). In contrast, neither of these mutations had any effect on the binding of a positive control anti-V1/V2 mAb (1088), whose binding has been established to be independent of glycosylation (107). Together, these studies indicate that 4B6 binding is dependent on the PNGS at position 130.

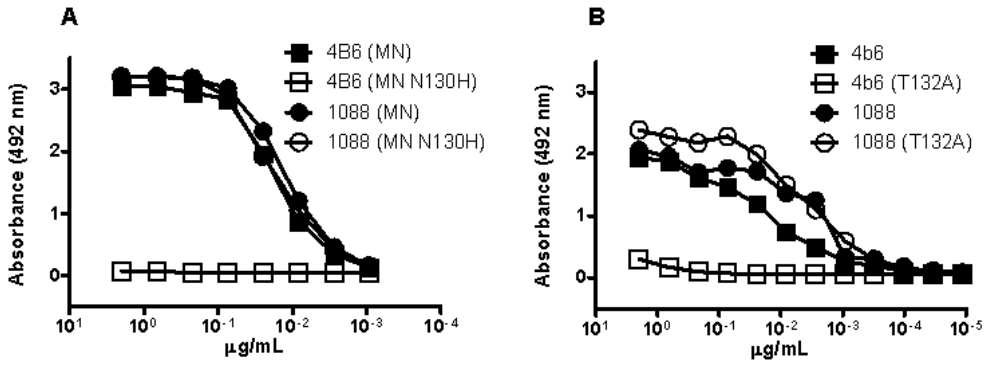

Figure 1-4 4B6 binding to MN V1/V2 fragments mutagenized to delete the N130 glycosylation site. The N130 glycosylation site was disrupted by two independent mutations targeting either the asparagine (N) at position 130 or the threonine (T) at position 132 in the N-X-S/T sequon. (A) Comparison of the binding of the glycan-dependent 4B6 mAb (squares) or the non-glycan-dependent 1088 mAb (circles) to the native V1/V2 fragment (shaded symbols) or to the V1/V2 fragment with the N130H mutation (open symbols). (B) Comparison of the binding of the glycan-dependent 4B6 mAb (squares) or the non-glycan-dependent 1088 mAb (circles) to the native V1/V2 fragment (shaded symbols) or to the V1/V2 fragment with the T132A mutation (open symbols).

PNGase F treatment destroys the epitope recognized by the 4B6 mAb

To verify that 4B6 recognizes a glycan-dependent epitope, we treated the MN V1/V2 fragment with peptide-N-glycosidase F (PNGase F). This enzyme cleaves N-linked glycans at the first N-acetylglucosamine (GlcNac), effectively removing any carbohydrates on a glycoprotein. In ELISA assays (**FIGURE 1-2**B), we observed that PNGase F treatment destroyed the binding of the 4B6 mAb to the MN V1/V2 domain fragment. To confirm that the PNGase F treatment went to completion, and to verify the identity of the species bound by 4B6, immunoblot studies were carried out. For these experiments, the mock- and enzyme-treated proteins were probed with either 4B6 (**FIGURE 1-5**A) or an anti-gD control mAb, 34.1 (**FIGURE 1-5**B). We observed that the native and mock treated V1/V2 fragment exhibited a

molecular mass that was higher than expected, approximately 50 kDa. This anomalous migration was attributed to the high carbohydrate content of the V1/V2 domain which contains 9 PNGSs in 131 amino acids, including the gD tag. As expected, treatment with PNGase F resulted in a molecular mass consistent with the calculated (17kDa) value. These results further suggested that 4B6 recognizes a GDE in the V1/V2 domain.

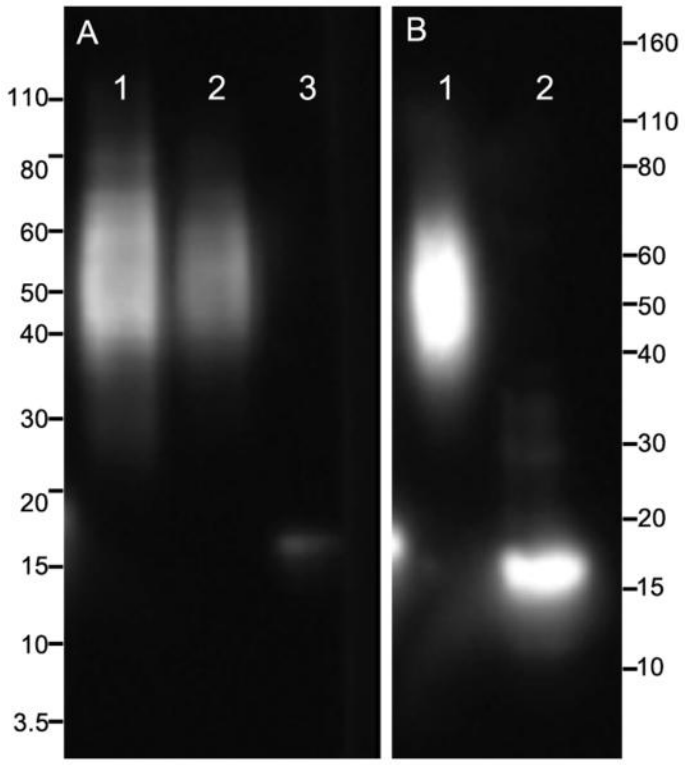

Figure 1-5 Analysis of 4B6 binding to PNGase-treated MN V1/V2 fragments by immunoblot. A fragment corresponding to the V1/V2 domain of MN-rgp120, expressed in 293 cells, was either treated with PNGase or treated with PNGase digest buffer alone (mock treated), and subjected to polyacrylamide gel electrophoresis. The proteins were then transferred to nitrocellulose paper (Novex, Life Technologies, Carlsbad, CA) and allowed to react with either the 4B6 mAb (panel A) or with 34.1, a mAb to the gD flag epitope (panel B). When probed with 4B6, untreated and mock-treated V1/V2 fragment migrates as a diffuse band of approximately 50 kDa (panel A, lanes 1 and 2); when treated with PNGase, the V1/V2 fragments runs as a sharp band of approximately 17 kDa (panel A, lane 3). When probed with the 34.1 mAb to HSV gD, untreated V1/V2 fragment migrates as a diffuse band of approximately 50 kDa (panel B, lane 1); when treated with PNGase, the V1/V2 fragment runs as a sharp band of approximately 17 kDa (panel B, lane 2). The mobility of molecular weight standards is shown in the left and right margins.

Glycan target of 4B6

Later binding studies further elucidated the epitope for 4B6. Interestingly, 4B6 bound with similar EC50 to an undigested, Endo H, and neuraminidase digested form of MN gp120.

The Endo H enzyme is derived from *Streptomyces plicatus*, and cleaves between the two N-acetylglucosamine residues of the diacetylchitobiose core of high mannose or hybrid oligosaccharides of N-linked glycans(115). Neuraminidase digest cleaves α2-3, α2-6, and α2-8 sialic acid terminal glycans from N-linked glycans(116) . Digest of MN gp120 with either of these glycosidases did not affect binding of 4B6. Assuming the digests were performed to completion, the lack of 4B6 binding to the neuraminidase-digested material indicates that 4B6 epitope does not contain a sialic-acid terminal glycan. This conclusion is supported by the observation that 4B6 additionally binds to the MN V1V2 glycosylated fragment when expressed in GNTI- cells (**FIGURE 1-6**)

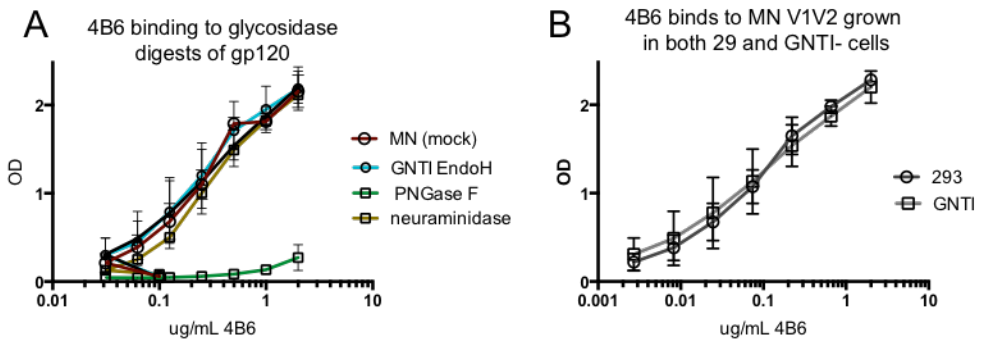

Figure 1-6 4B6 binding to MN-rgp120 expressing different glycoforms. A, mAb 4B6 binding to: mock enzyme digest, or glycan lacking (PNGase F digest) variants of MN-rgp120 were tested, and the EC_{50} was calculated for each binding curve. B, mAb 4B6 binding to MN-rgp120 grown in either 293 cells or to MN-rgp120 grown in GNTI- cells (and therefore expressing glycans containing exclusively oligomannose terminal monosaccharides). Error bars represent the standard error of the mean.

The GNTI- cell line is a HEK 293 derived cell line that is deficient in N-acetylglucosaminyltransferase I enzyme (ATCC No. CRL-3022). Expression of proteins in the GNTI- line results in limitation of N-linked glycans to mannose-5 terminal structures

(American Type Culture Collection Manassas, VA). When 4B6 was assayed for binding to mock- or Endo H-digested GNTI- expressed MN V1V2 fragments, binding curves overlapped. This was significant in that, as all glycans in GNTI- cells are constrained to the oligomannose glycoform, all glycan structures should therefore be susceptible to digest by Endo H.

Location of N130 in the V1/V2 domain structure

Recent structural studies have shown that the V1/V2 domain forms a 4-stranded β-sheet structure with the different strands identified as A, B, C, and D (89, 117) (**FIGURE 1-7**). The N130 is located near the middle of the A strand, between cysteines C126 and C131 that form disulfide bonds with cysteines located within in the D and B strands. Comparison of gp120 sequences showed that the N130 glycan is conserved among clade B viruses (94). Examination of the 3-D structure of the V1/V2 domain showed that this N130 is located in close spatial proximity to the N160 and N156 glycosylation sites that are critical for the binding of the broadly neutralizing PG9 mAb (**FIGURE 1-7**) (88, 89). However, when we measured PG9 binding to envelope proteins lacking the N130 glycosylation site, the binding of PG9 appeared to be unaffected (data not shown).

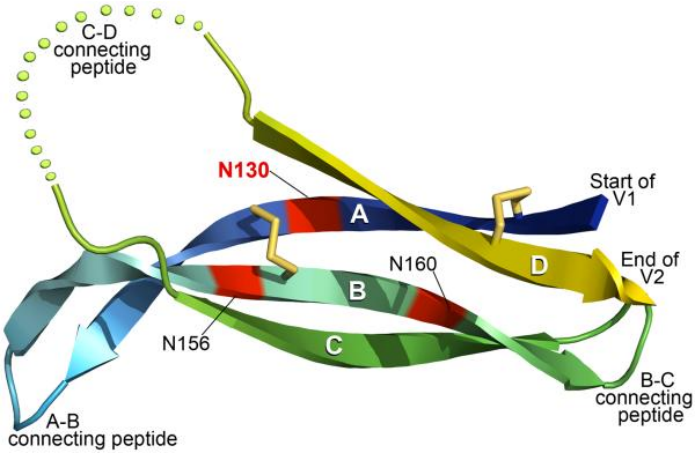

Figure 1-7 Diagram of the V1/V2 domain. The 4-stranded β-sheet structure of the V1/V2 domain reported by McLellan et al. (89) was modified to show the approximate location of glycosylation sites (red segments) recognized by the 4B6 mAb (N130) and the broadly neutralizing PG9 mAb (N156 and N160) (88). Letters (A-D) indicate each strand of the β-sheet structure. The two disulfide bonds at positions C126 and C131 flanking the N130 glycosylation site are also indicated (yellow). Other features including the B-C connecting peptide required for PG9 binding are also shown.

Neutralization Assays

4B6 does not neutralize various clade B or C viruses in a TZM-BL neutralization assay. When a TZM-bl neutralization assay (111) was used to evaluate the neutralization potential of 4B6, it was found that 4B6 was unable to neutralize any of the clade C isolate MW693 clade B isolates MN, 108060_Q655R, QHO692, PV04, and JR-FL nor the clade C isolate MW693 (**SUPPLEMENTAL TABLE 1-2**).

1.5 Discussion

This study documents the isolation of a mouse mAb (4B6) to a novel GDE in the V1/V2 domain of the HIV envelope protein, gp120. Four new findings derive from these

studies. First, we show that antibodies to GDEs in the V1/V2 domain of gp120 can result from immunization with recombinant gp120, whereas previously such antibodies have been isolated only from HIV-infected humans or chimpanzees (36, 66, 87, 88, 118, 119). Second, we show that antibodies to GDEs can result from a relatively short immunization schedule and that continuous exposure to gp120 over a long period of time, as occurs during chronic HIV infection, is not required to elicit antibodies to GDEs. Third, we show that the 4B6 epitope is common among clade B viruses. Finally, we show that while 4B6 binds to GDEs in the V1/V2 domain, this binding to a GDE in the V1/V2 domain alone is not sufficient for virus neutralization, and that additional factors determine whether an antibody possesses virus neutralizing activity.

Historically, N-linked glycans have been considered poorly immunogenic, and it has been surprising to discover that a large percentage of the broadly neutralizing antibodies in sera from HIV-infected individuals are directed to GDEs on gp120 (87, 88, 90). While it has been well documented that N-linked glycans found on the HIV envelope protein function as a "glycan shield" to protect large regions of the gp120 structure from antibody binding by steric hindrance, we now know that this shield is imperfect, and that glycans can themselves become targets for neutralizing antibodies(120). Recent studies of mAbs from HIV-infected humans have identified at least two different clonal lineages of bNAbs that recognize GDEs in the V1/V2 domain. These include the PG9 lineage that recognizes glycans at positions 156 and 160, and the PGT121/122 lineage that recognizes glycans at position 137 (121, 122). Thus far, antibodies from humans recognizing the N130 GDE have not been described. However, recent analysis of VAX003, VAX004, and RV144 vaccine trials revealed that the portion of the V1/V2 domain containing N130 PNGS is highly immunogenic [40]. The observation that the N130 site is contained within a region that is particularly visible to the

humoral immune response supports the hypothesis that antibodies to the N130 GDE may additionally be found in human sera.

Studies showing that GDEs are major targets of bNAbs have prompted considerable interest in developing vaccines able to elicit antibodies to this class of epitope. However, numerous uncertainties remain concerning the best approach to elicit antibodies to GDEs in gp120. We know little regarding the optimal formulation or immunization regimen to elicit antibodies to GDEs. In humans, bNAbs to GDEs are seldom found until 2-3 years post-infection, following years of continuous exposure to viral antigens (66, 87, 88). Based on these kinetics, it has been postulated that antibodies to GDEs might only occur as the result of continuous exposure to highly glycosylated viral antigens, or as a consequence of breakdown in immune tolerance of the glycan structures resulting from HIV infection. Indeed, several groups are pursuing the possibility of “guided” immunization strategy with viral proteins recovered from the sequential virus isolates thought to have guided the evolution of antibodies to GDEs with broadly neutralizing activity (121, 123, 124). It is postulated that this approach might be effective in driving the evolution of antibodies with the atypical structures found in most bNAbs, such as long CDR H3 domains (>20 amino acids) resulting from unusual VDJ splicing, additional N-linked glycosylation sites, or highly mutated antibody genes (>100 nucleotide changes) resulting from unusually high levels of somatic mutation (121). Moreover, bNAbs to GDEs often appear to bind simultaneously to two different glycan moieties (e.g., N156 and N160 in the case of PG9, and N302 and N332 in the case of PGT128) (125). Our isolation of 4B6 demonstrates that antibodies to GDEs can arise in healthy, uninfected animals as a result of a short intensive immunization regimen with recombinant envelope protein. Further work to sequence and solve the structure of this antibody would provide insight as to whether its inability to neutralize HIV results from a lack of structural features (e.g., long CDR H3 domain, etc.) common to bNAbs.

The potential binding of 4B6 antibody to the primary N-acetylglucosamine residue on MN carries interesting implications. The reliance of 4B6 binding on the N-acetlyglucosamine residue indicates the immunogenicity and exposure of the base of the N130 glycan to the humoral immune response in the context of the 108060 gp140. Additionally, as glycans are large, bulky components, it is possible that the 4B6 antibody may have unique characteristics to allow binding to an epitope located at the "base" of such a glycan tree. Ultimately, this mAb, despite its non-neutralizing characteristics, can be used as part of a "molecular toolbox" for understanding the antigenicity of the N130 glycan epitope in the context of relevant (amino acid epitope sharing) clade B immunogens.

Finally, these studies highlight the possibility that antibodies to GDEs are more common than previously appreciated. This insight has implications for our understanding of the protective immune responses to the highly glycosylated proteins of other pathogens such as cytomegalovirus (126), SARs-CoV, influenza, and West Nile virus (127). Until recently, vaccines were developed to epitopes that were primarily amino acids or carbohydrates, but not a combination of both. It now appears that another important class of epitope exists, exemplified by 4B6 and by bNAbs to HIV that depend on both amino acid and N-linked glycan contacts. Further studies evaluating the frequency and specificity of these antibodies, as well as studies aimed to elucidate the best method to elicit such antibodies, may present important medical insights and applications.

1.6 Supplemental Material

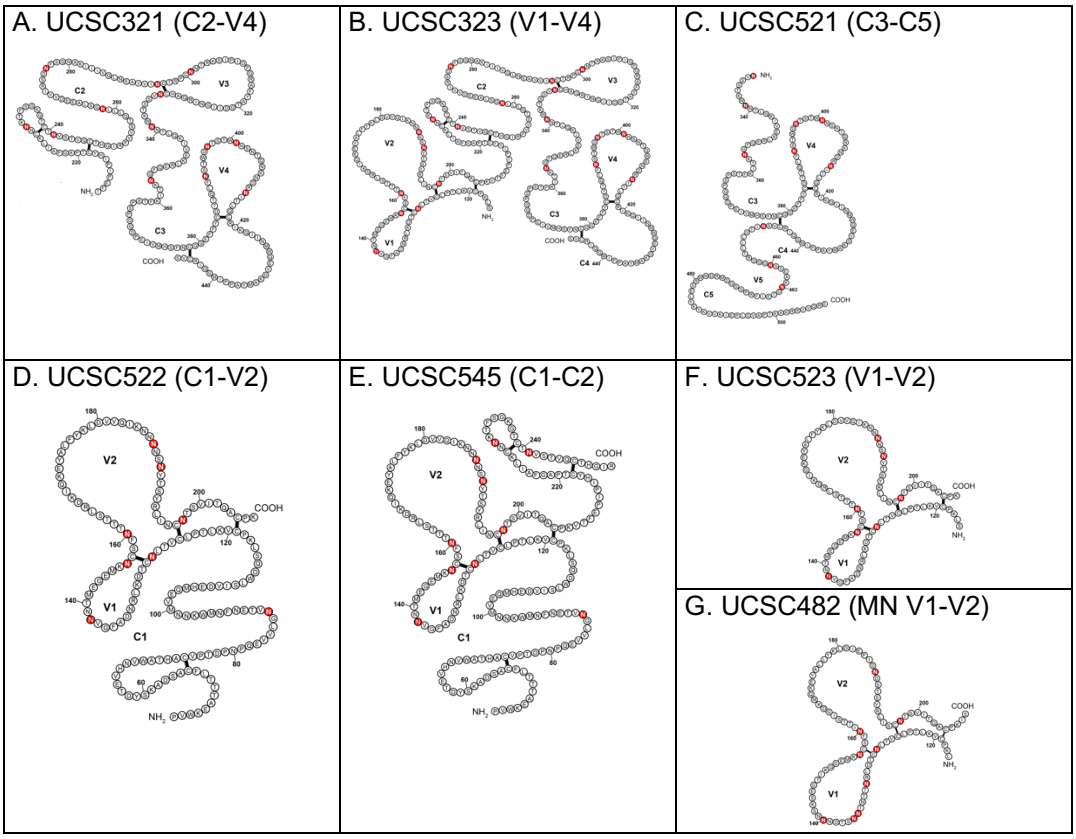

Supplemental Figure 1-1: Constructs of 108060_Q655R and MN used for 4B6 epitope mapping. A panel of overlapping fragments of the 108060-rgp120 protein (Figures A-F) were constructed based on the 2-dimensional structures from Leonard et al. [J Biol Chem 1990, 265:10373-82]. Fragment G is a V1/V2 fragment of MN. All fragments were used for epitope mapping in a manner similar to that described [Nakamura et al., PLoS One 2012, 7:e39045]. Disulfide bridges afforded by the primary sequence allowed the fragments to maintain a degree of secondary structure. All fragments were appended with the signal sequence and 27 amino acid N-terminal domain of the gD protein from type 1 herpes simplex virus, and expressed in the 293 human embryonic kidney adenocarcinoma cell line. MAb binding to the shortest fragments (F, G) were used to identify mAbs that bound to epitopes in the V1/V2 domain. All numbering is based on HXB2, with predicted N-linked glycosylation sites indicated at residues shaded.

Fragment	Absorbance	
	4B6	Rabbit polyclonal
QSLKPCVKLTPLCVT	0.052	0.057
PCVKLTPLCVTLNCT	0.084	1.878
LTPLCVTLNCTDLRN	0.059	0.303
CVTLNCTDLRNTTNT	0.076	0.053
NCTDLRNTTNTNNST	0.053	0.053
LRNTTNTNNSTANNN	0.051	0.052
TNTNNSTANNNSNSE	0.052	0.056
NSTANNNSNSEGTIK	0.051	0.054
NNNSNSEGTIKGEM	0.052	0.054
NSEGTIKGGEMKNCS	0.060	0.055
TIKGGEMKNCSFNIT	0.052	0.064
GEMKNCSFNITTSIR	0.053	0.069
NCSFNITTSIRDKMQ	0.051	0.064
NITTSIRDKMQKEYA	0.051	0.064
SIRDKMQKEYALLYK	0.051	0.454
KMQKEYALLYKLDIV	0.051	0.117
EYALLYKLDIVSIDN	0.051	0.069
LYKLDIVSIDNDSTS	0.051	0.079
DIVSIDNDSTSYRLI	0.051	0.076
IDNDSTSYRLISCNT	0.052	0.052
STSYRLISCNTSVIT	0.051	0.052

RLISCNTSVITQACP	0.051	0.067
CNTSVITQACPKISF	0.052	0.070
VITQACPKISFEPIP	0.051	0.054
ACPKISFEPIPIHYC	0.065	0.485
MN V1/V2	1.864	2.759

Supplemental Table 1-1 Binding of 4B6 to synthetic peptides. To map the epitope of the 4B6 mAb, we measured the binding of the mAb to a set of 15mer overlapping fragments of MN spanning the V1/V2 domain. Peptides were coated on a microtiter plate at a concentration of 5 μg/mL, and mAb 4B6 was tested for binding to peptides by ELISA. Rabbit polyclonal sera was used as a positive control. The left column indicates the sequence of the peptides tested. The N130 glycosylation motif is underlined. A glycosylated fragment of MN-rgp120 known to bind to 4B6 (UCSC482, comprising the V1/V2 domain and expressed in mammalian cells) was included as a positive control. Values presented represent the average of duplicate experiments.

Virus/Clade	Tier	4B6	Tri-Mab ug/ml
JR-FL/B	2	<20 dilution	0.01
MN-3/B	1	>50* ug/mL	<0.01
108060_024/B	2	>50 ug/mL	0.24
QHO692/B	2	>50 ug/mL	1.82
PV04/B	3	>50 ug/mL	4.01

Supplemental Table 1-2 Results of mAb 4B6 neutralization assays. Cell culture supernatant from 4B6 monoclonal hybridomas or purified antibody was tested for neutralization capability against a panel of viruses expressing envelope proteins for six different strains. IC50 values are expressed as the inverse dilution factor of hybridoma supernatant or ug/mL of purified 4B6. A TZM-bl neutralization assay [Montefiori et al., Curr Protoc Immunol 2005, 64:12.11.1-17] was used to determine 4B6 neutralization against the clade C isolate MW693 and the clade B isolates MN, 108060_Q655R, QHO692, PV04, and JR-FL. A Tri-Mab control consisting of a mixture of the monoclonal Abs b12, 2G12, and 2F5 was used as a positive control.

Funding for this work was supported by grants from the National Institutes of Health, National Institute of Drug Abuse (R01 DA 26801-01A1) and National Institute of Allergy and Infectious Disease (R01 AI 089378 01). The content is solely the responsibility of the authors and does not necessarily represent the official views of the National Institutes of Health. Additional funding was provided by the Henry Jackson Foundation (#683948).

Acknowledgments

We thank Dr. Aaron Vollrath for his assistance with sequence analysis, and Ann Durbin for expert technical assistance in the production of the manuscript.

Chapter 2

Improving the antigenic structure of the gp120 immunogens used in the RV144 clinical trial

2.1 Foreword

This chapter contains text and figures from the following manuscript:

> Doran, R. C., Tatsuno, G. P., O'Rourke, S. M., Yu, B., Alexander, D. L., Mesa, K. A., Berman, P. W., .Glycan modifications to the gp120 immunogens used in the RV144 vaccine trial improve binding to broadly neutralizing antibodies. PLoS One 13, doi:10.1371/journal.pone.0196370 (2018).

The work was completed as a collaboration between all authors; RCD, GT, KM, and PWB designed MN mutants, RCD, KAM, and PWB designed A244 mutants, RCD and SMO were involved in protein expression, BY performed protein purification, DLA contributed to assay design. PWB was responsible for conceptualization, oversight, and attaining funding.

2.2 Introduction

The RV144 clinical trial has been the only human clinical trial to show that vaccination can provide protection from HIV infection (46). The RV144 vaccination protocol consisted of immunization with the ALVAC (VCP1521) canarypox virus vector (128), designed to elicit a robust cell-mediated immune response, followed by co-immunization with the bivalent AIDSVAX B/E gp120 vaccine, designed to elicit an anti- gp120 antibody response (41, 103, 129). This regimen provided statistically significant protection (Vaccine Efficacy= 31.2%, P=0.04) over 3.5 years, with up to 60% efficacy within the first year after vaccination (46). Follow-up analysis revealed that protection correlated with: antibodies to the V2 domain of gp120, high levels of antibody-dependent cellular cytotoxicity (ADCC) (52), and HIV-1 specific IgG3 antibodies (82), but not with gp120-specific CD8+ T-cell responses (46). Together, these studies indicated a role for anti-gp120 antibodies in the modest but significant level of protection afforded by the vaccine. The importance of the antibody response was further supported by additional antibody binding studies (48, 49) and sieve analysis of breakthrough viruses (130). Such studies associating protection with anti-gp120 antibodies provided a rationale for further development of gp120-based immunogens.

Since the completion of the RV144 trial, we have accumulated considerable insight regarding the structure of gp120, as well as of the specificity of neutralizing antibodies against it. The isolation of bNAbs from HIV-infected individuals revealed highly conserved protein and glycopeptide epitopes on gp120 that were unknown when the AIDSVAX/BE vaccine was first developed. Of particular relevance was the identification of oligomannose terminal glycans targeted by multiple families of bNAbs. These glycans are located at conserved N-linked glycosylation sites in the V1/V2 domain (N301 and N332), near the apex of the gp120 trimer, and near the stem of the V3 domain (65-67, 88, 101, 131-136), referred to as the “high mannose patch” (135). The apparent preference of these bNAbs for gp120

within trimeric structures, as compared to monomeric gp120, suggested a requirement for quaternary structure for bNAb binding (65, 88). However, it is becoming apparent that differences in glycan processing and glycan accessibility between monomeric and trimeric gp120 structures, in part, can account for this preference. While trimeric gp120, the functional unit of gp120 displayed on the surface of virions, is enriched for oligomannose glycans, recombinant monomeric gp120 without the gp41 subunit displays predominantly complex, sialic acid-terminal, glycans (32, 137). This discrepancy is at least partially explained by incomplete glycan processing in the ER and Golgi Apparatus, thought to be a consequence of steric hindrance to glycosidase enzymes during trimer formation (136, 138). The AIDSVAXB/E immunogens were produced in a Chinese Hamster Ovary (CHO) cell line, and consequently possessed a high degree of N-linked glycan sialylation (40). High sialic acid content is desirable for a majority of biotherapeutics, as its presence in recombinant glycoproteins is known to impart a longer in vivo half-life (139, 140). However, it is now apparent that sialic-acid moieties on gp120 can prevent binding of bNAbs (40, 141, 142). Although previously unappreciated in HIV vaccine design, N-linked glycosylation is now recognized as a significant determinant of the antigenic structure of HIV envelope glycoproteins (131, 133). Here we describe our efforts to improve the antigenic structure of the vaccine immunogens used in the RV144 clinical trial by altering the location of no more than two critical N-linked glycosylation sites and constraining the types of glycoforms incorporated. These simple changes improved the antigenic structure of gp120 immunogens used in the RV144 trial, as measured by improved binding by three major families of bNAbs. The glycan-optimized gp120 proteins we describe represent second-generation vaccine immunogens that possess epitopes recognized by multiple bNAbs not present on the vaccine immunogens used in the RV144 trial. By enhancing the potential to elicit bNAbs associated

with protection from HIV infection in passive transfer studies (70, 80, 143), the immunogens described might improve the efficacy of the RV144 vaccine regimen.

2.3 Materials and Methods

Production and purification of rgp120 glycan variants

Site-directed mutagenesis was used to create the MN- and A244-rgp120 glycosylation site mutants using a Gibson Assembly master mix (New England Biolabs, Ipswich, MA). The MN_{GNE} sequence differs from the MN sequence published by Gurgo et al. (144) by 18 amino acids within the gp120 sequence, and contains a 27 amino acid N-terminal purification tag from herpes simplex virus glycoprotein-D (gD). The $A244_{GNE}$ sequence from the RV144 trial is unaltered from the original sequence described by McCutchan et al. (145) except for the addition of the N-terminal gD tag (41). The mature recombinant A244-gp120 (A244-rgp120) protein contains the same primary amino acid sequence as the A244-rgp120 incorporated into the AIDSVAXB/E vaccine. The MN_{GNE} and $A244_{GNE}$ sequences have been described in detail and submitted to Genbank under the accession numbers MG189370 and MG189369, respectively. Nucleotide and protein alignments were performed with Geneious software (version 6.0; http://www.geneious.com, Kearse et al., 2012) (146), and all sequences and notations employ HXB2 numbering. Plasmids containing rgp120 were transiently transfected in either 293 $GNTI^-$ HEK (ATCC CRL-3022) cells, deficient in the enzyme Mannosyl (Alpha-1,3-)-Glycoprotein Beta-1,2-N-Acetylglucosaminyltransferase I ($GNTI^-$ 293 cells), or CHO-S cells (Invitrogen, Carlsbad, CA) using electroporation (MaxCyte STX, Gaithersburg, MD). All rgp120s contained an 11 amino acid N-terminal deletion, replaced by the N-terminal gD tag that was used for affinity chromatography protein purification as previously described (40). Proteins were analyzed for molecular mass with

SDS PAGE on 4-12% Bis-tris gel (Life Technologies, Carlsbad, CA). Purified, CHO-derived MN-rgp120 (MN_{GNE}), was obtained from GSID (GSID, South San Francisco, CA).

Physical characterization of gp120 proteins

Immunoprecipitations using Dynabeads™ Protein G magnetic beads (Life Technologies, Carlsbad, CA) were performed on MN gp120 glycan variants preceding Endo H digest. Briefly, 300μL of supernatant from gp120 transient transfections were incubated with 2.5μg purified mouse monoclonal antibody (34.1), raised against the N-terminal gD tag, to form rgp120/mAb immune complexes. Beads were re-suspended and incubated in transfection supernatant containing rgp120/34.1 immune complexes. All incubations were performed for one hour on a rotating platform, at room temperature. The beads were washed three times in PBST with a final wash in PBS, and used directly in glycosidase digests. Endo H digest was purchased from New England Biolabs (Ipswich, MA) and used to digest $GNTI^-$ and CHO expressed rgp120 proteins according to the manufacturer's instructions. Briefly, ~10μg of recombinant protein was denatured and reduced with 10X denaturation buffer, then boiled at 100°C for 10 min. Samples were incubated with 10X G5 reaction buffer and 5,000 units Endo H for 12h at 37°C. Digested and mock-digested samples were analyzed by polyacrylamide gel electrophoresis (PAGE) using precast polyacrylamide gels (4–12% Bis-Tris) in MOPS running buffer (NuPAGE®, Invitrogen, Carlsbad, CA). Blots were probed with the 34.1 mAb and visualized with a goat-anti-mouse HRP conjugated polyclonal (American Qualex Antibodies, San Clemente, CA).

Immunoassays

A Fluorescence Immunoassay (FIA) was used to measure antibody binding to gp120. A FIA, which replaces the more common enzymatically catalyzed chemiluminescent

readout (ELISA) with fluorescently labeled secondary polyclonal, is slightly less sensitive, but provides the benefit of a higher dynamic range of sensitivity in addition to higher reproducibility (147). Briefly, 2μg/mL of an anti-gD mouse monoclonal antibody (mAb 34.1) was diluted into PBS and incubated overnight in 96 well black microtiter plates (Greiner, Bio-One, USA). Plates were blocked in PBS containing 1% BSA+0.05% normal goat serum in 0.01% thimerosal for two hours. Wells were incubated with either 6μg/mL of purified rgp120, or 25-200μL of rgp120 containing growth conditioned cell culture supernatant, overnight at 4°C. Three-fold serial dilutions of bNAb or polyclonal control sera were added starting at 10μg/mL, followed by incubation with a 1:3,000 dilution of goat-anti-human AlexaFluor 488 conjugated polyclonal antibody (Jackson ImmunoResearch Laboratories, West Grove, PA, Life Technologies, Carlsbad, CA). Dilutions were performed in a 1% BSA solution in PBS containing 0.01% thimerosal, and all incubations were performed for 90 min at room temperature followed by a 4Xwash in PBST buffer unless otherwise noted. Cell culture supernatants were normalized to contain approximately 2μg/mL of rgp120 for screening assays, or 4μg/mL for binding to the assays to an extended bNAb panel, and captured with 1μg/mL (for screening assays), or 2μ/mL of immobilized anti-gD 34.1 monoclonal antibody. Broadly neutralizing antibody binding curves were performed in quadruplicate for statistical confidence. Human IgGK was used as a negative control, protein-G purified rabbit polyclonal sera raised against rgp120 (PB94), was used as a coating control. Absorbance was read using an EnVision Multilabel Plate Reader (PerkinElmer, Inc, Waltham, MA) using a FITC 353 emission filter and FITC 485 excitation filter. The PG9 mAb was purchased from Polymun Scientific (Klosterneuburg, Austria), and the CH01-CH03 antibodies were gracious gifts of Dr. Barton Haynes at Duke University (Durham, NC). The following reagents were obtained through the NIH AIDS Reagent Program, Division of AIDS, NIAID, NIH: PGT126, PGT128, PGT 121, VRC01, and 10-1074, or were a gift from Dennis Burton (La Jolla, CA).

Statistical Analysis

Statistical analyses were performed with GraphPad Prism software (v5.0). A Kruskall-Wallis test with a Dunn's post-hoc test, to correct for multiple comparisons, was used to determine statistically significant differences in EC50 ($p<0.05$) measurements of bNAb binding between CHO-derived, RV144 based immunogens and GNTI$^-$-expressed gp120 glycan variants. Error bars represent the standard error of the mean (SEM).

2.4 Results

Improvements of the antigenic structure of the A244-rgp120

We analyzed the A244-rgp120 primary sequence for presence of bNAb-associated glycans. Glycans can obscure even distant epitopes in the context of primary protein structure (35, 95). We therefore aimed to introduce a minimal number of additional potential N-linked glycosylation sites (PNGS), and limited our investigation to highly conserved (~70% across clade) (148) glycans incorporated into a minimal V3 stem bookended by the N289 and N334 PNGS (

FIGURE 2-1A and B). Analysis of the A244-rgp120 sequence revealed that it lacked a PNGS located at HXB2 position N332, containing instead a glycan at position N334 that is highly typical amongst clade AE viruses. Based on these observations, we modified the A244-rgp120 sequence to contain point mutations E332N and N334S. These mutations resulted in the ablation of the N334 PNGS and introduction of a PNGS at N332. As the A244-rgp120 sequence contained all other highly conserved PNGSs within the considered range, no other glycan variants were investigated

FIGURE 2-1C).

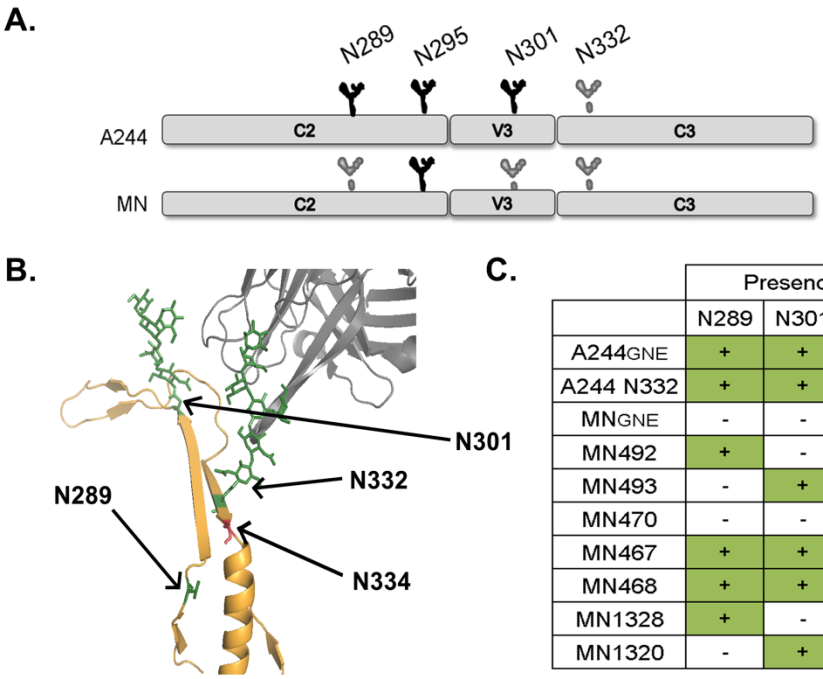

C.

	Presence of PNGS			
	N289	N301	N332	N334
A244GNE	+	+	-	+
A244 N332	+	+	+	-
MNGNE	-	-	-	-
MN492	+	-	-	-
MN493	-	+	-	-
MN470	-	-	+	-
MN467	+	+	-	-
MN468	+	+	+	-
MN1328	+	-	+	-
MN1320	-	+	+	-

Figure 2-1 Modification of N-linked Glycosylation Sites in MN- and A244-rgp120. (A) The A244-rgp120 or MN-rgp120 sequences were analyzed for the presence of highly conserved glycans known to be important for bNAb binding within the C2-C3 domains. Glycosylation sites are represented as either black (present in RV144 immunogen) or grey (absent in original RV144 immunogen) structures. (B) A ribbon diagram depicts the 3-dimensional arrangement of the N289, N301, N332, and N334 PNGS. The structure is based on crystal structure of the BG505 SOSIP.664 gp140 trimer (in gold) bound to the PGT122 bNAb (in grey) (117). The N301 and N332 glycan structures immobilized by the PGT122 antibody are indicated in green, while the asparagine residues at the base of relevant PNGS are indicated in red. (C) Site directed mutagenesis was used to create MN- or A244-rgp120 variants introducing one or more of the indicated PNGS. A summary of the PNGS variant constructs assayed is shown. The constructs with identical number and location of PNGS to the RV144 rgp120 immunogens are marked with an asterisk.

Because multiple bNAbs bind mannose-5 or mannose-9 glycan epitopes, and such epitopes are destroyed when sialic acid terminal glycans are incorporated, we expressed the gp120 variants in GNTI$^-$ 293 cells that limit N-linked glycosylation to predominantly mannose-5 terminal moieties (40). To verify that the proteins produced in GNTI$^-$ cells lacked complex

sialic acid containing glycans, gp120 variants were treated with Endoglycosidase H (Endo H). Endo H is an enzyme that cleaves high mannose, but not complex, sialic acid containing N-linked oligosaccharides. Endo H treatment results in cleavage of uniquely oligomannose terminating N-linked glycosylation moieties, leaving behind only the base N-acetyl glucosamine residue from the original diacetylchitobiose core of the original glycan base. When digested with Endo H and run on an SDS page gel, the GNTI$^-$ derived A244 gp120 glycan variants migrated as a ~60kD band, the predicted molecular weight of non-glycosylated gp120, while the sialic acid containing gp120 produced in normal CHO cells, like that used in the RV144 trial, remained showed only a small shift in mobility indicative of a lesser degree of oligomannose incorporation (**FIGURE 2-2**).

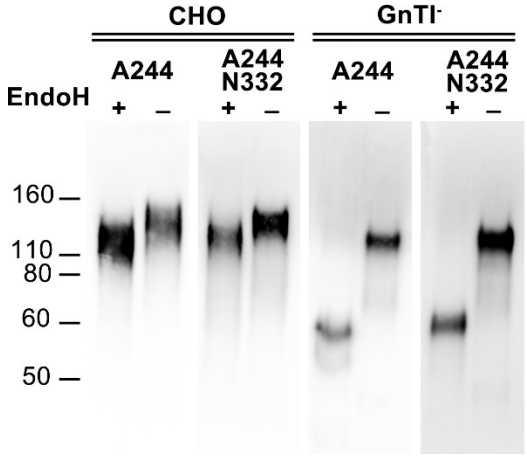

Figure 2-2 Endo H Digest and Immunoblot of A244 gp120 Glycan Variants. A244-rgp120s containing either N332 or N334 based PNGS were expressed in either CHO-S (lanes 1-4) or HEK 293 GNTI$^-$ cells (lanes 5-8) via transient transfection. Purified protein was subjected to Endo H or mock digest (digest buffer alone) and analyzed for mobility on 4-12% reducing SDS-PAGE gels. Immunoblots were probed with the mouse monoclonal 34.1 that binds a conformation independent epitope in the N-terminal gD tag of all expressed proteins, and visualized with goat-anti-mouse HRP conjugated polyclonal sera.

Previously, we have reported that rgp120s exhibit higher affinity for PG9, the prototypic V1V2 glycan dependent bNAb, when expressed in GNTI$^-$ 293 as compared to CHO cells (40). We expressed A244-rgp120 N332 glycosylation site variants in both CHO and GNTI$^-$ 293 cells. The resulting proteins ($A244_{N332}$CHO and $A244_{N332}$GNTI$^-$) were purified via affinity chromatography (see Materials and Methods) to investigate how the global change in glycoform processing would affect binding to a panel of bNAbs. Recombinant gp120 based on the A244-rgp120 sequence from the RV144 trial, containing the N334 PNGS, was expressed in CHO and GNTI$^-$ 293 cells. The resulting proteins ($A244_{GNE}$ and $A244_{N334}$GNTI$^-$, respectively) were assayed by FIA to identify how position of the PNGS or the type of glycosylation affected bNAb binding. EC50s derived from antibody binding curves were used to quantitate improvements to presentation of epitopes recognized by bNAbs. The binding curves and derived EC50s are summarized in **FIGURE 2-3**.

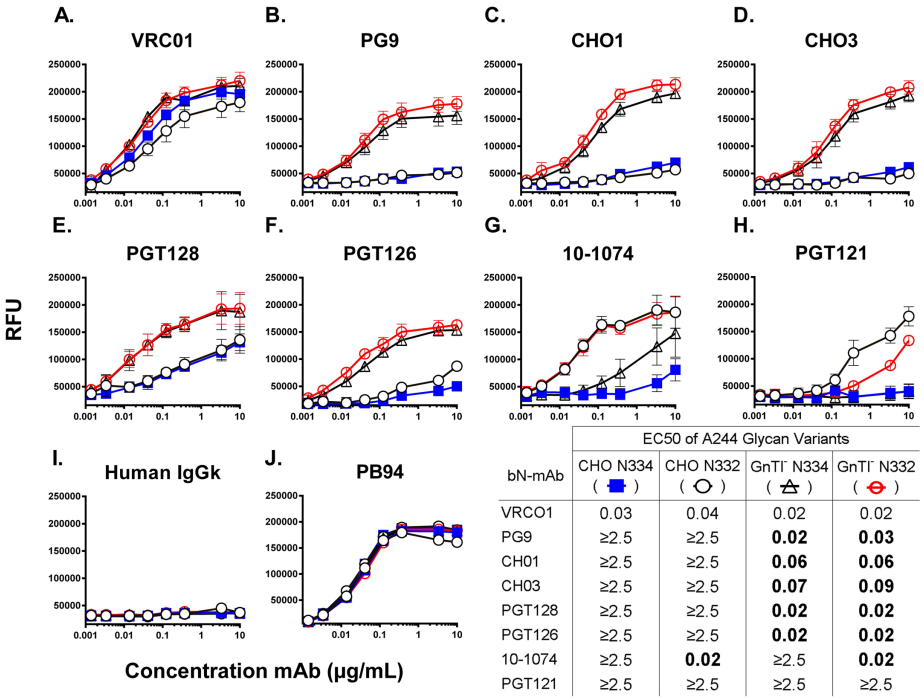

bN-mAb	EC50 of A244 Glycan Variants			
	CHO N334 (■)	CHO N332 (○)	GnTI⁻ N334 (△)	GnTI⁻ N332 (⊖)
VRCO1	0.03	0.04	0.02	0.02
PG9	≥2.5	≥2.5	**0.02**	**0.03**
CH01	≥2.5	≥2.5	**0.06**	**0.06**
CH03	≥2.5	≥2.5	**0.07**	**0.09**
PGT128	≥2.5	≥2.5	**0.02**	**0.02**
PGT126	≥2.5	≥2.5	**0.02**	**0.02**
10-1074	≥2.5	**0.02**	≥2.5	**0.02**
PGT121	≥2.5	≥2.5	≥2.5	≥2.5

Figure 2-3 Binding of A244-rgp120 Glycan Variants to bNAbs. Purified A244-rgp120 glycan variants were compared by FIA for binding to a panel of bNAbs. Results are reported as the half maximal effective concentration (EC50) in µg/mL, or the concentration of antibody required for a half-maximal binding, measured in Relative Fluorescence Units (RFU) on a titration-binding curve. Values are reported as ≥2.5µg/mL if titration curves did not plateau, or mean EC50 was calculated as ≥2.5µg/mL. Each curve represents the average of four independent assays. The EC50 values of the rgp120 glycan variants that are significantly different ($p<0.05$) from the $A244_{GNE}$ EC50 to the same bNAb are highlighted in bold. Human IgGK polyclonal antibody was used as a negative control, and binding curves to purified rabbit polyclonal antibody (PB94) raised against rgp120 were used as a coating control. Error bars represent standard error.

To verify that rgp120 glycan variants maintained relevant secondary and tertiary structure, we assayed gp120 binding to the bNAb VRCO1 that recognizes a conformation dependent protein epitope at the CD4 binding site of gp120 (149). Both N332 and N334 $GNTI^-$ expressed gp120 variants exhibited slight, though not statistically significant, improvements to the VRC01 bNAb as compared to CHO expressed rgp120 (**FIGURE 2-2**A).

The PG9 bNAb that recognizes a mannose-5 dependent epitope in the V2 domain exhibited negligible binding to $A244_{GNE}$, but bound with high affinity to both $GNTI^-$ expressed N332 and N334 variants (EC50 of 0.02 and 0.03 μg/mL, respectively) (**FIGURE 2-3**B) While PG9 binding appeared dependent on the mannose-5 glycans resulting from $GNTI^-$ expression, it did not distinguish between the N332 and N334 variants (150). A similar binding preference was observed with the CH01 and CH03 antibodies that recognize a glycan-dependent epitope in the V2 domain (66).

The PGT128 and PGT126 antibodies belong to a family of bNAbs whose epitope lies at the base of the V3 domain and requires oligomannose glycans at N301 and N332 (65, 88, 151). Both the N332 and N334 A244-rgp120 variants exhibited weak binding to PGT128 and PGT126 when produced in CHO cells. However, expression in $GNTI^-$ 293 cells resulted in significant improvements in EC50 for both the A244 N332 and N334 variants. Both the $A244_{N332}GNTI^-$ and $A244_{N334}GNTI^-$ displayed binding curves with EC50s of 0.01μg/mL for PGT128 and 0.02μg/mL to PGT126 (**FIGURE 2-3**E and F). While the bNAbs PGT121 and 10-1074 bNAbs have been reported to accommodate an N334 in place of an N332-based PNGS in a strain-dependent manner (67, 135), we found that both the A244 and MN-rgp120s required the N332 glycosylation site for optimal presentation of the PGT121 and/or 10-1074 bNAb epitopes. A244-rgp120 binding appeared to be strictly dependent on the presence of the N332 glycan. The $A244_{N332}$ exhibited high affinity binding to 10-1074 (EC50 ~0.02μg/mL) regardless of cell expression system (**FIGURE 2-3**G). However, PGT121 exhibited marginally better binding to the CHO produced A244-rgp120, in concordance with the observation that PGT121 exhibits a preference for complex glycans (**FIGURE 2-3**H) (67). Other members of the PGT family of bNAbs (PGT 130 -145) exhibit absolute dependence on quaternary structure afforded by the trimeric form of gp120, and were therefore not included in our analysis (65). These studies indicate that the antigenic structure of A244-rgp120, as

measured by the binding of bNAbs from the PG9, PGT128, and PGT121 families, can be improved by replacement of complex glycans with oligomannose glycans and incorporation of the N332 PNGS.

Improvement of the antigenic structure of MN-rgp120

Sequence analysis of MN-rgp120 revealed that the V3 stem lacked conserved PNGS at positions 289, 301, and 332. To evaluate the effects of these PNGS on the MN-rgp120 antigenic structure, we designed a series of glycosylation variants with single, double, or triple PNGS mutations. The first series of glycosylation mutants (MN492, MN493, and MN470) added a single PNGS at positions 289, 301, or 332, respectively. MN-rgp120 variants that incorporated two additional PNGS included: MN467 (two additional PNGS at N289 and N301), MN1320 (two additional PNGS at N301 and N332), and MN1328 (two additional PNGS at N289 and N332). Finally, the MN468 mutant introduced three additional PNGS at 289, 301, and 332. These rgp120 variants are summarized in

FIGURE 2-1C. The MN-rgp120 gene encoding the same sequence of MN-rgp120 used in the RV144 trial was included as a comparator for bNAb binding studies. MN glycan mutant constructs were expressed in GNTI$^-$ 293 and CHO cells via transient transfection. When expressed in CHO cells, the MN-rgp120 variants exhibited extensive proteolysis, rendering CHO-expressed protein unsuitable for assay. This proteolysis is consistent with previous observations that clade B gp120 sequences are particularly susceptible to digestion by secreted cellular proteases that clip at the GPGR motif within the tip of the V3 crown (43, 152). Due to this extensive proteolysis, we were unable to produce sufficient, un-cleaved CHO-MNrgp120. However, we were able to obtain the highly purified CHO expressed MN-rgp120 immunogen (MN_{GNE}) that was incorporated into the AIDSVAXB/E vaccine of the RV144 trial, to use for comparison.

Cell culture supernatants from transiently transfected GNTI$^-$ cells expressing MN rgp120 with glycan epitope insertions were normalized for gp120 concentration and subjected to Endo H glycosidase digests to confirm size and oligomannose content (**FIGURE 2-4**). All mock-digested rgp120 GNTI$^-$ expressed glycan variants ran as ~110kDa bands. Some MN rgp120 glycan mutants (UCSC 358, 470, 492, and 493) showed a minor amount of proteolysis which resulted in the appearance of a faint ~70kDa (undigested gp120) or ~50kDa (Endo H digested gp120) band on the immunoblots (**FIGURE 2-4**).

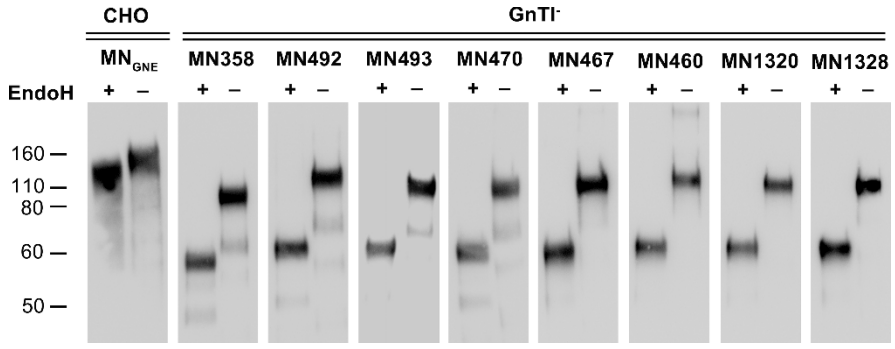

Figure 2-4 Endo H Digest and Immunoblot of MN gp120 Glycan Variants. Wildtype MN rgp120 expressed in CHO GNTI$^-$ cells, or MN glycoform mutants with single, double, or triple glycan additions were expressed in GNTI$^-$ cells via transient transfection. Purified MN_{GNE} or GNTI$^-$ cells supernatants containing expressed rgp120 were immunoprecipitated via a monoclonal antibody to an N-terminal gD tag bound to protein-G coated beads. Immunoprecipiated rgp120 variants were subjected to Endo H or mock digest (digest buffer alone), and analyzed for mobility on 4-12% reducing SDS-PAGE gels. Immunoblots were probed with the mouse monoclonal 34.1 and visualized with goat-anti-mouse HRP-conjugated polyclonal sera.

We used a FIA to screen the panel of eight GNTI$^-$ expressed MN gp120 glycan variants for binding to bNAbs, and the EC50s derived from these results are summarized in **FIGURE 2-5**. Binding to the CD4 binding bNAb VRCO1 was unaffected by the addition of

PNGS. While the bNAbs PGT128 and PGT126 required the addition of both the N301 and N332 PNGS, binding to MN constructs by the10-1074 bNAb was conferred by the addition of the N332 PNGS (**FIGURE 2-5**). The addition of the N289 PNGS appeared to have no effect on binding of any bNAbs tested.

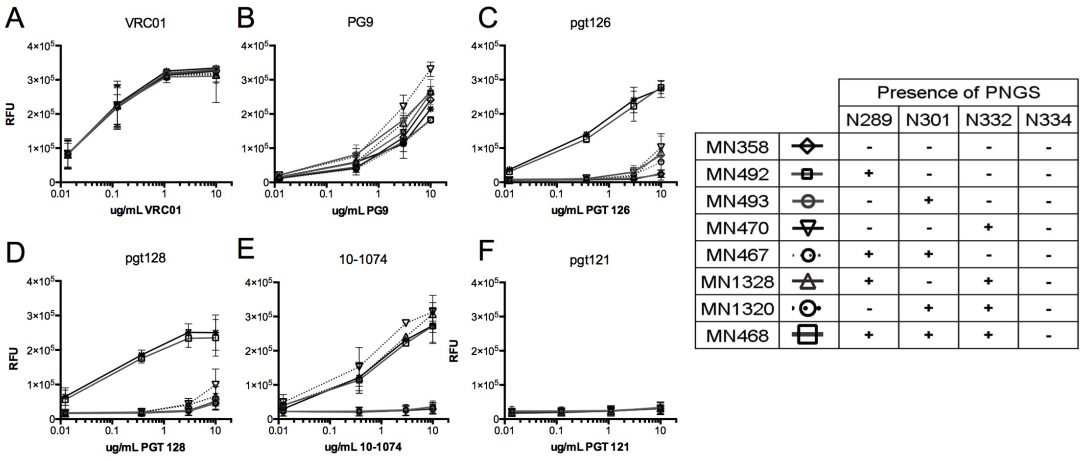

	Presence of PNGS			
	N289	N301	N332	N334
MN358	-	-	-	-
MN492	+	-	-	-
MN493	-	+	-	-
MN470	-	-	+	-
MN467	+	+	-	-
MN1328	+	-	+	-
MN1320	-	+	+	-
MN468	+	+	+	-

Figure 2-5 Screen of MN Glycan Mutant Supernatants for Improvements to bNAb Binding. A FIA was used to identify 293 GNTI$^-$ expressed MN-rgp120 glycan variants exhibiting improved bNAb binding profiles as compared to the wildtype MN sequence expressed in GNTI$^-$ (MN358). Recombinant gp120s were expressed in GNTI$^-$ 293 cells via transient transfection, and transfection supernatants were normalized to contain ~2μg/mL. MN-rgp120 variants were captured onto 96 well black plates using a 1μg/mL concentration of mouse monoclonal antibody to an N-terminal gD tag. Binding curves to the VRCO1 bNAb, which binds a conformation dependent epitope in the CD4 binding site, were used to assay for maintenance of overall secondary and tertiary structure. All screening assays were performed in duplicate, and error bars depict the standard error. MN-rgp120 glycan variants were assayed for improved antigenicity to a panel of glycan dependent bNAbs to be considered for further analysis.

From the original panel of seven MN-rgp120 PNGS mutants assayed, we identified MN1320 GNTI$^-$ as the construct containing the fewest PNGS additions (at N301 and N332) to

confer improved bNAb antigenicity. We investigated the binding the MN1320 glycan variant to an extended panel of bNAbs (**FIGURE 2-6)**. For comparison, we included MN_{GNE}, as well as its GNTI$^-$ 293 produced cognate, MN358. Binding curves of the VRC01 bNAb were not statistically different amongst any of the MN-rgp120 glycan variants, regardless of additional PNGS or cell expression system (**FIGURE 2-6**A). In agreement with previous observations (150), the epitope defined by the PG9 bNAb was poorly represented on the MN_{GNE}, but could be improved with incorporation of oligomannose glycoforms. However, expression of the MN358 and MN1320 in GNTI$^-$ 293 cells was able to introduce weak binding. The PG9 epitope was not significantly affected by the insertion of PNGS in the V3 stem. Insertion of PNGS at N301 and N332 were necessary to introduce high binding to the V3 stem glycan binding bNAbs 10-1074, PGT126, and PGT128. However, CH01 and CH03 and PGT121 bNAbs exhibited no binding to any of the MN-rgp120 variants (**FIGURE 2-6**).

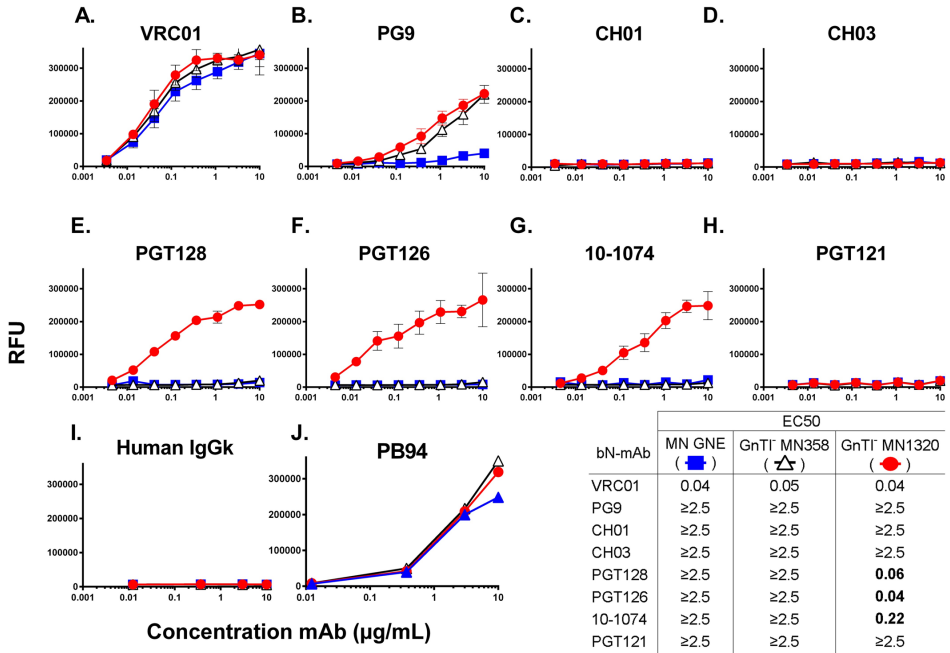

bN-mAb	EC50 MN GNE	EC50 GnTI⁻ MN358	EC50 GnTI⁻ MN1320
VRC01	0.04	0.05	0.04
PG9	≥2.5	≥2.5	≥2.5
CH01	≥2.5	≥2.5	≥2.5
CH03	≥2.5	≥2.5	≥2.5
PGT128	≥2.5	≥2.5	**0.06**
PGT126	≥2.5	≥2.5	**0.04**
10-1074	≥2.5	≥2.5	**0.22**
PGT121	≥2.5	≥2.5	≥2.5
PGT122	≥2.5	≥2.5	≥2.5

Figure 2-6 Binding of MN Glycan Variants to Extended Panel of bNAbs. The MN-rgp120 variants MN358 and MN1320 expressed in GNTI$^-$ cells were compared to MN_{GNE} for improved binding to an array of bNAbs. Recombinant gp120s were expressed in GNTI$^-$ 293 cells via transient transfection. Purified MN_{GNE} or transfection supernatants were normalized to contain 4µg/mL rgp120 and captured using 2µg/mL of mouse monoclonal antibody 34.1, then assayed by FIA for bNAb binding. Results are reported in µg/mL as (EC50), the concentration of antibody required for a half-maximal binding, measured in Relative Fluorescence Units (RFU) on a titration-binding curve. Values are reported as ≥2.5µg/mL if titration curves did not plateau or if mean EC50 was ≥2.5µg/mL. Binding curves to bNAbs were performed in quadruplicate, and error bars indicate the standard error of the mean (SEM). The rp120 constructs exhibiting statistically significant differences in EC50 values ($p<0.05$) from the MN_{GNE} are noted in bold. Human IgGK polyclonal antibody was used as a negative control and purified goat polyclonal antibody raised against rgp120 (PB94) was used as a coating control.

2.5 Discussion

Following the RV144 correlates of protection analysis, various strategies have been pursued to improve the level of protective immunity observed (reviewed in Stephenson et al.) (153, 154). Ongoing clinical trials have been designed to investigate variations on the RV144

protocol, including the use of envelope proteins from different clades or more robust viral vectors (154). Other studies have been designed to maintain the original AIDSVAX/BE gp120 immunogens but alter such variables as number of booster injections, interval between booster injections, or risk-factor of the clinical trial population. However, little effort has been allocated to optimize the original rgp120 immunogens used in the trial. In this paper we use insights gained since the conclusion of the RV144 trial to improve the A244 and MN-rgp120 immunogens of the AIDSVAX B/E vaccine. The improvement of an existing vaccine with a modest record of efficacy offers several advantages. First, this approach builds upon a gp120 vaccine formulation with a demonstrated record of safety. Second, it utilizes existing manufacturing and production knowledge used to create similar molecules for commercial scale. Finally, the incremental improvement of a vaccine efficacy from the 31.2% observed in RV144 to the level of 50% or more thought to be required for product registration (155) presents a less formidable task than the development of an entirely new vaccine concept.

We found that we could significantly improve the antigenic structure of the AIDSVAXB/E immunogens by the addition of no more than two glycosylation sites, and by the modification of glycoform incorporated. The PG9, CH01, and CH03 bNAbs are members of a major class of neutralizing antibodies that binds a glycan-dependent epitope within the V1V2 domain. While $A244_{GNE}$ displayed negligible binding to PG9, CH01, and CH03, the $GNTI^-$ derived A244gp120 constructs (containing both N332 or N334 PNGS) exhibited drastic improvements in antigenicity to these antibodies. The dependence of $GNTI^-$ expression for the $A244_{N332}$ and $A244_{N334}$ gp120s for binding to CH01, CH03, and PG9 antibodies supports a dependence of these antibodies on the mannose-5 glycan epitopes, as opposed to elements associated exclusively with quaternary structure (150, 156). Additionally, the glycan optimized MN construct ($GNTI^-$ expressed MN1320) exhibited improved binding to only the PG9 bNAb in a manner dependent on glycoform but not additional PNGS. However, MN1320 did not

bind CH01 and CH03, regardless of cell expression system. This is likely a consequence of absent amino acid, rather than glycan epitope determinants, that were not covered in the scope of this study.

Both the MN and A244 glycan-optimized constructs additionally displayed statistically significant improved binding to the V3 glycan binding bNAbs PGT128 and PGT126 as compared to their respective RV144 cognates. Surprisingly, GNTI$^-$ expression of both A244- and MN-rgp120 was found to enhance binding to the PGT126 and PGT128 bNAbs for both the N332 or N334 PNGS variants. While these bNAbs have been reported to recognize a mannose-5 glycoform at N301, the N332 glycoform recognized by the PGT128 family is characteristically mannose-8 or mannose-9 (132). One potential explanation for improved binding profile of GNTI$^-$ produced antigens to these bNAbs is that the accessibility of mannose-8/9 epitope at N332 is maintained, if not enhanced, in the context of the neighboring mannose-5 terminal glycans of GNTI$^-$ 293 expressed gp120 proteins. These data indicate that production of gp120 immunogens in GNTI$^-$ 293 cells can improve antigenicity not only to mannose-5 binding bNAbs, but also to mannose-8 or -9 dependent bNAbs (72, 78). The CD4 binding site, recognized by the VRC01 bNAb, is a conserved, glycan-independent epitope. Although the VRC01 antibody does not make contact with any glycan residue (157), we additionally observed a minor but consistent improvement in binding of both the MN and A244 gp120 proteins to VRC01 when expressed in GNTI$^-$ cells. This improvement was not dependent on the addition of any PNGS, and may, like improvement observed for the epitopes bound by the PGT128 family of bNAbs, be a result of improved protein epitope accessibility in the context of smaller, less bulky glycans. The 10-1074 and PGT121 bNAbs displayed a requirement for an N332 based PNGS. This preference was glycoform independent; binding to $A244_{N332}$ could not be improved with GNTI$^-$ expression. Of note,

PGT121 exhibited better binding to the CHO expressed $A244_{N332}$ as compared to $GNTI^-$ expressed $A244_{N332}$; likely due to the preference of PGT121 for complex glycoforms (67).

Since the completion of the RV144 trial, at least five major sites of virus vulnerability on the HIV envelope protein have been reported. Three of these sites within gp120 are defined by the VRC01, PG9, and PGT128 epitopes. Outside of gp120, bNAbs target epitopes within the MPER domain of gp41 and at the interface between gp120 and gp41 subunits (65, 158-161). Recent passive transfer studies with bNAbs indicate that a successful bNAb eliciting vaccine should raise at least two of these bNAb families to contend with expected viral escape mutants (70, 80, 81). Different variations of envelope-protein based immunogens such as trimeric gp140s, gp120s, or scaffolded fragments, have as of yet not been able to consistently elicit broadly neutralizing antibodies to any of these sites (162-164). Additionally, it has not been established how modifications to the RV144 protocol, via glycan optimization, trimerization of gp120, or use of different germline-targeting immunogens will affect the immunogenicity of the non-neutralizing V1V2-binding antibodies correlated with protection in the RV144 trial (46). In this regard small modifications to the gp120 backbone such as those described here may be preferable to avoid major changes in antigenic structure associated with gp140 trimers or scaffolds that may disrupt presentation of critical V1V2 epitopes. Further immunogenicity studies may be required provide insight to these questions.

As the AIDSVAX B/E, in conjunction with the VCP1521 canarypox vector, established a baseline of vaccine efficacy, building upon this immunization protocol offers a logical approach to optimizing a safe and effective vaccine. We propose that evaluating the efficacy of the immunogens described herein represents a systematic, stepwise modification in structure to improve vaccine efficacy. Various promising pathways exist for investigating modifications on a gp120-based vaccine protocol, including strategies that use a DNA prime-gp120 boost (165), more potent vector primes (154), or germline gene targeting strategies

(78). The immunogens using the glycan optimization strategies outlined in this report can be used in follow up studies in conjunction, or in parallel with RV144 follow-up studies investigating the role of A244, MN, or other gp120 immunogens in the elicitation of a protective immune response.

Chapter 3

Development of a Stable MGAT1- CHO Cell Line to Produce Clade C gp120 with Improved Binding to Broadly Neutralizing Antibodies

Foreword

The following chapter contains text and figures from a manuscript of the same name. The work was completed as a collaboration between all authors, Rachel C. Doran, Bin Yu, Meredith Wright, Sara M. O'Rourke, Lu Yin, Jennie M. Richardson, Gabriel Byrne, Kathryn A. Mesa, Phillip W. Berman. RCD, SMO, and PWB contributed to study design. KAM contributed to construct design. RCD and BY performed binding assays. JM performed phylogenetic analysis, and MW and SMO performed cell culture and cell line development. BY and LY designed and performed purification methods. GB provided the MGAT1$^-$ CHO cell line and culture system. All authors contributed to manuscript revision.

3.1 Abstract

The high rate of new HIV infections, particularly in Sub-Saharan Africa, emphasizes the need for a safe and effective vaccine to prevent acquired immunodeficiency syndrome (AIDS). To date, the only HIV vaccine trial that has exhibited protective efficacy in humans was the RV144 study completed in Thailand. The finding that protection correlated with antibodies to gp120 suggested that increasing the quality or magnitude of the antibody response that recognize gp120 might improve the modest yet significant protection (31.2%) achieved with this immunization regimen. However, the large-scale production of rgp120 suitable for clinical trials has been challenging due, in part, to low production yields and difficulties in purification. Moreover, the antigens that are currently available were produced

largely by the same technology used in the early 1990s and fail to incorporate unique carbohydrates presented on HIV virions required for the binding of several major families of broadly neutralizing antibodies (bNAbs). Here we describe the development of a high-yielding CHO cell line expressing rgp120 from a clade C isolate (TZ97008), representative of the predominant circulating HIV subtype in Southern Africa and Southeast Asia. This cell line expresses high levels (1.2g/L) of the TZ97008 rgp120 antigen that incorporates oligomannose glycans required for binding to multiple glycan dependent bNAbs. The resulting rgp120 displays lower of glycoform heterogeneity as compared to rgp120s produced in normal CHO cells. This lowered glycoform heterogeneity results in decreased net charge variation in the resulting protein population, which subsequently facilitated purification by filtration and ion exchange chromatography methods, eliminating the need for expensive custom-made lectin or immunoaffinity columns. The results described herein document the availability of a novel cell line for the large-scale production of clade C gp120 for clinical trials. Finally, the strategy used to produce a TZ97008 gp120 in the MGAT$^-$ CHO cell line can be applied to the production of other candidate HIV vaccines.

3.2 Introduction

While the availability of anti-retroviral drug prevention and treatment strategies has significantly reduced mortality associated with HIV infection, the persistence of HIV transmission remains a major public health concern. This is particularly true for Sub-Saharan Africa and South Asia, where the majority of new infections are predicted to occur over the next decade (166). Thus, an effective vaccine remains an important strategy to stop the spread of HIV. The RV144 HIV vaccine trial completed in Thailand (2003-2009) provided evidence that a prime-boost vaccine could provide modest protection (31%, p=0.04) from HIV

infection (44, 46). The RV144 protocol employed a recombinant canarypox virus vector (VCP1521) to stimulate a cell-mediated immune response, with bivalent recombinant gp120 (rgp120) immunogens (AIDSVAX B/E), to promote an anti-gp120 antibody response (44). Follow-up studies correlating protection in RV144 with non-neutralizing antibodies against gp120, but not cell-mediated immunity, supported a role for the rgp120 immunogen in the observed protection (46). Following the RV144 trial, multiple families of broadly neutralizing antibodies (bNAbs) that bind oligomannose structures were identified, highlighting the importance of specific glycoforms (mannose-5 and mannose-9) on the HIV envelope glycoprotein (Env) (32, 88, 89, 133, 135). However, the rgp120 immunogens used in the RV144 trial were expressed in CHO cells, and therefore enriched for complex, sialic acid containing N-linked glycans that preclude binding glycan dependent bNAbs (40). Together, these observations provided justification for investigation of gp120-based immunogens incorporating the oligomannose (mannose-5 and mannose-8/9) glycoforms found on native virions and targeted by bNAbs (32, 136, 167).

We screened a diverse panel of clade C gp120 protein isolates expressed in HEK 293 cells to identify a clade C envelope protein that displayed above average binding to different bNAbs. To express the clade C rgp120, we employed a novel cell line (MGAT1^{-}CHO), created in our laboratory through the use of the CRISPR/Cas9 gene editing to inactivate the Mannosyl (Alpha-1,3-)-Glycoprotein Beta-1,2-N-Acetylglucosaminyltransferase (MGAT1) gene (168). The resulting cell line expresses rgp120 proteins containing N-linked mannose-5 or earlier intermediate glycoforms that are recognized by various families of glycan dependent bNAbs. This strategy is advantageous to previous approaches to manipulate glycosylation on rgp120 (i.e. expression in HEK 293 GNTI^{-} cells, or with the use of glycosidase inhibitors such as kifunensine) in that it can be used as part of a biopharmaceutical production system amenable to current Good Manufacturing Practices

(cGMP). Additionally, expression of rgp120 in the MGAT1$^-$CHO cell expression system reduces heterogeneity in net charge as compared to CHO-expressed rgp120. Such homogeneity of MGAT1$^-$CHO derived rgp120s facilitated the development of an ion-exchange based purification method that obviated the need for custom affinity-chromatography resins previously used for purification of rgp120 immunogens (103). Here we compare the properties of a clade C rgp120, TZ97008, produced in normal CHO cells, resembling those used to produce gp120 for previous (44, 129, 169) and current clinical trials (170), with TZ97008-rgp120 produced in the MGAT1$^-$CHO cell line. Our results demonstrate that the MGAT1$^-$CHO expression system provides a cost-effective approach for the production of the clade C TZ97008 rgp120 displaying oligomannose glycoforms that both simplifies down-stream purification and improves the binding of bNAbs.

3.3 Materials and Methods

Clade C gp120 screening

The panel of clade C gp120s was assayed for bNAb binding by Fluoresence ImmunoAssay (FIA). Antigen was diluted to 2μg/mL in PBS and coated onto 96 well black-microtiter plates (Greiner, Bio-One, USA) at 4°C overnight. Plates were blocked in PBS with 1% BSA for two hours. Three-fold dilutions of antibody were added, followed by a 1:3,000 dilution of Alexa Fluor 488 conjugated goat-anti-human polyclonal secondary (Jackson ImmunoResearch Laboratories, West Grove, PA). Incubations were performed for 90 min (23°C) in blocking buffer and preceded by a 4x wash in PBST unless otherwise noted. The panel of 10 clade C, gD tagged envelope proteins was expressed in HEK 293 cells as described previously (110). Recombinant gp140 from the 1086 strain of HIV-1, contributed by Drs. Barton F. Haynes and Hua-Xin Liao, was obtained from NIH AIDS Reagent Program,

Division of AIDS, NIAID, NIH (47, 171). The TV1 gp120 expressed in 293 HEK cells was obtained from Immune Tech Corporation (New York, NY). The PG9, PGT121, PGT128, and VRC01 bNAbs were produced in our laboratory in 293 HEK cells based on published sequences. The 10-1074 bNAb was obtained through the NIH AIDS Reagent Program, Division of AIDS, NIAID.

Area under the curve (AUC) calculations were performed using GraphPad Prism version 6.0 for Mac, GraphPad Software, La Jolla California USA, www.graphpad.com. To obtain a relative ranking of overall bNAb antigenicity, individual area under the curve (AUC) analyses were taken of individual gp120 binding curves to each of the 5 bNAbs, and the sum of these AUC values for each gp120 antigen was ranked. Rank scores from 1-12 were awarded to the 12 envelope antigens based on calculated AUC values, with a rank score of one awarded to the envelope protein exhibiting the poorest binding (lowest calculated AUC) to a bNAb, to a rank score of 12 awarded to envelope antigen exhibiting the highest binding (highest calculated AUC). The AUC rank value scores were summed, and the subsequent values were used to determine relative gp120 antigenicity and to select a gp120 sequence for further development. A phylogenetic analysis of the clade C gp120 and reference sequences was constructed with RAxML using the maximum likelihood method and rapid bootstrapping (172). Sequences were pre-aligned with ClustalW (173). Branch lengths are drawn to scale and visualized using RainbowTree (174).

Development of a MGAT1$^-$ CHO cell line to express TZ97008-rgp120

Suspension adapted CHO-S cells were obtained from Thermo Fisher (Thermo Fisher, Life Technologies, Carlsbad, CA). The TZ97008 MGAT1$^-$ CHO cell line was developed following a protocol described previously (O'Rourke et al., 2018, in press). Cells were transfected with a modified pCDNA3.1 expression vector (175) encoding TZ97008 and

the gene encoding resistance to Geneticin. The gp120 transcription unit included an N-terminal purification tag from Herpes Simplex Virus glycoprotein D (gD) as described previously (103). The cells were transfected using an STX electroporation device (MaxCyte Inc., Gaithersburg, MD) according to manufacturer's protocols. Following transfection, cells were serially diluted from 500-5,000 cells/mL in semi-solid CHO-Growth A media with 1XHT and L-glutamine (Molecular Devices, Sunnyvale, CA), 500μg/ml G418, and 10μg/ml Alexa Fluor 488 conjugated goat anti-gp120 polyclonal antibodies reactive with clade B, AE, and C rgp120s as described previously (O'Rourke et al., 2018, in press). Colonies expressing rgp120 were selected on basis of fluorescence and default selection parameters using the ClonePix2 (Molecular Devices, Sunnyvale, CA).

Cell culture in shake flasks was performed in BalanCD® CHO Growth A medium (Irvine Scientific, Santa Ana, CA) supplemented with 1XHT (Corning, Corning NY), 10% Proyield® Cotton seed protein (DOMO, Netherlands), and 0.25mM glutaMAX (Sigma-Aldrich Chemicals, St. Louis, MO). Cell viability was assessed via with trypan blue exclusion and cell counts and viability were monitored using the TC20™ automated cell counter (BioRad, Hercules, CA). The concentration of rgp120 in growth conditioned cell culture supernatant was quantitated using a capture ELISA. Briefly, rgp120 in cell culture supernatant was captured on 96 well Maxisorp plates via a mouse monoclonal antibody (34.1) to an N-terminal purification tag (41), incubated with a 2μg/mL dilution of purified goat-anti-rgp120 polyclonal antibody, and detected with a 1:3,000 dilution of bovine-anti-goat HRP conjugated polyclonal and OPD substrate. Reactions were stopped with 3M sulfuric acid. Dilutions were performed in blocking buffer (1% BSA in PBS) and all assays were performed in duplicate. For comparison, CHO derived TZ97008-rgp120 was expressed via transient transfection using a method as previously described (176).

Purification of TZ97008 rgp120 proteins

Supernatants containing MGAT1$^-$ CHO expressed TZ97008 rgp120 were concentrated and buffer exchanged to 10mM TRIS, pH=8.0 buffer (Vivaflow 200 Sartorius, Göttingen, Germany). Eluent was monitored at the 280nm wavelength using an Akta purifier (GE healthcare Chicago, IL). Concentrated and buffer-exchanged MGAT1$^-$ CHO supernatant containing TZ97008 rgp120 was passed through a 5cm anion exchange (HiTrap Q FF column, GE Healthcare, Chicago, IL) and flow through fractions containing gp120 were collected. These fractions were further purified via size exclusion chromatography using a 60cm Highload Superdex 200pg column (GE Healthcare) in pH 8 TBS (Tris-buffered Saline) buffer. CHO-S expressed TZ97008 rgp120 was purified by affinity chromatography against the N-terminal gD tag, followed by size exclusion chromatography, as previously described (9).

Protein concentration and recovery calculations

Purified rgp120 from the relevant cell expression system was used as a standard to determine rgp120 concentration in cell culture supernatants, column flow-through, and eluates associated with each individual purification step. Protein was quantified using a concentration dependent analysis protocol with the Biacore X100+ software V2.0.1 (GE Health Sciences). The conformation-dependent but glycan-independent bNAb VRC01 was coupled to the chip via an anti-human Fc polyclonal and used as a capture mAb for concentration analysis. The concentration of either anion exchange- or immune-affinity chromatography purified TZ97008 rgp120 from MGAT1$^-$ CHO cell line was confirmed by BCA (Thermo Fisher, Waltham, MA).

Physical and antigenic analysis of purified rgp120

SDS-PAGE, isoelectric focusing (IEF), and endoglycosidase digestions

SDS-PAGE of purified rgp120 proteins was performed as previously described (177). Purified protein samples were run on a Bis-Tris 4-12% gradient gel (Invitrogen, Carlsbad, CA) and stained with SimplyBlue SafeStain (Invitrogen, Carlsbad, CA). Endoglycosidase H (Endo H) and PNGase F digest kits were purchased from New England Biolabs (Ipswich, Massachusetts). Briefly, 200μg of rgp120 was reduced with provided denaturation buffer and boiled for 10 min at 100 °C. Denatured rgp120 was then mixed with reaction buffer and 5,000 units of enzyme and digests were incubated for 24h at 37°C. TZ97008-rgp120 from CHO and MGAT1$^-$ CHO expression systems, were purified by affinity or ion exchange purification methods, respectively, and analyzed by two-dimensional isoelectric focusing gel analysis as previously described (40). Proteins were run on ReadyStrip^{TM} IPG strips (11cm, pH 3-10, Bio-Rad, Hercules, CA), and resolved using a Protean® IEF Cell (Bio-Rad, Hercules, CA) to establish the horizontal dimension based on the protein isoelectric focusing point. The vertical dimension, determined by protein molecular weight and shape, was established by running strips along 4-15% polyacrylamide tris-glycine gels (Bio-Rad, Hercules, CA). Proteins were stained with SimplyBlue SafeStain (Invitrogen, Carlsbad, CA). Amyloglucosidase from *Aspergillus niger (97 kDa, pI=3.6)* and/or carbonic anhydrase isozyme II (29kDa, pI=5.9) from bovine erythrocytes (Sigma-Aldrich Chemicals, St. Louis, MO) were included as internal pI standards.

Reverse Phase High Performance Liquid Chromatography (RP-HPLC)

RP-HPLC was performed using a Shimazu 10A VP serial HPLC system (Columbia, Maryland), and run on a 150mm*2.1mm Betabasic C18 column (Thermo Scientific, Waltham,

MA). Solutions were run at a 1% per minute (5% acetonitrile to 60% acetonitrile in water) gradient, and eluent was monitored at UV 214nm.

Antibody binding assays

Protein-antibody binding kinetics were assessed via surface plasmon resonance (SPR) using the Biacore X100+ (GE Healthcare, Chicago, IL). Standard amine coupling methods were used to couple anti-human Fc to a CM5 sensor chip. Assayed bNAbs were injected until 100-150 RU signal increase was achieved. After a base RU signal increase was achieved, serial dilutions from 0.25 to 80nM of TZ97008-rgp120 in HBS-EP buffer were injected, and ligand capture protocols (three min at 30 µL/min followed by 10 min dissociation) were used to determine kinetics. Channels were regenerated with 3M $MgCl_2$. Biacore evaluation software was used to subtract blank injection references and determine K_d measurements (V 2.0.1, GE Health Sciences). Fluorescence immunoassays were performed as capture fluorescence immunoassay as described previously (176).

3.4 Results

Screening clade C HIV envelope proteins

Previous studies have indicated that binding of gp120s to different bNAbs varies considerably as a result of primary sequence, glycan occupancy (how often a glycan is added to an existing N-X-S/T motif), and higher order structure (178, 179). Therefore, we assembled a panel of clade C envelope proteins to identify a clade C gp120 able to bind multiple families of bNAbs. The panel included rgp120s of diverse geographical origins such as Sub-Saharan Africa, China, and India (110), as well as the TV1-rgp120 and 1086-rgp140 sequences similar to those currently being tested in RV144 follow-up studies in South Africa (HVTN702) (180).

A fluorescence immunoassay (FIA) was used to compare gp120 binding to four diverse and genetically distinct families of bNAbs (PG9, PGT128, PGT121, and VRCO1). Area under the curve (AUC) value scores were derived from FIA binding curves and used to rank the magnitude and breadth of bNAb binding for the panel of envelope proteins (see Materials and Methods). The AUC rank value scores were summed. From these sums, the TZ97008-rgp120 was identified to possess the highest overall breadth and magnitude of binding to assayed bNAbs (**FIGURE 3-1**).

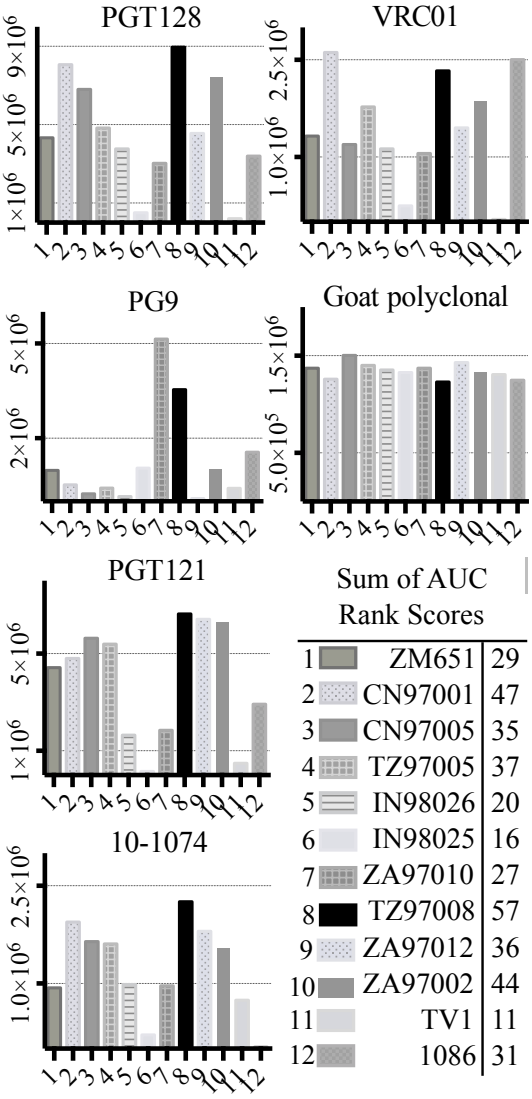

Figure 3-1 Screen of bNAb binding to clade C rgp120 proteins of diverse geographic origins. Clade C gp120 proteins expressed in 293 HEK cells were compared by FIA for binding to a panel of five prototypic bNAbs. All rgp120 proteins except the TV1 and 1086 are appended with an N-terminal gD purification tag as described previously (110). To obtain a relative ranking of overall bNAb antigenicity, individual Area under the Curve (AUC) analyses were calculated for individual envelope protein binding curves as described Materials and Methods. The AUC rank scores for all of the 5 bNAbs assayed were summed, and the cumulative AUC score of each envelope protein antigen is shown in in the included table.

The TZ97008 rgp120 exhibited the best binding to the PGT128 bNAb that binds a glycan epitope in the stem of the V3 domain (132). Additionally, the TZ97008 rgp120 was amongst the highest binding envelope proteins to the PG9, VRC01, and PGT121 bNAbs, that bind epitopes in the V1V2, CD4 binding-site, and V3 domains, respectively (67, 88, 149).

Development of the 3E5 cell line to express TZ97008 rgp120

Based on the bNAb binding results, we pursued development of a stable cell line expressing TZ97008-rgp120. To this end, we utilized a cell-line development method developed by O'Rourke et al (2018)(181). The MGAT1$^-$ CHO cell line was used as a parental cell line, as it possesses a mutation in the gene encoding Mannosyl (Alpha-1,3-)-Glycoprotein Beta-1,2-N-Acetylglucosaminyltransferase (Mgat1) and therefore incorporates predominantly mannose-5 or earlier (i.e. mannose-8/9) glycoforms (168). Such oligomannose glycoforms have been found to contribute to gp120 recognition by different families of bNAbs (65, 88). MGAT1$^-$ CHO cells were transfected via electroporation with a pCDNA3.1 expression vector containing the TZ97008-rgp120 gene. A total of 1.5 x 10^5 transfected cells was serially diluted and grown on semi-solid media containing G418 and anti-gp120 polyclonal antibodies labeled with Alexa Fluor 488 (see Materials and Methods). After 14 days, white light and fluorescent images were acquired using the ClonePix2 (**FIGURE 3-2**A).

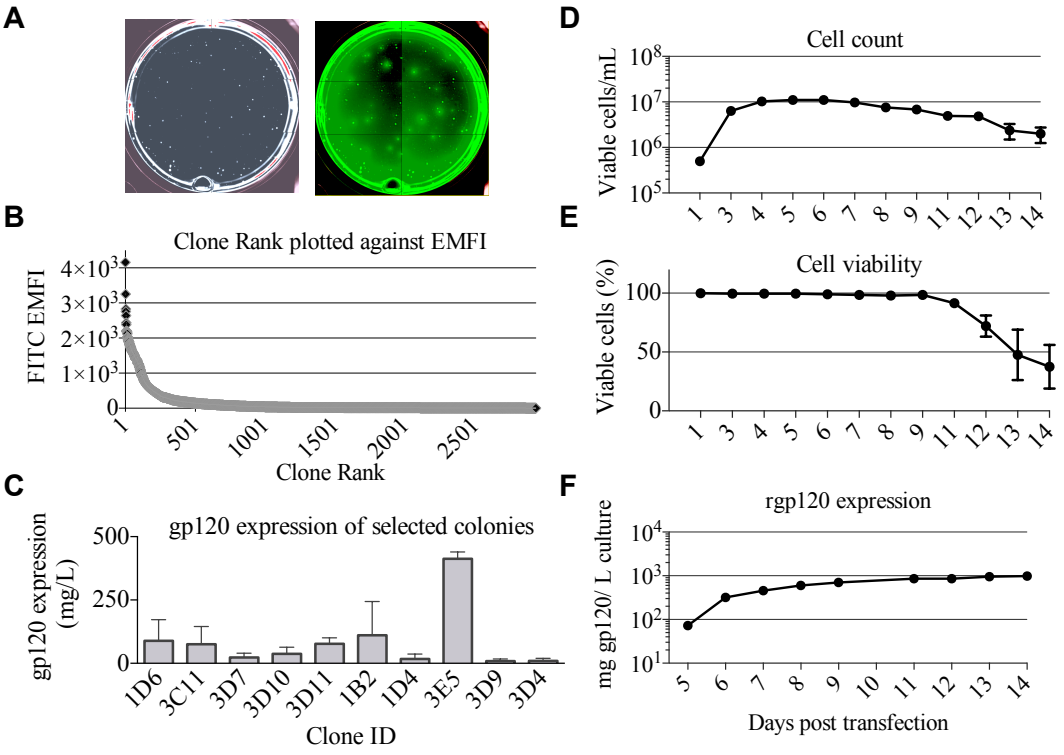

Figure 3-2 Colony selection of MGAT1 transfected cells. (A) 10,000 colonies of cells transfected with a plasmid encoding TZ97008-rgp120 were analyzed for rgp120 expression using the ClonePix 2 robot. The number of colonies was visualized under white light, and the relative magnitude of gp120 expression was determined by size and intensity of halos visualized under fluorescent light (470nm excitation and 535nm emission wavelength filters). (**B**) Colonies were ranked by exterior mean fluorescent intensity (EMFI) as readout of rgp120 expression and EMFI was plotted as a function of clone rank. **(C)** Following growth and selection, the 10 best growing clones were grown in six-day batch culture and assayed for gp120 expression by quantitative ELISA. Binding curves were compared to a standard curve of known protein concentration. From the expression screen, the highest expressing clone (3E5) was expanded for an 11-day fed-batch fermentation run. Cells were monitored for **(D)** cell count, **(E)** viability, and **(F)** rgp120 expression. Assays were performed in duplicate and error bars indicate Standard Deviation (SD).

Acquired images were used to screen the ~7,000 colonies and identify colonies actively secreting rgp120. The size and intensity of the fluorescent halo resulting from immunoprecipitation by Alexa Fluor 488 conjugated anti-gp120 polyclonal antibody around rgp120 secreting cells was measured as exterior mean fluorescence intensity (EMFI), and used in conjunction with additional default ClonePix2 selection parameters to select colonies for further development. **FIGURE 3-2**B depicts the relative EMFI of imaged colonies. A total of 384 colonies were selected and expanded into 96 well cultures. As colonies were passaged, cell growth, as determined by well confluence at time of passage, and rgp120 expression, as determined by ELISA, were monitored. Following four passages, the 10 clones exhibiting consistent growth and gp120 expression were quantified for rgp120 expression to select for the highest producing cell line, designated 3E5 (**FIGURE 3-2**C). From the expression screen, the highest expressing clone (3E5) was expanded to a 125 mL shake flask and monitored for cell count and viability over a 14-day fermentation process (**FIGURE 3-2**D, E). Growth conditioned cell culture medium was analyzed by ELISA for each clone and expression levels as high as 1200mg/L expression were obtained from fed batch cultures of the TZ97008 MGAT1$^-$ CHO 3E5 line (**FIGURE 3-2**F). The 3E5 clone was additionally entered into a 63-day stability assay, over which cells were passaged for an additional 30 passages (**FIGURE 3-3**A) and observed to maintain greater than 98% viability (**FIGURE 3-3**B).

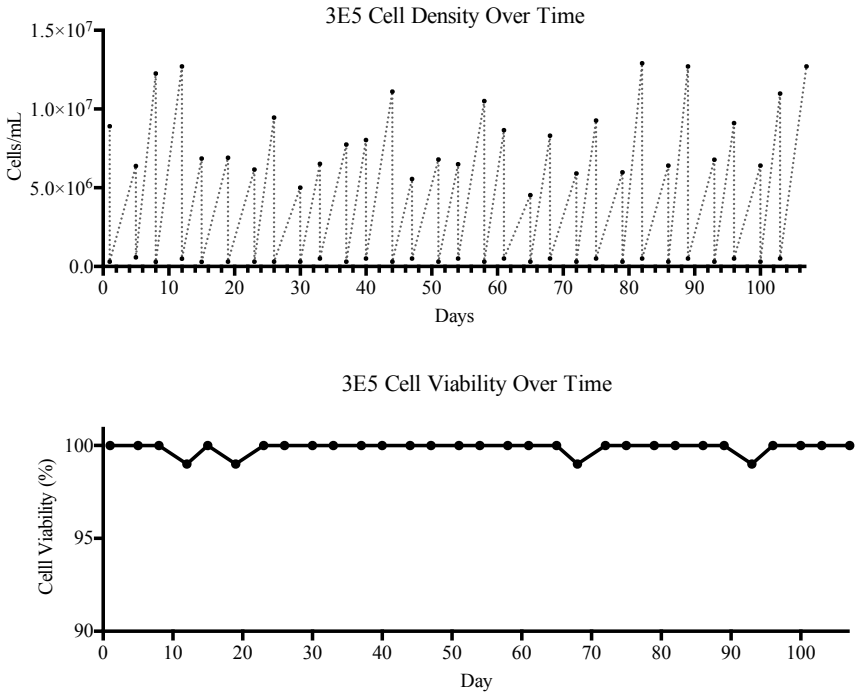

Figure 3-3 Cell viability over time. A 106-day study designed to determine cell line stability and viability over time was carried out. The TZ97008 expressing 3E5 MGAT1$^-$ CHO cell line was entered into a viability stability assay and carried for a total of 31 passages. The 3E5 cell line culture was adapted to suspension culture with a fractioned (300μg/mL) concentration G418 in BalanCD® CHO Growth A medium and incubated at 37°C. (**A**) Cell density and **(B**) cell viability was measured using Trypan Blue staining before cultures were diluted down to ~3E5 cell/mL. Following dilution, cells were allowed to grow for 3-4 days before cell counts and viability were measured and cultures were again diluted.

Development of a conventional purification process for TZ97008 rgp120

A high degree of net charge heterogeneity present on envelope proteins produced in CHO cell previously necessitated gp120 purification schemes to employ immunoaffinity or lectin affinity chromatography (103, 170, 182-185). To eliminate complications introduced by such methods and to efficiently process the large amounts of protein, we developed a purification process that does not rely on lectin or immunoaffinity based resins. While the

negatively charged sialic-acid incorporated into gp120 produced in CHO cell lines results in a product displaying a broad spectrum of isoelectric points (pI 3.5-7.5) (40), rgp120 expressed in cell lines incorporating exclusively oligomannose N-linked glycans and exhibit pIs of a smaller range (40). The lower degree of net charge heterogeneity on TZ97008-rgp120s produced in the 3E5 cell line permitted the use of ion exchange and size exclusion chromatography. The use of ion exchange and size exclusion chromatography additionally offers a cost-effective purification alternative that is amenable to optimization for high-throughput systems. For this method, growth conditioned cell culture medium from the 3E5 cell line was buffer exchanged to pH=8.0 in a low salt solution and passed through Hitrap Q FF anion exchange column. Using this strategy, CHO host cell proteins were mostly retained on the column, while rgp120 was present in the flow through fractions. The flow through containing rgp120 was then passed over a size exclusion column for final purification.

Size exclusion chromatographs of MGAT1$^-$ CHO expressed TZ97008-rgp12 purified by either the affinity or anion exchange methods are compared in **FIGURE 3-4**A. Supernatant, flow through and elution of affinity column and anion exchange column, and final TZ97008 rgp120 products from both methods were run on SDS-PAGE in **FIGURE 3-4**B. Together, the chromatographs and the SDS-PAGE gel demonstrate that the TZ97008-rgp120 can be isolated to a clean, homogenous protein by either affinity purification or anion exchange methods. Although some TZ97008-rgp120 bound to the QFF anion exchange column (**FIGURE 3-4**B, lane 10), the majority of the rgp120 could be found in the flow through (**FIGURE 3-4**B, lane 11). The yields of each purification step are summarized in **FIGURE 3-5**. In summary, roughly 74% of the original protein was recovered in the flow through of anion exchange chromatography, and 50% final recovery was reached after size exclusion chromatography. From a starting volume of 200mL of fed-batch 3E5 fermentation

supernatant containing an estimated 1.2mg/mL, 120mg of MGAT1^{-} CHO TZ97008 rgp120 was recovered for a scaled yield of 600mg rgp120/L of culture using the anion exchange method. While the anion exchange chromatography method exhibits a comparatively lower recovery than the traditional affinity chromatography approach (74% vs 93%), it offers distinct, technical advantages. First, this method removes the potentially denaturing low pH elution step used in previous affinity chromatography processes. Additionally, the use of an ion exchange column removes additional cost and documentation associated with production and maintenance of affinity chromatography resins under cGMP standards.

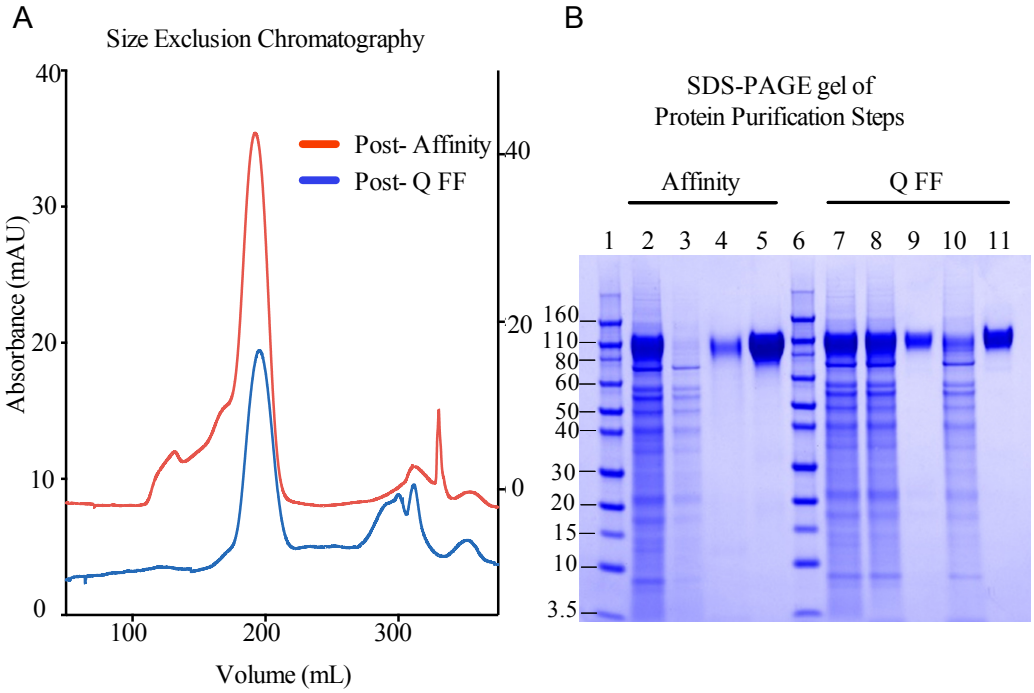

Figure 3-4 Comparison of immunoaffinity and ion-exchange chromatography purification strategies for 3E5 MGAT1$^-$ CHO expressed TZ97008-rgp120. Two methods were compared for the purification of 3E5 MGAT1$^-$ CHO expressed TZ97008-rgp120. The first method reconstructed the method used to purify the rgp120 immunogens used in the RV144 clinical trial (44) and incorporated an affinity chromatography column that purified gp120 via an N-terminal gD tag as previously described (103). Briefly, gp120 molecules retained on the affinity chromatography column were selectively eluted at low pH. Following neutralization and buffer exchange**.** The second method incorporated anion exchange chromatography (QFF) as described in Materials and Methods. Briefly, growth conditioned cell culture medium was concentrated and buffer exchanged. The resulting solution was passed through a HiTrap QFF column, wherein gp120 molecules flowed through the column with a large proportion of CHO proteins were retained on the column. Size exclusion chromatography (SEC) was used to further purify protein products from Affinity and QFF methods. (**A**) A chromatograph depicts the SEC elution profiles of the CHO or 3E5 derived TZ97008-rgp120 proteins initially purified by the Affinity method (red) and the QFF method, respectively (blue). The left Y-axis corresponds to the Post-Q FF chromatograph, and the right Y-axis corresponds to the Post- Affinity chromatograph. **(B)** The products resulting from the Affinity (lanes 2-5) and QFF (lanes 7-11) purification methods were compared by SDS-PAGE. Samples from each step of the purification were treated with SDS-PAGE sample buffer and loaded onto 4-12% Bis-tris gels. Starting cell culture supernatants from the 3E5 MGAT1$^-$ CHO fermentation cultures are shown (lanes 2 and 7). Flow through and eluate fractions of CHO culture supernatants after passage through immunoaffinity column (lanes 3

and 4, respectively) and the main rgp120 peak from the SEC column (lane 5) are shown. Flow through fractions of 3E5 MGAT1$^-$ CHO cultures following buffer exchange and the QFF column flow throughs are shown in lanes 8 and 9, respectively. Lane 10 and 11 indicate the proteins retained on the QFF column that eluted with salt solutions (predominantly CHO host cell proteins), and the major rgp120 containing fraction of SEC, respectively. Molecular weight standards are included (lanes 1 and 6).

	Pre-purification		STEP 1 yield		STEP 2 yield	Final yield
	Starting	Buffer Exchange	FT	Eluate	Eluate	
Affinity /Size Exclusion Chromatography	2650 ug (100%)	N/A	Affinity Chromatography		Size Exclusion Chromatography	**70%**
			25 ug (1%)	2460 (93%)	1848 (75%)	
Q FF/ Size Exclusion Chromatography	3350 ug (100%)	3350 ug (100%)	Q FF (anion exchange) Chromatography		Size Exclusion Chromatography	**50%**
			2496 ug (74%)	760 ug (23%)	1677 (67%)	

Figure 3-5 Comparison of methods for the purification of TZ97008-rgp120. The efficiency of the recovery process for the purification of TZ97008-rgp120 produced in CHO-S cells and MGAT1- CHO cells were compared. TZ97008 produced in CHO-S cells l was purified in two steps; an immunoaffinity chromatography column which captured rgp120 via the N-terminal gD tag (41), followed by size exclusion chromatography (top row). MGAT1$^-$ CHO expressed gp120 was purified using an anion exchange chromatography column (QFF), followed by a size exclusion chromatography (bottom row). Surface plasmon resonance (Biacore X100+) was used to determine the concentrations of gp120 before and after each individual purification step. Yields were calculated by dividing protein recovered after each purification step to starting supernatant. Protein not accounted for in the flow through (FT) or eluate calculations was lost during wash steps.

Biophysical characterization of purified TZ90008-rgp120

Both CHO and MGAT1$^-$ CHO expressed TZ97008-rgp120 preparations could be purified to >95% purity as measured by scanning densitometry of SDS-PAGE gels. However, the differences resulting from cell expression system that facilitated the different purification schemes became apparent upon analysis of purified rgp120 by isoelectric focusing. Whereas

purified rgp120 expressed in the MGAT1$^-$ CHO cell line resulted in a bulk protein product of pI ~8.4 (**FIGURE 3-6**A, right), purified TZ97008 rgp120 expressed in the CHO line displayed 25 different gp120 isoforms with PIs spanning pH 3.5 to 6 (**FIGURE 3-6**A, left). When analyzed by RP-HPLC, both CHO and MGAT1$^-$ CHO purified preparations ran as a single peak, with the MGAT1$^-$ CHO derived protein preparation displaying a slightly more symmetrical peak and smaller trailing shoulder as compared to the CHO derived preparation (**FIGURE 3-6**B). CHO and MGAT expressed proteins both exhibited absorbance peaks starting at 41 min with a minor shoulder eluting at 43min. However, the CHO expressed gp120 exhibited a wider peak base. Purified rgp120 was assessed for the presence of oligomannose carbohydrate by sensitivity to degradation by the glycosidase Endo H that uniquely degrades oligomannose terminal N-linked glycans. While CHO derived rgp120 remained largely resistant to Endo H digest, the MGAT1$^-$ CHO expressed TZ97008 rgp120 was sensitive to Endo H digest, running as a ~60kDa band post-digest digest (**FIGURE 3-6**C). Additionally, unreduced CHO-S derived TZ97008 rgp120 displayed a faint band at ~200kDa (**FIGURE 3-6**C), indicative of a small dimerized fraction not present in purified 3E5 MGAT1$^-$ CHO derived rgp120 samples. These data indicate that when expressed in a MGAT1$^-$ CHO cell line and purified with ion exchange/size exclusion chromatography, TZ97008 rgp120 displayed increased size and glycoform homogeneity and decreased aggregation as compared to when expressed in a normal CHO-S cell line and purified by affinity and size exclusion chromatography.

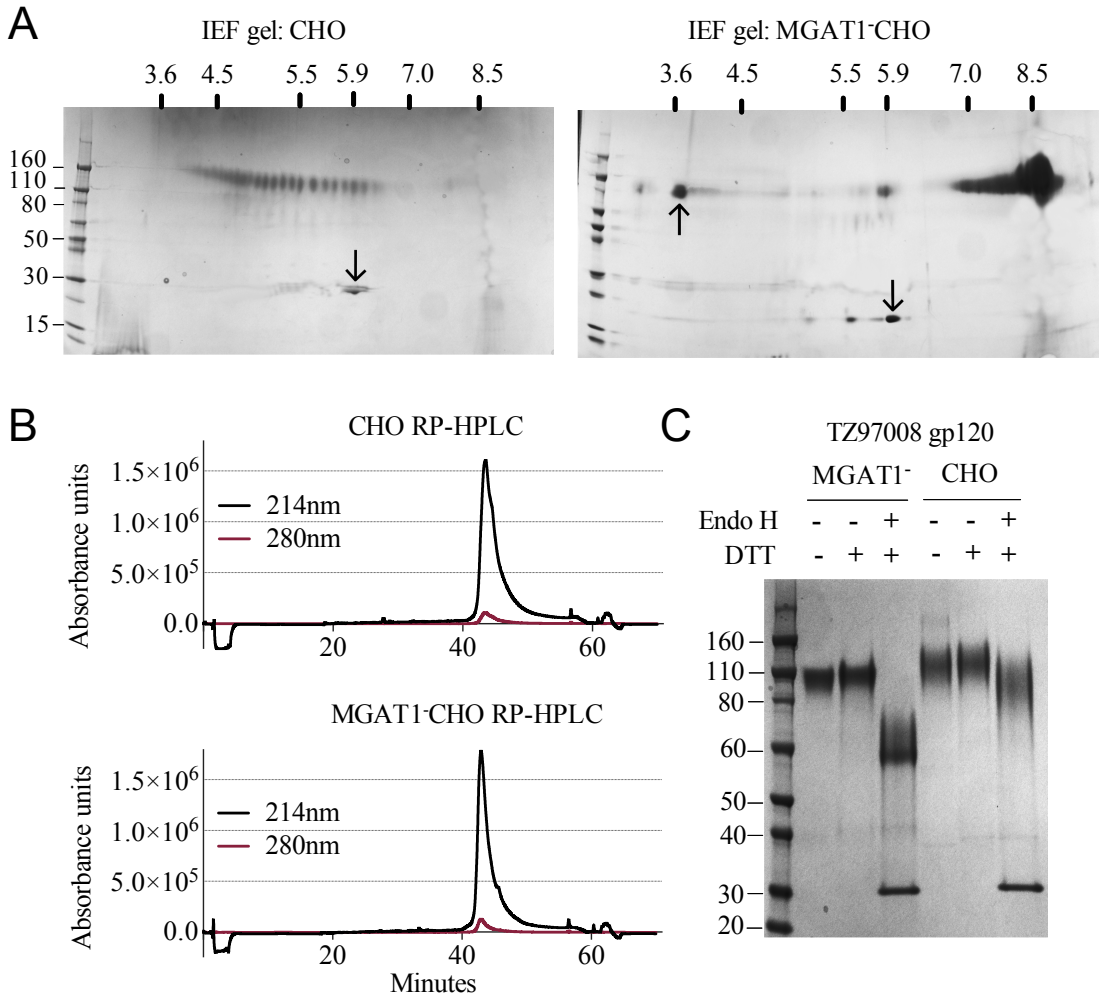

Figure 3-6 Characterization of purified TZ97008 rgp120 proteins by isoelectric focusing, reverse phase HPLC and endoglycosidase digestion. Purified protein preparations of TZ97008 expressed in CHO-S and MGAT1- CHO and cell lines were analyzed by a variety of methods. **(A)**, 2-dimensional isoelectric focusing gels of TZ97008-rgp120 purified from CHO-S and MGAT1$^-$ CHO cells (A left and right, respectively). Protein PI standards included the Amyloglucosidase from *Aspergillus niger (97kDa, pI=3.6, upward pointing arrow)* and/or bovine carbonic anhydrase isozyme II (29kDa, pI=5.9, downward pointing arrow) are indicated. A protein molecular weight ladder is included on the left-hand side of each panel. **(B)** Purified TZ97008 produced in CHO-S or MGAT1$^-$ CHO cells were assayed for purity by RP-HPLC. Absorbances were measured at 214nm (solid line) and 280nm (dashed line) wavelengths **(C)** Purified TZ97008 rgp120 proteins expressed in both cell lines were run on an SDS-PAGE gel to assess for purity, proteolytic degradation (clipping), the presence of dimers, and heterogeneity in N-linked glycosylation. Purified

TZ97008 rgp120 proteins expressed by the CHO or MGAT1$^-$ CHO 3E5 cell lines were run as reduced and non-reduced samples. Proteins were additionally assayed for Endo H sensitivity to evaluate for presence of simple oligo-mannose terminal glycans, or complex sialic acid containing carbohydrates. For Endo H digestion purified proteins were reduced and subject to Endo H digest overnight at 37°C (Panel C, lanes 3 and 6). The Endo H enzyme appears as a 30kDa band present in lanes 3 and 6.

bNAb binding to TZ97008-rgp120

TZ97008-rgp120 expressed in the MGAT1$^-$ CHO or CHO cell lines was assayed for bNAb binding by SPR and fluorescence immunoassay. SPR indicated that production of rgp120 in MGAT1$^-$ CHO cells improved TZ97008 binding to the PG9, PGT128, PGT121, and VRC01 bNAbs. The production of TZ97008 rgp120 in the MGAT1$^-$ CHO line provided almost four-fold improvement in K_d of PGT128 binding, six-fold improvement in K_d of PG9 binding, and over ten-fold improvement in K_d of VRC01 binding (ERROR! REFERENCE SOURCE NOT FOUND.). While the VRC01 antibody does not directly contact a glycan, improved binding may be partially explained by better accessibility of protein epitopes in the context of smaller glycoforms. Both the PGT121 and 10-1074 bNAbs bind glycans (based at N332 or N334) at the stem of the V3 domain and derive from the same inferred IgVH germ-line genes (67, 135). The 10-1074 bNAb exhibited binding to both CHO-S and MGAT1$^-$ CHO produced rgp120s. However, PGT121 improved binding to CHO derived gp120 as compared to MGAT1$^-$ CHO derived rgp120 (ERROR! REFERENCE SOURCE NOT FOUND.).

bNAb	Ka*E4 (association)		Kd*E-4 (dissociation)		Chi2		Kd*E-9(nM)	
	MGAT	CHO	MGAT	CHO	MGAT	CHO	**MGAT**	**CHO**
PG9	6.51	0.66	11.42	18.95	0.47	0.169	**17.56**	**288**
PGT128	6.59	1.92	1.73	3.73	0.71	0.339	**2.62**	**19.44**
10-1074	1.6	2.01	6.46	8.68	0.55	0.32	**40.51**	**43.16**
VRC01	1.59	0.97	6.64	2.8	0.193	0.041	**4.18**	**28.84**
PGT121	0.76	1.15	5.04	3.25	0.16	0.148	**65.99**	**28.22**

Table 3-1 Comparative bNAb binding affinities for TZ97008-rgp120 produced in CHO-S or MGAT1$^-$ CHO cells. Purified rgp120 was assayed for binding to a panel of panel of prototypic bNAbs that target three distinct sites of virus vulnerability of the gp120 envelope protein. These include antibodies to glycan dependent epitopes in the V2 domain glycan (PG9) or the stem of the V3 domain (PGT128, PGT121, and 10-1074), and a glycan independent epitope proximal to the CD4 binding site (VRC01). bNAbs were captured onto a CM5 sensor chip via a covalently immobilized anti-human F_C antibody. Serial dilutions of TZ97008 expressed in MGAT1$^-$ CHO or CHO cell lines were injected in HBS-EP buffer, at a flow rate of 30uL/min. Average measurements from blank injection were subtracted from analyte response measurements, and data was rejected if Chi2 values exceeded 1.0, or R_{max} values exceeded 100.

bNAB binding to the TZ97008 gp120 was also assayed by FIA. The results observed for SPR could be mostly recapitulated for fluorescence immunoassay (**FIGURE 3-7**). A small discrepancy was observed in the PGT121 binding, for which FIA indicated improved MGAT1$^-$ CHO expressed gp120 binding, while Biacore results showed improved affinity for CHO derived gp120. However, both methods showed that PGT121 is able to bind to TZ97008-rgp120. Overall, the MGAT1$^-$ CHO expressed rgp120 displayed better bNAb binding than CHO derived TZ9708 gp120 to three different families of bNAbs, indicating improved antigenic structure of neutralization sensitive epitopes to at least three different regions of the envelope protein.

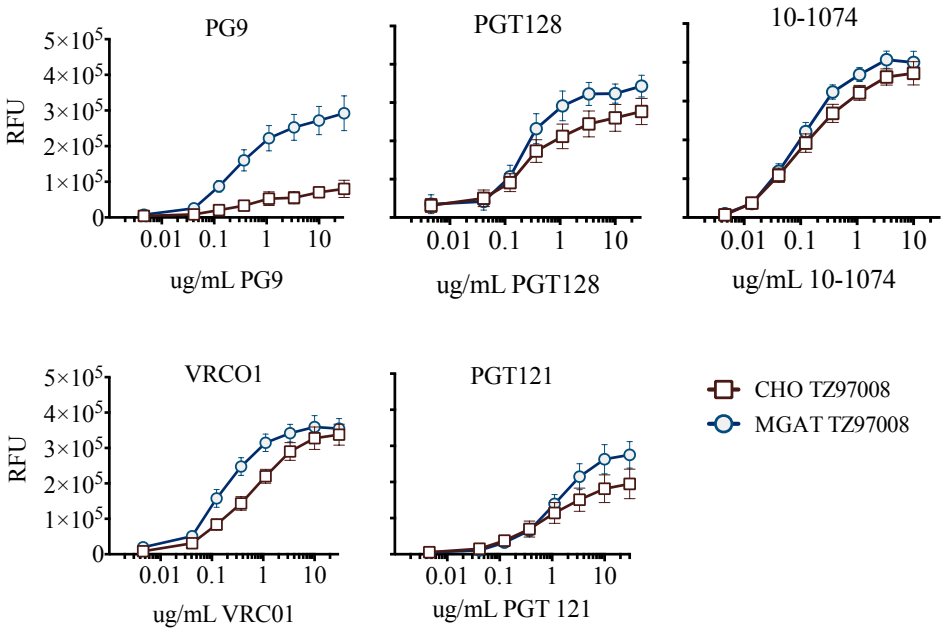

Figure 3-7 Binding of CHO and MGAT1$^-$ CHO produced TZ97008 gp120 to a panel of bNAbs. Purified protein preparations of TZ97008-rgp120 expressed in either CHO (open circles) or MGAT1$^-$ CHO cell lines (closed circles) were compared for binding to a panel of bNAbs by FIA. Plates were coated with 2μg/mL of 34.1 specific for the g N-terminal gD tag appended to each protein. The plates were washed, blocked, and incubated with 6μg/mL of purified rgp120. After a subsequent wash, captured antigen was incubated with one of six different bNAbs. The binding of bNAbs to rgp120 was detected with fluorescently labeled goat-anti-human polyclonal antibody. Each curve represents the average of a minimum of triplicate assays.

3.5 Discussion

Here we report: (1) the screening and selection of a clade C gp120 (TZ97008) with improved ability to bind a panel of bNAbs, (2) the development of a stable, high expressing (> 1g/L) MGAT1$^-$ CHO cell line that limits N-linked glycosylation for improved binding to glycan dependent bNAbs , (3) the development of an improved purification scheme for gp120 produced in the MGAT1$^-$ CHO cell line that eliminates the need for immunoaffinity

chromatography, and (4) initial biophysical characterization of the purified rgp120 product. Based on screening of a panel of diverse clade C envelope proteins, TZ97008-rgp120 displayed a superior antigenic structure with respect to binding to a panel of prototypic bNAbs. Phylogenetic analysis demonstrated that the TZ97008 immunogen was derived from an isolate that was representative of the clade C isolates circulating in Africa and Asia. From our screening experiment we found that TZ97008 is one of the few clade C gp120s able to bind the prototypic PG9 and PGT128 bNAbs. Notably, the TZ97008 rgp120 also displayed improved bNAb binding over the TV1 and 1086 clade C strains of which rgp120 immunogens currently being tested in human clinical trials are derived (170).

Previously, rgp120 purification methods required the use of lectin affinity or immunoaffinity columns for purification (41). These resins were required because the high degree of heterogeneity in net charge caused by variation in the sialic acid content precluded the use of conventional ion-exchange purification methods. Indeed, site-specific glycan analysis of gp140 proteins identified up to 70 unique glycoforms occupying a single N-linked glycosylation site (186). Production of HIV vaccine immunogens in the MGAT1^{-} CHO cell line eliminated the need for affinity purification strategies by reducing the net charge and sialic acid heterogeneity of the rgp120 product. The reduced heterogeneity in glycan structure and protein pI, facilitated downstream purification by allowing the use of ion exchange chromatography strategies similar to those described previously (170, 187). The final 3E5 MGAT1^{-} CHO TZ97008 cell line expressed approximately 1200 mg of TZ97008-rgp120 in an 11-day shake flask culture. The two-step chromatography method has a final yield of roughly 50%, resulting in about 600mg final protein product per L of culture. This yield represents an improvement compared to other cell lines producing gp120 for clinical studies, where yields of 5-100mg/L have been reported (170, 188). The yields of gp120 described here can be further improved in a setting intended for biopharmaceutical production incorporating

regulated fed batch bioreactors, optimized cell growth medium, and improved filtration and purification methods. The recovery process developed for MGAT1$^-$ CHO expressed TZ97008-rgp120 was based on its predicted isoelectric point (pI 8.4) and direct IEF measurements. We expect rgp120 from other strains of HIV produced by the MGAT1$^-$ CHO cell line to possess similar pIs, and therefore, to also be amenable to purification by this method.

Recently multiple gp120 immunogens have been advanced into human clinical trials (154, 170, 189, 190) in an effort to repeat and verify the results from the RV144 HIV vaccine clinical trials (44). The gp120s employed in these trials, like the gp120s used in the VAX003 (129), VAX004 (169), and RV144 clinical trials (41), were expressed in normal CHO cells lines. Thus, these vaccines failed to incorporate the knowledge gained since the RV144 trials related to the structure of glycans required for the binding of bNAbs. Both FIA and Biacore analysis indicated improved binding for MGAT1$^-$ CHO expressed TZ97008 rgp120 as compared to CHO expressed gp120 for the PG9, PGT128, 10-1074, and VRC01 bNAbs. While the improved binding of envelope proteins produced in the MGAT1$^-$ CHO cell to bNAbs does not necessarily translate to improved bNAb immunogenicity, the closer emulation of the glycan structures found on infectious virions and required for bNAb binding is a logical first step in the development of an improved vaccine formulation. In principle, improving the immunogenicity of any one of the four major epitopes described in this paper could potentially improve the level of protection achieved from 31% obtained in the RV144 trial to a level of 50% or more thought to be required for regulatory approval (155).

Previous studies comparing HEK 293 expressed TZ97008 have found it to induce comparable cross-clade anti-gp120 titers to a broad diversity of diverse clade C gp120 immunogens (110). Additionally, expression of A244 gp120 in the GNTI$^-$ HEK 293 cell line that limits glycoforms to oligomannose terminal glycans did not significantly decrease overall immunogenicity (150). Together, these data suggest that overall immunogenicity of TZ97008

MGAT1$^-$ CHO will not significantly change, despite the changes in glycoform and bNAb binding. However, in the face of the historically short lived anti-gp120 response, future studies investigating dosing, different adjuvants, and different immunization schedules will need to be performed to understand the full immunogenic potential of these immunogens. The question of how the immunogenicity of MGAT1$^-$ CHO TZ97008 rgp120 compares to the original RV144 rgp120 immunogens remains an open question. Characterized bNAbs against HIV often contain unusual characteristics such as high levels of somatic hypermutation or long complementarity domain regions that are difficult to elicit in animal models (88, 132, 149, 157, 191). Because of this, the antigenic potential of new vaccine immunogens may only be ultimately determined in human clinical trials. With this perspective in mind, the TZ97008-rgp120 is one a few gp120s that is designed to incorporate glycoforms required for bNAb binding and expressly produced for human clinical trials. The improvements described in this paper can be applied to facilitate the production and clinical testing of any HIV envelope-based vaccine concepts, including gp140 trimers (192) guided immunization (78, 193), DNA prime/gp120 boost protocols (165, 194) vector/gp120s boosts (153, 154) and envelope protein fragments (150, 195).

Chapter 4

Immunogenicity studies of oligomannose containing gp120 and gp120-fragments

4.1 Follow-up A244 N332 MGAT rgp120 immunogenicity experiments

The experiments outlined in Chapter 2 of this dissertation presented in this chapter documents improved antigenicity to bNAbs. However, improved antigenicity (ability of an epitope to bind an antibody) does not imply improved immunogenicity (ability to elicit antibodies to a presented epitope). The modifications described in are two-fold. First, the addition of the N332 glycan introduces a highly conserved bNAb epitope. Secondly, the expression of the gp120 in the GNTI- cell line restricts N-linked glycans to oligo-mannose terminal glycans. While the effect of the first change on the presentation of relevant epitopes (particularly those targeted by multiple families of bNAbs), the second change confers a larger effect, which can be observed by the change in molecular weight as well as the improved antigenicity to different bNAbs.

It is difficult to assess how these modifications change the immunogenicity of the investigated bNAbs. For reasons discussed in Chapter 1, there exist no ideal animal models to ask this question. However, animal models can still provide insight as to how glycan modifications can affect the immunogenicity of the gp120 as a whole, as well as insights to how presentation of other protection-associated epitopes, such as those to the V1V2 domain, and V3 loop, may be affected.

Assays for correlate of protection studies must be chosen that identify relatively independent immune functions (to reduce redundancy of readouts and cover the broadest possible immunological “space”), exhibit enough variability amongst vaccinees to identify correlations, but exhibit low degrees of experimental noise and background to optimize

statistical power(196). To evaluate correlates of protection in RV144, a consortium of various independent academic and non-academic groups (Thai AIDS Vaccine Evaluation Group) valuated 32 pilot assays that looked at antibody, T-cell, and innate immune responses, and of these, selected 17 assays based on “reproducibility, ability to detect post-vaccine responses, and uniqueness of responses detected”(46). These 17 assays were further whittled down to a total of 6 primary assay variables to maximize the power of results after multiplicity corrections. The assays used in the final analysis looked at binding of IgA antibodies to Env, avidity if IgG antibodies for Env, ADCC, HIV-1 neutralization, binding of IgG to V1V2, and level of Env-specific CD4+T cells(46).

With consideration to the limitations imposed on the number of assays that could be performed in the correlate of protection analysis (i.e. for cost and time efficacy, considerations to maintain statistical power), the identification of the correlates of protection from the Haynes et al paper(46) does not preclude the potential existence of other, unidentified correlates. It will be important to understand and document how such modifications might also change unidentified correlates. This is exemplified by the observations by Gottardo et al that increased antibody responses against a peptide epitope within the V3 domain additionally displayed inverse correlation with risk of infection (49). Such possibilities also support continued development of rgp120 immunogens in HIV vaccine design. To pursue this question for the glycan-modified gp120 immunogens, we designed an experiment to understand the role of gp120 glycoform may affect the antibody response to regions of the V1V2 and V3 domains targeted by antibodies that correlated to protection in RV144 and bNAbs.

Multiple lines of evidence, from the RV144 and broadly neutralizing antibodies against HIV, have emphasized the importance of the antibody response against the V1V2 and V3 domains. Thus, there may be an advantage to improve the immune response to

these regions. We attempted to create minimal variable domain fragments to improve upon the vaccine immunogen used in the RV144 studies. To do this, we designed protein fragments of the V1V2 and V3 domains of HIV gp120 with the aim of focusing the antibody response to these regions. We used x-ray crystallographic data of bNAbs binding to trimeric rg120 to inform the design of minimal gp120 fragments that maintains antigenicity to conformation dependent bNAbs. Previously, our group has described a V1V2 fragment that could be successfully expressed and purified and that retained the capability to bind the PG9 bNAb, despite being taken out of the full length gp120 context. Here we further describe a V3 fragment, as well as a fragment that contains the V1V2 and V3 loops to focus the immune response to relevant regions of the gp120 antigen. However, ultimately, low expression, aggregation, and lack of efficacy in preliminary animal trials discouraged the further development of these antigens.

The V3 domain has been identified as an important target of protective antibodies in the context of HIV infection. The V3 domain consists of a ~35 amino acid residue loop that is located near the apex of the gp120 trimer (117). The highly immunogenic crown of the V3 loop, containing the conserved GPGR/Q motif (residues 312-315 HXB2), has been implicated in both the autologous neutralizing antibody response and co-receptor usage (197, 198). The base of the loop, or the V3 stem, contains conserved amino acid residues important for co-receptor binding (197, 199) and targeted by multiple families of broadly neutralizing antibodies (132, 134). In the context of HIV infection, anti-V3 antibodies invoke immune pressure on infecting viruses (200, 201) and are a positive correlate of protection in both the RV144 clinical trial as well as in the context of mother-to-child transmission (49, 202). Finally, follow-up studies of early clinical trials associated V3-binding antibodies with ADCP and ADCC activity with reduced rates of infection (203, 204). Such evidence supports the role for an anti-V3 antibodies in a protective anti-gp120 immune response. Our lab has previously

designed gp120 fragments to focus the immune response to epitopes in the V1/V2 domain (150), and immunization protocols using similar fragments were found to improve the antibody titer against V1V2 based epitopes associated with protection in the RV144 clinical trial (46, 205). With the success of previous V1V2 and V3 (163) fragments, we aimed to design similar V3 fragments for use in immunization protocols with the A244 rgp120 immunogens described in earlier chapters.

Considering the relevance of both the V1/V2 (as detailed in Chapter 1) and the V3 domains, a logical path of research would be to develop an immunization strategy to focus the immune response to these domains (77, 133). The idea that the V1/V2 and V3 domains form a contiguous epitope is supported by observations that perturbations in epitopes in the V1 domain perturb presentation and immunogenicity of epitopes in the V3 domain and vice-versa (206-213). When only primary protein structure is considered, V1/V2 and V3 domains are geographically distinct, separated by the presence of the C2 domain. However, cryo-electron microscopy and crystallographic structures of the trimeric Env protein (117, 214) revealed that, in the properly folded trimeric structure, the V1/V2 and V3 domains interrelate to form a contiguous epitope located at the apex of the trimeric gp120 spike, and mediate both inter- and intra-molecular interactions amongst gp120 monomers (117, 214). From this, we reasoned that the V1/V2 and V3 domains could be fused to create an immunogen that mimicked the apex of the gp120 trimer that did not present the same magnitude of additional, non-neutralizing epitopes that are displayed on the complete gp120 monomer. We used the published crystal structure of trimeric BG505 SOSIP.664 bound to the monoclonal antibody Pgt122 to design V1V2V3 (V123) fragments derived from the CM244 clinical isolate that was used in the AIDSVAX and Rv144 clinical trials. The first half of this section describes the design, expression, and characterization of glycosylated V3 fragments to be used in conjunction with A244 gp120 based immunization protocols. The second half of this section

describes the development of a single antigen containing glycosylated V1V2 and V3 fragments.

4.2 Materials and Methods

Design and expression of glycosylated variable domain fragments

Recombinant variable domain fragments were constructed as codon-optimized Gene-strings and verified by confirmatory sequencing. The sequences of gp120s compared were aligned using MAFFT (112), and protein modeling was performed using Pymol (The PyMOL Molecular Graphics System, Version 2.0 Schrödinger, LLC). The numbering of the amino acids is provided using the HXB2 standard reference sequence (Los Alamos National Laboratories, HIV Sequence Compendium, Los Alamos, NM, hiv.lanl.gov/content/sequence/HIV/compendium.html).

Recombinant proteins for assay were expressed via transient transfection in FreeStyle™ 293-F cells (Invitrogen, Carlsbad, CA) as previously described (40). Proteins for immunogenicity experiments were expressed using electroporation. To control N-linked-glycosylation to the oligomannose-terminal glycoforms, fragments were expressed in the presence of 100uM kifunensine using a protocol adapted from Eggink et al. (215), or in cells deficient in the MGAT1 gene. Proteins expressed for bNAb binding and immunogenicity assays contained a flag epitope from herpes simplex virus glycoprotein D (gD) fused to the amino terminus and used for affinity chromatography as previously described (40).

Because of the highly immunogenic nature of this gD tag, the V1V2 fragment used in sera-derived-antibody binding assays replaced the gD tag with an N-terminal hexahistidine tag as described previously (150). The -poly-histidine tagged V1V2 construct was purified using nickel-Sepharose affinity chromatography (HisTrap column, GE Healthcare

Biosciences). Protein preparations were buffer-exchanged into PBS and analyzed for purity via SDS-PAGE on 4-12% Bis-Tris protein gels (Invitrogen). Western blots of SDS-PAGE gels were probed using an in-house mouse mAb (34.1) against the N-terminal gD tag. HRP-conjugated Polyclonal goat-anti-mouse sera from AffiniPure, Jackson Immuno Research (West Grove, PA) was used a secondary antibody.

Guinea pig Immunizations

Eight groups of six white D. Hartley guinea pigs per group (female, ages 2-3 months old) were immunized with an IACUC-approved protocol (Pocono Rabbit Farm and Laboratory, Canadensis, PA). Guinea pigs were immunized via the intramuscular route with 50ug of immunogens incorporated into Complete Freund's adjuvant (CFA) for the first immunization (Week 0). Two booster immunizations were and incorporated into Incomplete Freund's adjuvant (IFA) and were performed week 4 and week 8, with test bleeds two weeks after the first and second immunizations (weeks 2 and 6), and a final bleed two weeks after the third immunization (week 10). Animal experiments were performed according to the guidelines of the Animal Welfare Act. The immunization protocol (PRF2A) was reviewed and approved by the Animal Care and Use Committee of the Pocono Rabbit Farm and Laboratory, a facility that is fully accredited by AAALAC International with a current Animal Welfare Assurance on file (OLAW A3886-01).

Assays to detect the binding of guinea pig antibodies

Serum titers to full length gp120, gp120 fragments, or synthetic linear peptide epitopes were assayed using a direct FIA. Full-length gp120 or V1V2 fragments incorporating Man-5 glycoforms were expressed with a C terminal 6x His-tag. Synthetic linear peptides were synthesized by GenScript (Piscataway, NJ) to >98% purity. Direct FIAs were carried out

by coating a dilution of 2ug/mL protein or 5ug/mL synthetic peptide antigen in PBS onto 96 well black-microtiter plates (Greiner, Bio-One, USA) overnight. After a 4x wash in PBS-Tween, plates were blocked in a solution of PBS containing 1% BSA and 0.05% normal goat serum. Following, plates were incubated with serial dilutions of guinea pig sera starting at a 1:20 dilution. Plates were again washed 4x, and incubated with a 1:3,000 dilution of AlexaFluor 488 labeled goat-anti-guinea pig IgG (Jackson ImmunoResearch, West Grove, PA). Unless otherwise noted, dilutions were performed in solution of PBS containing 1% BSA with 0.05% normal goat serum and 0.01% thimerosal, and incubations were carried out for 90 min at room temperature. Incubations were followed by a 4x wash in PBST. Antibody binding was recorded as relative fluorescence units (RFU) using an EnVision Multilabel Plate Reader (PerkinElmer, Inc Waltham, MA) with a FITC 353 emission filter and a FITC 485 excitation filter. Final bleed titers are reported as the average of a minimum of triplicate independent assays, and pre-immune titers are the average of a minimum of duplicate assays. Results are reported as the inverse dilution for which the fluorescence measured was equal to 4x that of the background values minus measured pre-immune titers.

Neutralization Assays

The neutralizing antibody responses against tier 1 and 2 HIV-1 Env pesudoviruses from different clades were measured using a TZM.bl neutralization assay as previously described (216). Neutralization titers against the Murine leukemia virus (MLV) were included as a negative control to show that neutralization against HIV was virus specific. Tier 1A HIV-1 Env pseudoviruses tested included isolates clade CRFO1_AE THO23.6, clade C MW965.26, and the clade B SF162.LS. Tier2 isolates tested included two clade CRF01_AE (CM244.c0 and CNE55), as well as one clade C (Ce116_A3) from a standard neutralization panel.

V3 Fragment Immunoassays

To assay binding of gp120 or V3 fragments to bNAbs, 96 well microtiter plates (Nunc Maxisorp, Rochester, NY) were coated with 50μL of 2μg/mL of gp120, or 5μg/mL of V3 fragments overnight (4°C). Plates were washed 4 times in PBS containing 0.05 Tween-20, and blocked (at room temperature) for 2 hrs with PBS containing 1% BSA. Serial dilutions of monoclonal or control antibody were added and incubated for one hour at room temperature. Human IgG1 isotype control sera from Sigma Aldrich (St. Louis, MO) served as a negative control, while the in-house mAb against the gD tag, 34.1, served as a coating control. Plates were washed 4 times in PBS with 0.05% Tween, and incubated in a 1:5,000 dilution of Fc-specific peroxidase-conjugated goat-anti human or goat-anti-mouse IgG (AffiniPure, Jackson Immuno Research, West Grove, PA). Following a final wash, plates were developed using OPD substrate (Fisher Scientific, Pittsburg, PA) for 10 min and stopped with 50μL of 3M H_2SO_4. Light absorption was read in a spectrophotometer at 492nm (Spectramax 190, Molecular Devices, Sunnyvale, CA). Dilutions were performed in PBS with 0.1% BSA and incubations were performed on a shaking platform.

Deglycosylation studies

Glycosidase digests using peptide-N-glycosidase F (PNGase F) and Endoglycosidase H (Endo H) were performed on the gp120 fragments to remove N-linked glycans as per manufacturer's instructions (New England Biolabs, Ipswich, Mass). Briefly, 20μg of protein was denatured in the 10x denaturation buffer and boiled at 100°C for 10 min. Samples were then mixed with their respective reaction buffer and 5,000 units of glycosidase. Digests were carried out for 12 hrs at 37°C. The resulting digest products were analyzed by SDS-PAGE and Western blotting as described above.

Production of V3 fragments and immunoassay reagents

The rgp120-based immunogens were produced as described in Chapter 2. The A244 V3 fragment was expressed via transient transfection of CHO-S cells using the same CHO-S electroporation protocol, with the addition of 100μM kifunensine (Glycosyn, Lower Hutt, New Zealand) that was added to cell culture media 24hr post-transfection. Purified immunogens were analyzed for size and purity via SDS-PAGE analysis and for antigenicity to mAbs by capture FIA using a method described in Doran et al, 2018 (176).

Expression and purification of V123 fragments

The V123 fragments were constructed in the same manner as the V3 fragments. GNTI$^-$ cells were transfected using PEI as described in Chapter 1, and 80 hours post-transfection, 100μM of kifunensine was added to the culture. Protein preparations to be used for bNAb binding assays were purified via affinity chromatography as described above, and protein preparations for immunization (#558 and #598) were purified via affinity chromatography and size exclusion chromatography. Molecular weights of fragments without glycans were predicted with the molecular weight prediction calculator at http://www.bioinformatics.org/sms/prot_mw.html.

V123 fragment characterization and bNAb binding assays

For immunoassay, purified proteins were coated overnight onto 96 well microtiter plates (NUNC Maxi-sorp Rochester, NY) at a concentration of 5μg/mL. Plates were incubated with serial dilutions of various bNAbs for 1.5 hours and bound mAb was detected with a 1:5,000 dilution of Fc specific peroxidase-conjugated goat anti-human IgG (AfinniPure,Jackson Immuno Research, West Grove, PA). Incubations were performed one

and a half hours and dilutions were made in PBS containing 0.05% Tween-20 (PBST) with 1% BSA, and preceded by a 4X wash in PBST unless otherwise stated. Plates were developed with OPD substrate (Fisher Scientific, Pittsburg, PA) for 10 min, and the reaction was stopped with 50uL 3M H_2SO_4. Absorbance was read at 492nm (Spectramax 190, Molecular Devices, Sunnyvale, CA). The capture ELISA method was used to directly assay cell culture supernatants and varied only slightly from the direct ELISA method. Briefly, microtiter plates (Nunc Maxisorp, Rochester, NY) were coated with 2 μg/ml of 34.1 and incubated overnight at 4C. Plates blocked overnight with PBS containing 1% BSA. Cell culture supernatants were normalized for gp120 concentration and 50 μL of the normalized supernatant was added to each well and incubated with agitation for 1.5 hours at room temperature, with subsequent steps performed as described above.

Quantitative SDS-PAGE to assess V123 expression levels.

Cell conditioned supernatant was harvested 5 days post-transfection, and 10 μL of protein were reduced and loaded onto an SDS-PAGE gel. Gels were probed with the 34.2 antibody and visualized with anti-mouse HRP-conjugated polyclonal. Known concentrations of purified A244 V123 scaffold grown i293 $GNTI^-$ treated cells were loaded as a standard. was probed with anti-gD 34.2.

V123 fragment Immunizations and antibody binding titer assays

Rabbits in the RI-01-15 protocol were immunized with 200μg of V123 (serial #558 or #598) fragments per animal at weeks 0, 2, and 6 of an immunization schedule. Immunogens were incorporated in Complete Freund's adjuvant (CFA) for the first immunization, and Incomplete Freunds's adjuvant (IFA) for the two subsequent immunizations. Bleeds were assayed from sera sampled at week 8 of the schedule – two weeks after the third

immunization. Full length gp120 or V1V2 fragments incorporating Man-5 glycoforms were expressed with a C-terminal polyhistidine tag. Antibody binding titers were assayed, and Area under the Curve (AUC) calculations were performed as described in Chapter 2. Animal experiments were performed according to the guidelines of the Animal Welfare Act. The immunization protocol was reviewed and approved by the Animal Care and Use Committee of the Pocono Rabbit Farm and Laboratory, a facility that is fully accredited by AAALAC International with a current Animal Welfare Assurance on file (OLAW A3886-01).

4.3 Results

Production and characterization of full length and gp120 fragments

Full-length gp120 or gp120 fragments based on the subtype AE $A244_{N332}$ gp120 sequence were cloned into a PUC expression vector as previously described(150, 217). The primary sequences of the expressed immunogens are displayed in **FIGURE 4-1.**

MGGAAARLGAVILFVVIVGLHGVRGKYALADASLKMADPNRFRGKDLPVLDQL

LEVPVWKEADTTLFCASDAKAHETEVHNVWATHACVPTDPNPQEIDLENVTE

NFNMWKNNMVEQMQEDVISLWDQSLKPCVKLTPPCVTLHCTNANLTKANLT

NVNNRTNVSNIIGNITDEVRNCSFNMTTELRDKKQKVHALFYKLDIVPIEDNND

SSEYRLINCNTSVIKQACPKISFDPIPIHYCTPAGYAILKCNDKNFNGTGPCKNV

SSVQCTHGIKPVVSTQLLLNGSLAEEEIIIRSENLTNNAKTIIVHLNKSVVINCTR

PSNNTRTSITIGPGQVFYRTGDIIGDIRKAYCNISGTEWNKALKQVTEKLKEHF

NNKPIIFQPPSGGDLEITMHHFNCRGEFFYCNTTRLFNNTCIANGTIEGCNGNI

TLPCKIKQIINMWQGAGQAMYAPPISGTINCVSNITGILLTRDGGATNNTNNET

FRPGGGNIKDNWRNELYKYKVVQIEPLGVAPTRAKRRVVEREKRAVGIGAMF

LGFLGA*

Figure 4-1 Amino acid sequence of A244 gp120 immunogens. The N terminal gD tag is underlined.

The full length A244 rgp120 was expressed in either CHO cells, similar to the cell line used for production of the RV144 immunogens, or the MGAT1 cell line, a CHO-S cell line in which the Mannosyl (Alpha-1,3-)-Glycoprotein Beta-1,2-N-Acetylglucosaminyltransferase enzyme was mutated to limit glycosylation to oligo-mannose glycoforms(103) (168)**.**The gp120 V1V2 fragment was also expressed in the MGAT1 cell line, to maintain the mannose-5 glycoform that is necessary for PG9 bNAb binding(150). The glycosidase inhibitor kifunensine restricts glycan processing to mannose-8 or mannose-9 glycoforms. Twenty four hours post transfection, 100 uM kifunensine was added to cell culture media to ensure the incorporation of the mannose-8 and -9 glycoforms required for binding by V3 glycan binding bNAbs. Purified gp120 proteins and gp120 fragments were run on gels, shown in **FIGURE 4-2**. While

the CHO-expressed gp120 ran as a ~120kDa band, the MGAT1 expressed gp120 ran as an approximately 110kDa band, indicative of the smaller, mannose-5 glycoforms incorporated.

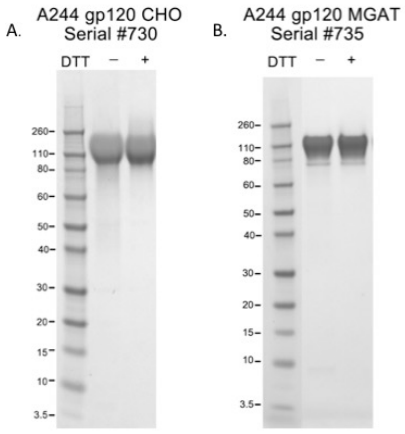

Figure 4-2 SDS PAGE analysis of affinity purified gp120 and gp120 fragment immunogens. Affinity-purified rgp120 or rgp120 fragments (V1V2 or V3) were run as either reduced or non-reduced proteins on SDS PAGE (see Materials and Methods). Protein was visualized using Coomassie Blue staining. Protein standards and size designations (kD) are labeled to the left of each gel.

Immunizations

Groups of Hartley white guinea pigs (6 guinea pigs per group) were immunized with either MGAT or CHO-expressed rgp120. The immunization protocol detailing immunogen sequences is summarized in **TABLE 4-1,** and a timeline of the protocol is depicted in **FIGURE 4-3**. The effect of the magnitude and specificity of the antibody response to each immunogen was evaluated by sera binding assays to fragments, full-length gp120, or linear peptides of epitopes within the gp120 protein.

Group	Guinea Pig #	Immunization 1 (week 0)	Immunization 2 (week 4)	Immunization 3 (week 8)
1	1-6	A244 MGAT-gp120	A244 MGAT-gp120	A244 MGAT-gp120
2	6-12	A244 CHO gp120	A244 CHO gp120	A244 CHO gp120

Table 4-1 Guinea pig immunization and bleed schedule. MGAT denotes that the MGAT deficient CHO cell line was used for production. Unless noted as MGAT or KIF, immunogens were produced in CHO-S cells. Each immunization consisted of 50ug of gp120 protein.

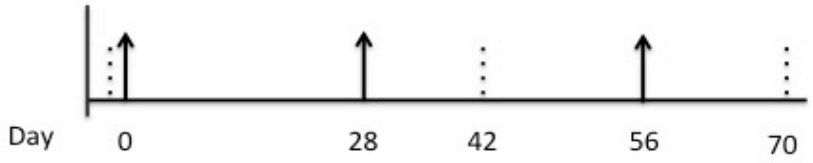

Figure 4-3 Timeline of immunizations and bleeds. Arrows indicate dates of immunization; dotted lines indicate dates of bleeds. Bleeds were collected before the first immunization, two weeks after the second immunization, and two weeks following the final immunization for a total of three bleeds spanning a period of 10 weeks.

Antibody titer characterization

We assayed for the overall gp120 titers the full-length gp120 protein expressed in MGAT cells, the V1V2 MGAT expressed fragment, and a panel of peptides covering the V1V2 and V3 domains. The amino acid sequences of the peptides used in assay are shown in

TABLE 4-2. We first measured titers of guinea pigs to the A244 N332 gp120 protein expressing Mannose-5 glycoforms, and a HIS tag replaced the N-terminal gD tag. We found there was no statistically significant difference between the groups immunized with either

MGAT expressed rgp120 (group1) or CHO expressed rgp120 (group 1) (**FIGURE 4-4**). However, the MGAT gp120-immunized animals exhibited overall greater variation in titer, while the CHO gp120-immunized group exhibited generally a higher and more consistent antibody response against the full length gp120 protein. When we assayed titers obtained from the first bleed (following the second immunization), we found that there was a significant difference between the MGAT and CHO rgp120 immunized groups (p=0.0260). These data indicate that while MGAT-expressed A244 rgp120 may initially induce lower titers to the gp120 antigen, this difference is minimized after subsequent boosts.

Peptide	**Sequence**
A244 V2	SFNMTTELRDKKQKVHALFYK
1086 V2	ATTELKDKKHKVHALFYKLD
A244 V3	NCTRPSNNTRTSITIGPGQVFYRTGDIIGDIRKAYCNISGT
A244 V3 stem	NCTRPSNNTKTVLPVTPMSQLVFHRTGDIIGDIRKAYCNISGT

Table 4-2 Amino acid sequences of peptides used in immunogenicity assays. The A244 and junction and the 1086 V2 peptides contain peptide sequences to the peptide sequence associated with protection in two studies(49, 218). All V3 peptide sequences are based on the A244 gp120 sequence; the V3 with wt crown contains no differences from the A244 gp120 sequence, while the peptide "V3 stem" replaces the V3 crown sequence from A244 gp120 with an SIV crown sequence (underlined).

We next investigated how immunization with MGAT- or CHO-derived rgp120 affected immunogenicity of epitopes within the V1V2 domain. To do this, we assayed titers to a V1V2 glycosylated fragment of A244 appended with an N-terminal His tag, expressed in the MGAT1 cell line, in addition to the glycosylated clade B V1V2 fragment associated with protection in RV144 follow up studies (46). Of note, the clade B V1V2 fragment used in immunoassay was expressed in HEK293 cells, and therefore displays complex, type sialic acid terminal glycans. The anti-V1V2 titers were overall robust amongst both groups. While the group immunized with CHO rgp12 displayed a significantly higher titer to the A244- V1V2 immunogens after the first bleed, (p=0.0411), this difference disappeared following the subsequent boost. These observations mimic the trend observed for titers against the full length A244 gp120 antigen. Interestingly, there was no difference in cross-clade reactivity against the clade B, V1V2 fragment, regardless of when the samples were collected.

IgG titers against a peptide spanning A244 V2 peptide have been found to be inversely correlated with risk of infection in the RV144 (46, 49). We investigated how the immunogenicity of this region was affected when A244 n332 rgp120 was expressed in the MGAT and CHO cell lines. We investigated titers to an A244 V2 peptide, as well as a V2 peptide clade C isolate (1082) for which binding titers have been associated with protective immune responses(49). Immunization with CHO-expressed A244 N332 rgp120 appeared to elicit significantly higher titers to A244 V2 peptide than MGAT A244 N332 rgp120 in both the first and final bleeds ($p = 0.015$). This trend was additionally reflected in titers against the 1082 V2 peptide ($p = 0.0087$) (**FIGURE 4-4**).

Both the MGAT and CHO rgp120 immunized groups displayed similarly high titers to the V3 peptide. The V3-SIV peptide is similar to the V3 peptide with the exception that the highly immunogenic V3 crown epitope has been replaced with the sequence of a V3 crown from the related but genetically distinct Simian Immunodeficiency Virus (SIV) (**TABLE 4-1**).

Antibody binding titers to this peptide should therefore represent the antibody response to the V3 peptide that does not bind the V3 crown. Immunization with MGAT gp120 resulted in significant decrease in titers to V3 stem as compared to CHO gp120 for the first bleed ($p = 0.013$) as well as for the final bleed ($p=0.041$). However, titers against the V3 stem peptide exhibited over a 10 fold average increase between the first and second boosts in MGAT-immunized animals, while the anti- V3 stem titers of CHO-gp120 immunized groups exhibited only a 2-fold increase between boosts. The trend suggests that an additional boost might result in equally high titers for these and perhaps other relevant epitopes. These data indicate that the differences in immunogenicity may exist, but could be accounted for with a minimum of two booster immunizations.

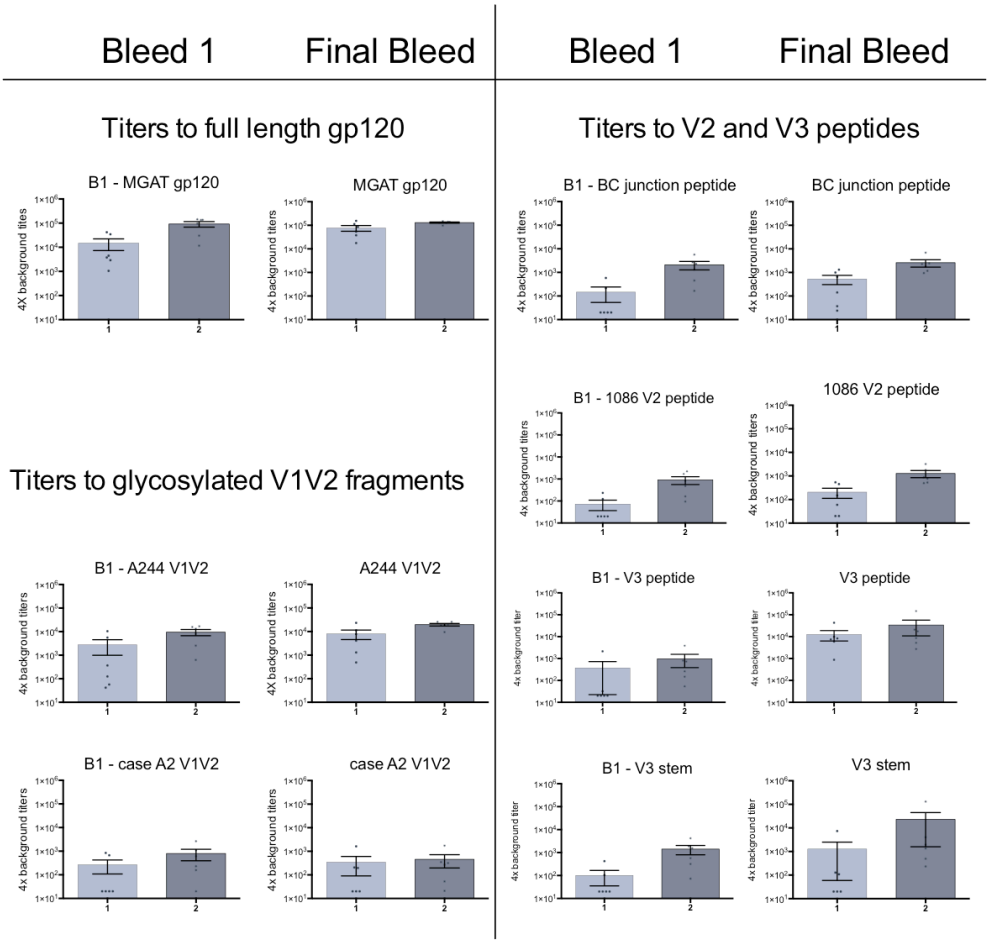

Figure 4-4 Immunized guinea pig sera binding titers to full length, V1V2 gp120 fragments, and peptide fragments of gp120. Sera from immunized guinea pigs were assayed for binding to full-length rgp120, V1V2 fragments, or peptides spanning regions in the V2 and V3 domain. Full-length rgp120, V1V2 fragments, or peptides were coated onto 96 well black microtiter plates and blocked overnight. Serial dilutions of guinea pig sera, starting at a 1:20 dilution was added and incubated in antigen-coated wells for 1.5 hours at room temperature. After a 4x was, bound antibody was probed with AlexaFluor 488 conjugated goat-anti-guinea pig polyclonal antibody, and fluorescence was read using an EnVision Multilabel Plate Reader. Bar graphs depict the average of 6 biological replicates (indicated as a data point), with pre-immune titers were subtracted and each assay was performed in triplicate. Reported titers were calculated from binding curves and reported as the inverse dilution of sera that results in a fluorescence readout 4x background. Error bars represent the standard deviation.

PG9 competition assays

PG9 competition assays were performed on sera sampled before the first immunization and two weeks after the final immunization (final bleed). Sera were diluted 1:50 and incubated with a pre-determined IC50 of PG9. Group 1 sera (immunized with MGAT expressed A244 N332 rgp120) displayed high variability in PG9 blocking ability, particularly in pre-immune sera (**FIGURE 4-5**). Group 1 (immunized with CHO-expressed A244 N332 rgp120) exhibited higher PG9 blocking ability, blocking over 60% on average of PG9 binding. Group 2 sera displayed positive PG9 blocking, as opposed to Group 1 sera, which did not significantly increase in PG9 blocking ability as compared to pre-immune titers.

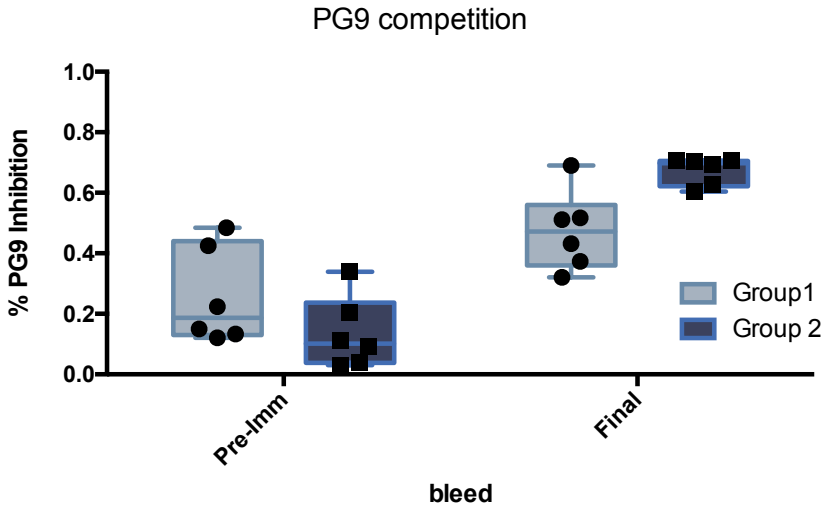

Figure 4-5 PG9 competition assays. PG9 competition assays were performed on sera sampled before the first immunization and two weeks after the final immunization (final bleed). Sera were diluted 1:50 and incubated with a pre-determined IC50 of PG9. Values reported are the average of triplicate individual experiments, and results are reported as percent competition compared to negative control (normal guinea pig) sera. Assays were considered positive if they blocked 80% of PG9 binding.

Neutralization assays

Individual sera from the guinea pigs was assayed for neutralization activity against a panel of 6 pseudoviruses (See Materials and Methods). The sequence of THO23 gp120 resembles the A244 primary sequence, and both group 1 and group 2 immunization groups exhibited the highest titers of neutralizing antibodies to the pseudeovirus expressing the TH023 envelope (average IC50 titers of 1:2923 and 1:2187, respectively) (**FIGURE 4-6**). Both groups expressed weak neutralization against the clade C MW965.25 strain (average IC50 titers of 1:88 and 1:418, for groups 1 and 2, respectively). Neither group exhibited neutralization activity against the Tier 1A clade B or Tier 2 Cm244.c01, CNE55, Ce1176_A3 strains tested. Overall, both autologous and heterologous neutralization was weak.

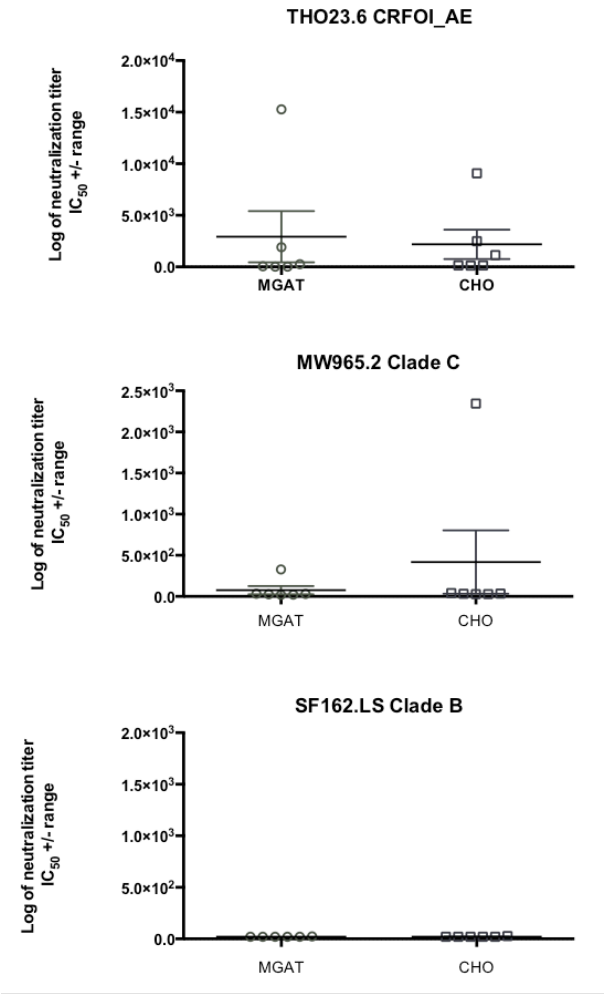

Figure 4-6 Neutralization assays. Individual guinea pig sera were assayed for presence of neutralizing antibodies in a TZMBL neutralization assay. Neutralization titers against the Murine leukemia virus (MLV) were included as a negative control.

Design of V3 glycosylated fragments

We selected sequences from five strains of gp120 to be made as V3 fragments. These strains included the clade B isolates Bal, MN468, and 108060, as well as the clade C isolates TZ97008 and CN97001. The V3 fragments begin at the Arg273 located within the C1 domain, and end at the residue 340 (**FIGURE 4-7**).

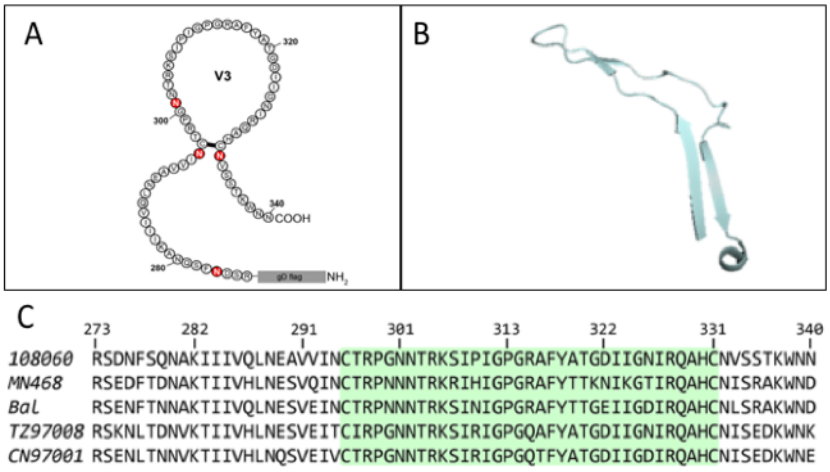

Figure 4-7 Design of V3 glycosylated fragments. **(A)** 2D rendition of the V3 fragment. The Potential N-linked glycosylation sites (PNGS) are marked in red, and the location of a single disulfide bridge was preserved to maintain gross secondary and tertiary structure. **(B)** A 3D structure of the V3 loop adapted from the crystal structure of a BG505-SOSIP co-crystallized with the V3 binding, glycan dependent bNAb PGT122(117). The anti-parallel beta sheets that form the base of the V3 loop are depicted towards the bottom of the structure. **(C)** Alignment of the V3 fragments. The V3 fragments of 108060, MN 468, and Bal are derived from clade B sequences, while TZ97008 and CN97001 are derived from clade C envelopes. The V3 loop is highlighted in green, with the V3 crown sequence boxed in grey. Within the V3 loop, the flanking sequences to the V3 crown are bookended by cysteines C295 and C331.

The nucleotide and amino acid sequences of the full-length V3 constructs designed and expressed in these experiments are summarized in **SUPPLEMENTAL TABLE 4.1.** All the

V3 fragments contained an endogenous disulfide bridge at the base of the V3 loop, based on previous findings indicating that V3 peptides constrained by a DS bridge yield a 30-fold stronger HIV neutralizing response than unconstrained peptides(219). All fragments contain the N301 and N332 Potential N-linked Glycosylation Sites (PNGS) that are relevant for 128 binding (90) However, the Bal V3 fragment contains 5 PNGS, while the other V3 fragments contain 4 PNGS.

Production and physical characterization of glycosylated V3 fragments

The V3 fragments were expressed via transient transfection in HEK 293 cells and purified via affinity chromatography to the N-terminal gD tag. The protein expression levels and final purification yields for each construct is summarized in **TABLE 4-3.** SDS-PAGE gels of representative V3 fragments containing four PNGS are shown in **FIGURE 4-8.** Purified V3 fragments containing 4 PNGS ran as roughly 40kD bands while the Bal V3 fragment, which contains 5 PNGS, ran as a diffuse band based at 55kDa **FIGURE 4-8**

Serial #	Fragment ID	Description	Amount recovered from supernatant volume	Final yield
350	UCSC 907	MN V3 + kif	.8mg/70mL	11.7 mg/L
351	UCSC 908	CN97008 V3 + kif	0.7 mg/70 mL	9.7 mg/L
352	UCSC 909	TZ97008 V3 + Kif	.7 mg/70mL	9.7 mg/L
353	UCSC 910	Bal V3 + Kif	1.1 mg/ 70 mL	16/3 mg/L
609	UCSC 703	108060 V3 + Kif	.6 mg/ 600 mL	1.1 mg/L

Table 4-3 Purification yields of V3 constructs. V3 fragments were expressed in HEK 293 cells in the presence of kifunensine and purified by affinity chromatography. Final yields of purified V3 protein concentration was assessed by BCA.

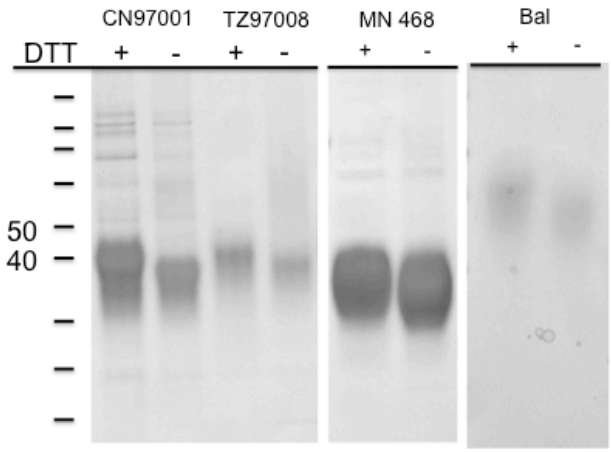

Figure 4-8. SDS-PAGE image of representative V3 fragments expressed in HEK 293 cells V3 fragments were produced in HEK 293 cells. Transient transfections were performed in 200-300 mL batches. Five days post-transfection, supernatants were harvested, and the fragments were purified by immunoaffinity chromatography with an anti-gD antibody against the gD flag-tag. Proteins were buffer exchanged into Tris buffered saline (TBS) and analyzed, in either reduced (10 min boiling in DTT) or non-reduced forms, by SDS-PAGE with 4-12% precast gradient gels.

The V3 fragments were expressed in 293 HEK cells in the presence of 100çM kifunensine. Kifunensine is an alkaloid glycosidase inhibitor produced by the actinobacterium *Kitasatosporia kifunense,* and inhibits the mannosidase I (ERM1) enzyme of the endoplasmic reticulum, resulting in presentation of predominantly Man9GlcNac2 (mannose-9) glycoforms on expressed proteins (220). The mannose-9 glycoform at the N32 PNGS has been identified as a critical component of the neutralization-mediating epitope recognized by bNAbs like PGT 128 (87). When the V3 constructs expressed in the presence of kifunensine (V3-Kif) were purified and analyzed by SDS-PAGE, they ran as two distinct bands (**FIGURE 4-9**). The V3-kif constructs with 4 PNGS ran as a major band at ~35kDa and a minor band at ~29kDa. The Bal construct, with 5 total PNGS, also ran as two bands, with a major band at ~38kDa and a minor band at ~35kD. When run as un-reduced preparations, CN97001 and TZ97008 constructs contained minor bands at ~51kDa. These bands are likely dimers, owing to the fact they were not observed when the preparations are run under reducing conditions (with DTT).

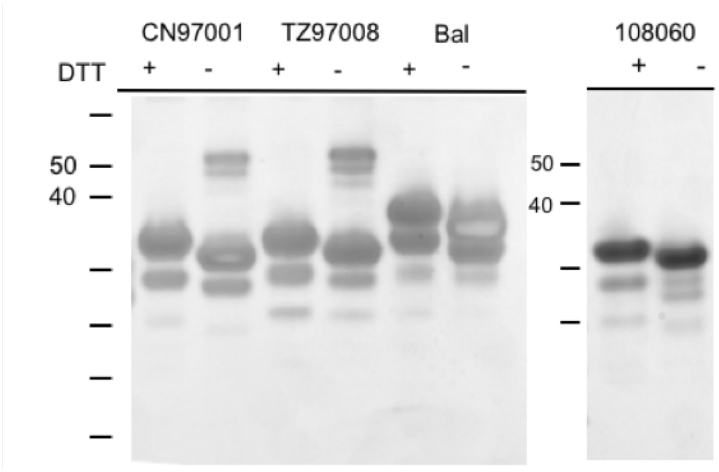

Figure 4-9 SDS PAGE image of representative V3 fragments expressed in 100uM kifunensine. V3 fragments were produced in HEK 293 cells treated with kifunensine. Transient transfections were performed in 200-300 mL batches. Five days post-transfection,

supernatants were harvested, and the fragments were purified by immunoaffinity chromatography with an anti-gD antibody against the gD flag-tag. Proteins were buffer exchanged into Tris buffered saline (TBS) and analyzed, in either reduced (10 min boiling in DTT) or non-reduced forms, by SDS-PAGE with 4-12% precast gradient gels.

The presence of two distinct bands with similar molecular weight (~29 and 35kDa) may be the result of different PNGS occupancy or processing. Previous studies have shown heterogeneous occupation of PNGS amongst individual protein of a single antigen production lot, however, such observations have been previously limited to full-length gp160 proteins in a trimeric form (186). The difference between the molecular weight of the V3 constructs from Bal and the other clades may also be explained by the occupancy of an extra PNGS found in Bal but not the other constructs.

Endoglycosidase digests using PNGase F and Endo H digest were performed on the CN97001, as a representative of a four-PNGS containing constructs, and Bal, a five-PNGS containing construct (**FIGURE 4-10**). When treated with PNGase F and analyzed by gel electrophoresis, both V3 fragments of Bal and CN97003, regardless of expression system (normal 293 or kifunensine treated 293 cells) migrated as a ~11kDa band **(FIGURE 4-10 PANEL A**). Endo H (Endoglycosidase H) is a glycosidase that cleaves glycans with oligomannose, but not complex, -terminating N-linked glycans. When grown in normal 293 cells, both Bal and CN97001 Endo H digests migrated the same distance as the mock (enzyme-free) controls (**FIGURE 4-10**, panel B). This indicated that fragments grown in normal 293 cells did not contain complex-terminal glycans, so were resistant to Endo H. However, when grown in the presence of kifunensine, the fragments ran as ~11-13kDa proteins, indicating that fragments grown in the presence of kifunensine carried the expected oligomannose terminal PNGS.

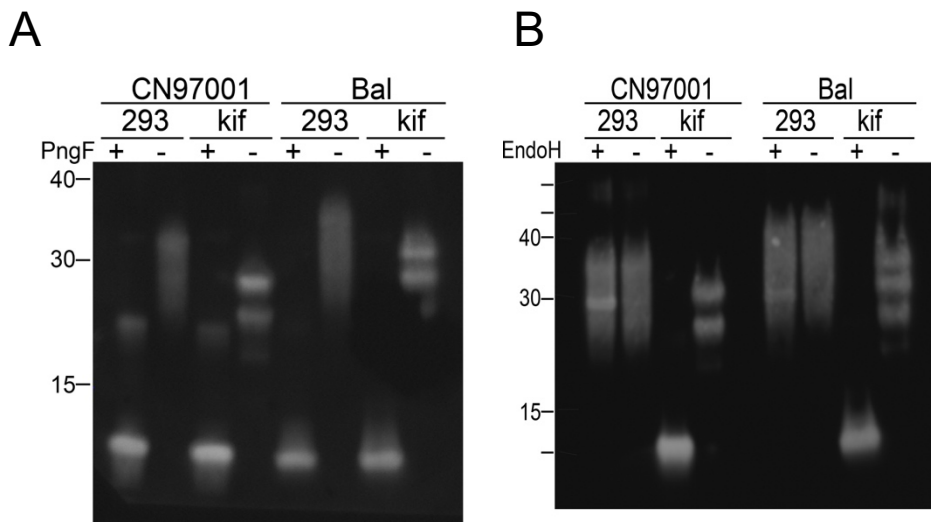

Figure 4-10PNGase F and Endo H digests of V3 fragments. PNGase F and Endo H digests were performed on purified V3 fragments expressed in 293 cells with or without the presence of the glycosidase inhibitor kifusnensine. Representative V3 fragments carrying four (CN97001) or five PNGS (Bal) were subjected to PNGase F Endo H, or mock digests, and resulting protein preparations were analyzed by SDS-PAGE. SDS-PAGE gels of PNGase F and mock digests are shown in Panel A, and SDS-PAGE gels of Endo H digests are shown in Panel B. Molecular weight standards are indicated as bars to the left of each gel.

The V3 fragment expressed in HEK 293 cells, HEK 293 cells in the presence of kifunensine, and GNTI$^-$ cells (gels not shown) were screened by ELISA for binding to the PGT 128 and PGT 121 bNAbs, as well as to the 34.1 mouse monoclonal antibody that recognizes a linear, peptide epitope contained within the N-terminal gD tag appended to the N-terminus of each fragment. The binding of the 34.1 mAb served as a coating control, as binding to this mAb should be unaffected by primary sequence or glycosylation. While all the V3 fragments, regardless of clade or primary sequence, bound to the PGT128 bNAb, the same V3 fragments expressed in normal 293 or GNTI$^-$ cells did not bind (**FIGURE 4-11**). None of the V3 fragments showed robust binding to the PGT 121 bNAb, regardless of cell expression conditions or substrates. The consistent binding to the 34.1 mAb of all V3 fragments,

regardless of clade, primary sequence, or cell expression conditions, indicated that coating was comparable amongst all experiments.

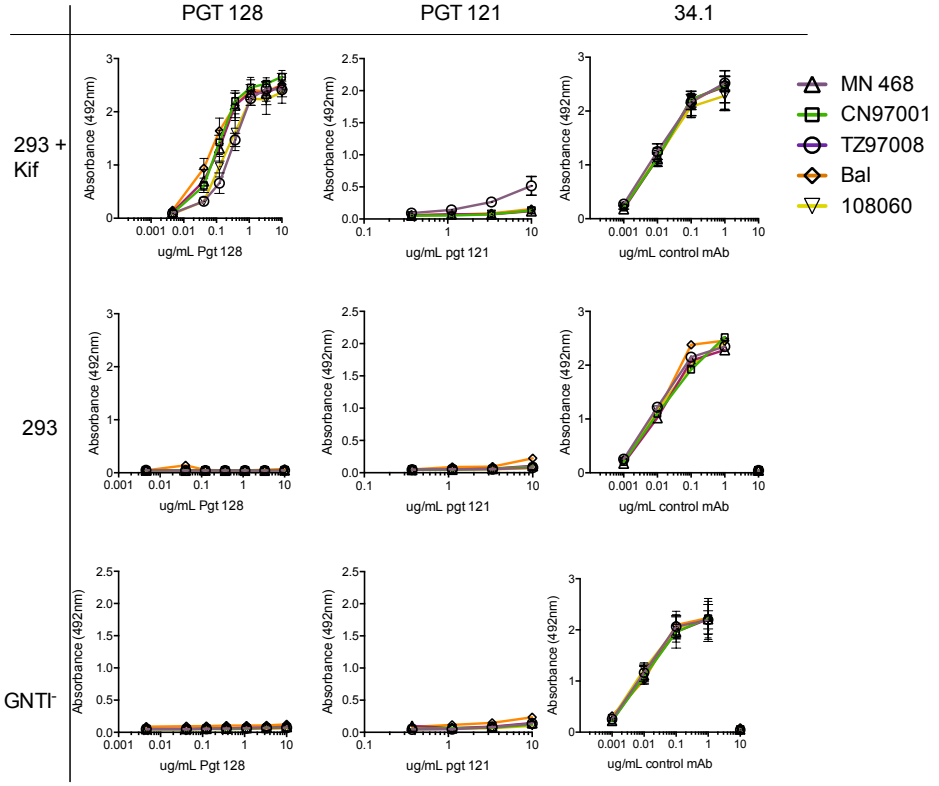

Figure 4-11 Binding of V3 fragments to bNAbs PGT 121 and PGT 128: Affinity purified V3 fragments expressed in HEK 293 cells in the presence of kifunensine, normal 293, or GNTI$^-$ cells. Plates were coated (overnight at 4°C) on microtiter plates at a concentration of 3 µg/ml in PBS. The plates were washed 4 times with PBS containing 0.05% Tween-20, and blocked for 1 hour with PBS containing 1% BSA. Serial dilutions of PGT128, PGT 121, or an isotype matched control antibody were added. Following a 1 hour incubation and a wash step, Fc specific peroxidase-conjugated goat anti-human IgG added at a 1:10,000 dilution. Following a one-hour incubation and subsequent wash step, plates were developed with OPD substrate for 10 min, and the reaction was stopped with 50 µL 3 M H_2SO_4. and absorbance was measured at 492 nm. Error bars represent standard error.

We further assayed the V3 fragments expressed in kifunensine (V3-kif) for binding to an expanded panel of anti-V3 bNAbs; PGT 126, PGT 128, 10-1074, and 447-52D (**FIGURE 4-12**). All of the V3-kif fragments bound to the bNAb PGT 128 and 447-52D with similar EC50's. The mAb 10-1074 is clonal variant of the bNAb PGT 121. Interestingly, the fragments bound to this mAb with varying EC50's. Fragments grown in GNTI$^-$ or normal 293 cells did not bind to PGT128, indicating that the Man9GlcNac2 glycoform was required for PGT 128 binding.

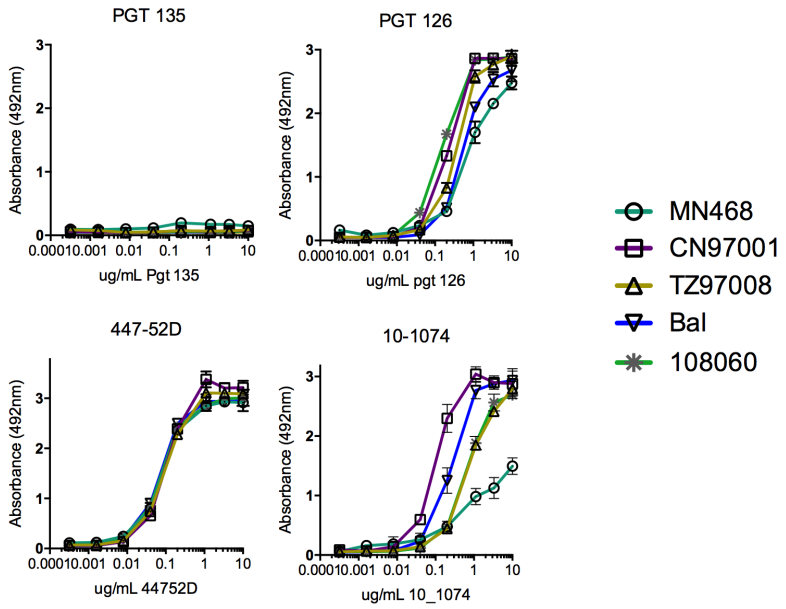

Figure 4-12. Binding of V3 fragment to an expanded panel of V3 bNAbs. Purified fragment was coated (overnight at 4°C) on microtiter plates (Nunc Maxisorp, Rochester, NY) at a concentration of 3 µg/ml in PBS. The plates were washed 4 times with PBS containing 0.05% Tween-20, and blocked for 1 hr with PBS containing 1% BSA. Serial dilutions of PGT128, PGT 121, or an isotype matched control antibody were added. Following a one hour incubation and a wash step, Fc specific peroxidase-conjugated goat anti-human was added at a 1:10,000 dilution. Following a one-hour incubation and subsequent wash step, plates were developed with OPD substrate for 10 min, and the reaction was stopped with 50 µL 3 M H_2SO_4 and absorbance was measured at 492 nm. ELISAS were run in duplicate and error bars represent standard error.

V3 immunogenicity studies

Full-length gp120 or gp120 fragments based on the subtype AE $A244_{N332}$ gp120 sequence were cloned into a PUC expression vector as previously described(150, 217). The primary sequences of the expressed immunogens are displayed in **TABLE 4-4**.

gD-A244-rgp120 MGGAAARLGAVILFVVIVGLHGVRGKYALADASLKMADPNRFRGKDLPVLDQLLEV PVWKEADTTLFCASDAKAHETEVHNVWATHACVPTDPNPQEIDLENVTENFNMW KNNMVEQMQEDVISLWDQSLKPCVKLTPPCVTLHCTNANLTKANLTNVNNRTNVS NIIGNITDEVRNCSFNMTTELRDKKQKVHALFYKLDIVPIEDNNDSSEYRLINCNTSV IKQACPKISFDPIPIHYCTPAGYAILKCNDKNFNGTGPCKNVSSVQCTHGIKPVVST QLLLNGSLAEEEIIIRSENLTNNAKTIIVHLNKSVVINCTRPSNNTRTSITIGPGQVFYR TGDIIGDIRKAYCNISGTEWNKALKQVTEKLKEHFNNKPIIFQPPSGGDLEITMHHFN CRGEFFYCNTTRLFNNTCIANGTIEGCNGNITLPCKIKQIINMWQGAGQAMYAPPIS GTINCVSNITGILLTRDGGATNNTNNETFRPGGGNIKDNWRNELYKYKVVQIEPLG VAPTRAKRRVVEREKRAVGIGAMFLGFLGA*
gD-A244-V3 fragment MGGAAARLGAVILFVVIVGLHGVRGKYALADASLKMADPNRFRGKDLPVLDQLLEV PRSENLTNNAKTIIVHLNKSVVINCTRPSNNTRTSITIGPGQVFYRTGDIIGDIRKAYC NISGTEWNK*

Table 4-4. Amino acid sequence of proteins used in immunization studies.

The full length A244 rgp120 was expressed in either CHO cells, similar to the cell line used for production of the RV144 immunogens, or the MGAT1 cell line, a CHO-S cell line in which the N-acetylglucosamine transferase 1 enzyme was mutated to limit glycosylation to oligo-mannose glycoforms (103, 168). The glycosidase inhibitor kifunensine restricts glycan processing to mannose-8 or mannose-9 glycoforms. The V3 gp120 fragment was expressed in the presence of 100 uM kifunensine to ensure the incorporation of the mannose-8 and -9

glycoforms required for binding by V3 glycan binding bNAbs. Purfied gp120 proteins and gp120 fragments were run on gels, shown in **FIGURE 4-13**. Immunogens were assayed by a capture fluorescence immunoassay (FIA) for antigenicity to a panel of bNAbs (**FIGURE 4-14**). While preliminary, small scale production batches of A244 V3 grown in kifunensine treated CHO cells showed binding to the PGT128 bNAb (data not shown), the V3 fragment used in the immunization protocol failed to bind PGT128.

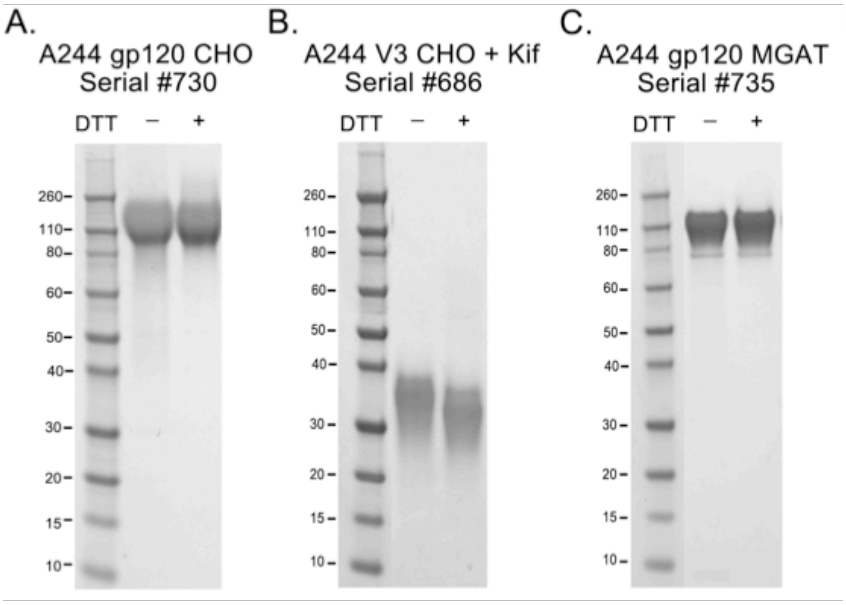

Figure 4-13. SDS-PAGE analysis of affinity purified gp120 and V3 fragments. Affinity purified rgp120 or rgp120 fragments (V1V2 or V3) were run as either reduced or non-reduced proteins on SDS-PAGE (see Materials and Methods). Protein was visualized using Coomassie Blue staining. Protein standards and size designations (kD) are labeled to the left of each gel.

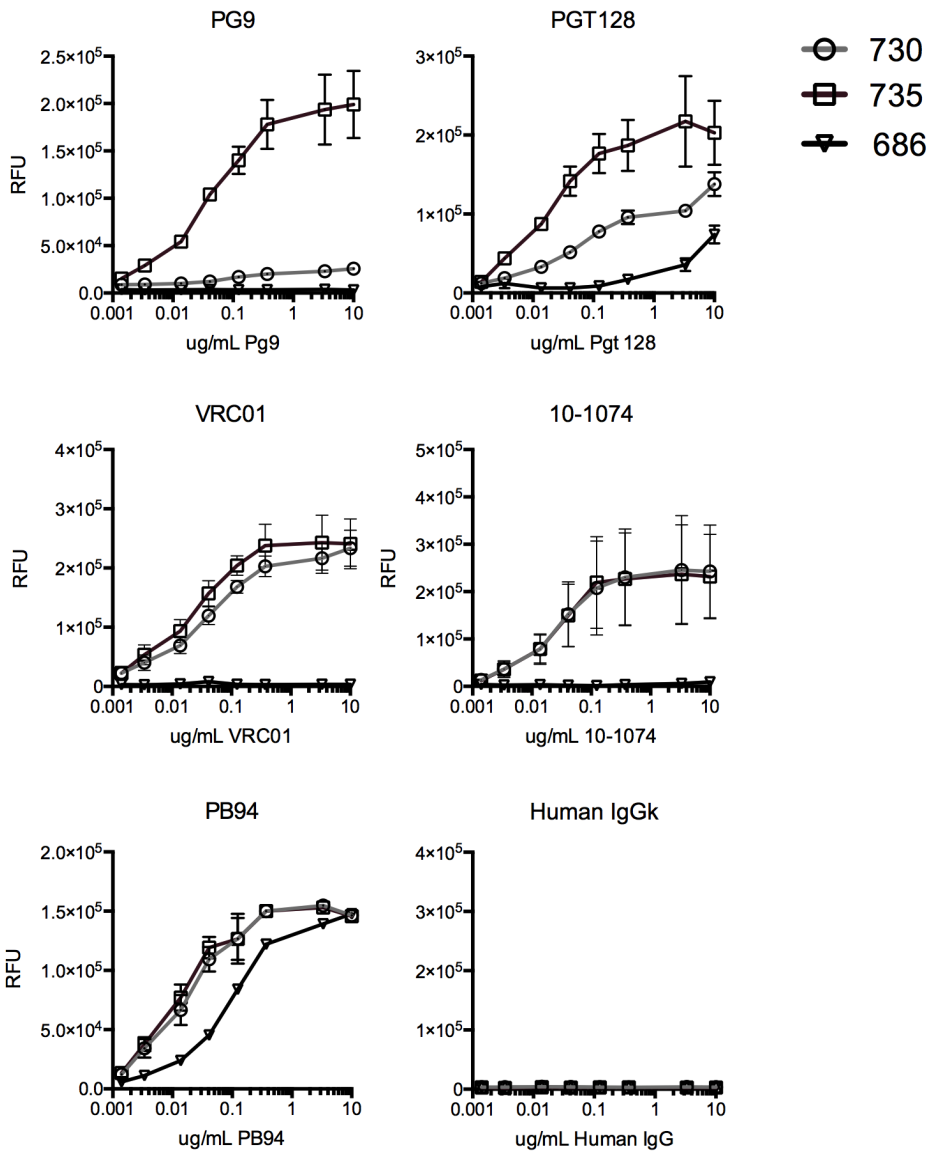

Figure 4-14. bNAb binding to gp120 and V3 fragment immunogens. The full length gp120 produced in CHO (serial # 730) or MGAT (serial # 735) cells and V3 fragment immunogens (serial # 686) were assayed for bNAb bindng by a capture FIA assay. Purified protein was capture onto a 96 well plate using the 34.1 mouse monoclonal antibody and incubated with serial dilutions of primary antibody. Captured antibody was detected using Alexa-Fluor 488 conjugated goat-anti-human polyclonal. PB94, a rabbit polyclonal sera against the full length gp120 was used as a coating control, and human isotype (IgGk) was used as a negative binding control.

To ask the question of how priming with a gp120 V3 fragment affected the specificity and magnitude of the immune response to regions within the fragments, groups of Hartley white guinea pigs (6 guinea pigs per group) were immunized following a protocol in which fragments were used as either a prime immunogen, or a boost immunogen. In an immunization protocol that consisted of 3 immunizations over the course of 8 weeks, fragments were either administered at weeks 0 and 4 (prime), or at week 4 and 8 (boost). Full-length gp120 or fragments were administered at each time point (weeks 0,4, and 8) for comparison. The immunization protocol is summarized in **TABLE 4-5**, and a timeline of the protocol is depicted in **FIGURE 4-15**.

Group	Guinea Pig #	Immunization 1 (week 0)	Immunization 2 (week 4)	Immunization 3 (week 8)
1	1-6	A244 MGAT- gp120	A244 MGAT- gp120	A244 MGAT- gp120
2	6-12	A244 CHO gp120	A244 CHO gp120	A244 CHO gp120
3	13-18	V3 KIF	V3 KIF	V3 KIF
4	19-24	A244 MGAT- gp120	V3 KIF	V3 KIF
5	25-30	V3 KIF	V3 KIF	A244 MGAT- gp120

Table 4-5 Rabbit immunization and bleeding schedule. KIF denotes proteins were expressed in CHO-S cells in the presence of kifunensine. MGAT denotes that the MGAT deficient CHO cell line was used for production. Unless noted as MGAT or KIF, immunogens were produced in CHO-S cells. Each immunization with gp120 consisted of 50μg of gp120 protein. Each immunization with a V3 fragment consisted of 25μg of fragment.

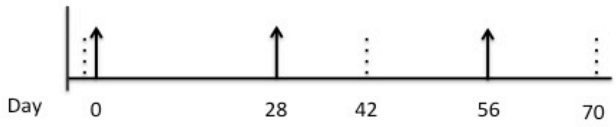

Figure 4-15 Timeline of Immunizations and bleeds. Arrows indicate dates of immunization; dotted lines indicate dates of bleeds. Bleeds were collected before the first immunization, two weeks after the second immunization, and two weeks following the final immunization for a total

Differences in the magnitude and specificity of the antibody response elicited by the different protocols were evaluated by sera binding assays to fragments, full-length gp120, or linear peptides of epitopes within the gp120 protein. To investigate whether a prime or boost protocol could better focus the immune response to critical epitopes, we assayed antibody titers from all five groups to an array of fragments and peptides spanning the V3 domains, summarized in **TABLE 4-6**. The V3 peptide encompasses the V3 loop, which includes the exceptionally immunogenic V3 crown motif, an addition to the N and C terminal flanking sequences that, in the context of the trimer, and held together by a disulfide bridge.

V3 peptide	NCTRPSNNTRTSITIGPGQVFYRTGDIIGDIRKAYCNISGT
V3 stem	NCTRPSNNTKTVLPVTPMSQLVFHRTGDIIGDIRKAYCNISGT
C terminus of V3 stem	RTGDIIGDIRKAYCNISGT

Table 4-6 Amino acid sequences of peptides used in immunogenicity assays. All V3 peptide sequences are based on the A244 gp120 sequence; the V3 peptide contains no differences from the A244 gp120 sequence, while the peptide "V3 stem" replaces the V3 crown sequence from A244 gp120 with an SIV crown sequence (underlined).

There appeared to be no statistically significant difference for V3 titers amongst any group. The immunodominance of the V3 domain was evident; the similarity amongst the groups to responses to the V3 peptide suggested that the V3 peptide was equally targeted amongst the different immunization protocols (**FIGURE 4-16**). The V3 stem peptide is similar to the V3 peptide with the exception that the highly immunogenic V3 crown epitope has been replaced with the sequence of an SIV V3 crown (**TABLE 4-6**). Antibody binding titers to this peptide should therefore represent the antibody response uniquely to the epitopes that flank the crown epitope at the base of the V3 loop. Immunization with MGAT gp120 resulted in significant decrease in titers to V3 (SIV crown) as compared to CHO gp120. However, this trend did not hold for groups immunized with full length-gp120 as a prime or boost (**FIGURE 4-16**).

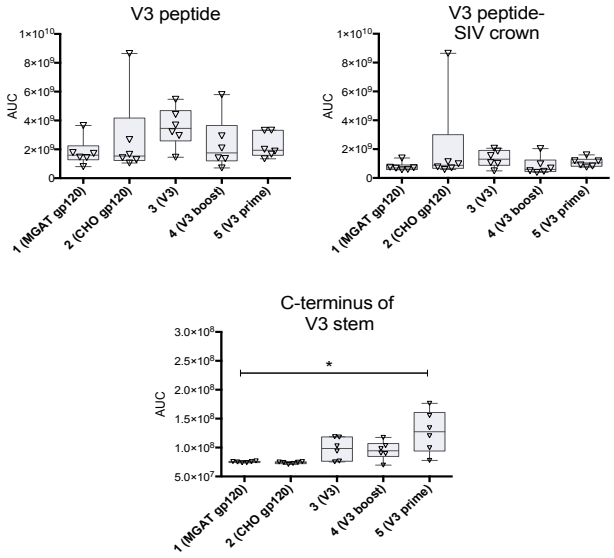

Figure 4-16. Binding titers of immunized guinea pigs to V3 peptides. Guinea pig sera from final bleeds (day 70) was assayed for binding to peptides spanning the V3 domain by FIA. Area under the Curve (AUC) values were calculated from FIA binding curves, and a one-way ANOVA and Kruskall-Wallis were used to identify statistically significant differences

between MGAT$^-$CHO gp120 immunized animals (Group 1), and groups immunized with CHO gp120 or V3 fragments. GraphPad Prism 2.0 was used for AUC calculations and statistical analysis. Values are significantly different (P = 0.0013) are marked with an asterisk.

The C-terminus V3stem peptide is a minimal peptide that contains only the 19 amino acids on the C terminus of the end of the V3 crown epitope and contains conserved amino acid residues targeted by the PGT128 bNAb family. Immunization with either the MGAT and CHO gp120 proteins elicited only negligible titers to C-terminus V3stem peptide, indicating that, in the context of the full length gp120 protein, this is an immunorecessive epitope. However, protocols in which V3 peptide was used as a prime antigen, elicited high titers to the C-terminus V3stem peptide, indicating that titers to this epitope could be rescued with a V3-fragment immunogen (**FIGURE 4-16**). The group that received a V3 fragment boost (Group 5), was the only group observed to have a statistically significant improvement to the C-termV3stem peptide (P = 0.0013). Sera were additionally assayed for neutralization activity against same (THO23 CRFO1_AE) and cross-clade pseduoviruses in a TZM.bl neutralization assay (**FIGURE 4-17**). Although slightly higher neutralization titers were observed in groups receiving V3 fragment immunogens (groups 3, 4, or 5), trends were not statistically significant when compared to the group receiving the MGAT1-CHO full length rgp120 protocol (group 1) as analyzed by one-way ANOVA.

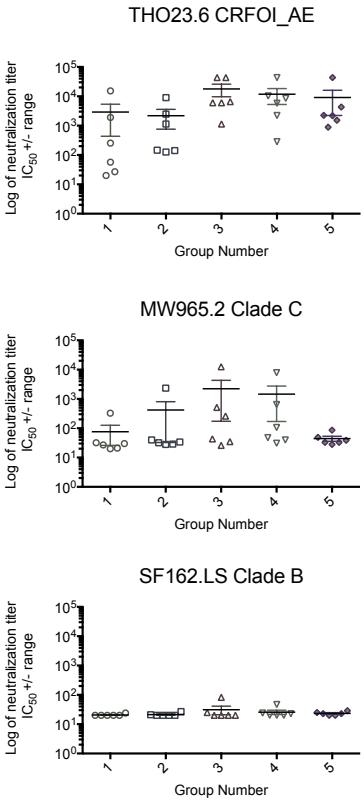

Figure 4-17. Neutralizing antibody titers 2 weeks after final immunization with different A244 gp120 and fragment immunization protocols. Guinea pig sera from final bleeds (day 70) was assayed for neutralization activity against tier 1 and tier 2 neutralization-sensitive pseudoviruses in a TZM.bl neutralization assay format. Horizontal bars represent mean titers and SEM. For each group, neutralization of a negative control (MLV) is included as a negative control and standard for sera cytotoxicity.

Design and expression of V123 fragments

A V1/V2/V3 fragment was designed using the A244_N332 gp120 sequence. Examination of the BG505 SOSIP.664 crystal structure revealed that a distance of 18.8 Å separated the bases of the V1/V2 and V3 loops (**FIGURE 4-18).** To fuse the V1/V2 and V3 domains into a single fragment, while maintaining at least ~20 Å distance to retain the

inherent V1V2 and V3 loop flexibility, we designed a (GGGGSx3) linker to give enough flexibility to the domains, allowing for conformational flexibility and potentially better bNAb binding. The GGGGS linker has an expected length of 5.7nm per repeat (221), so a 3X GGGGS linker should be approximately ~20kDa. We inserted the 15-amino acid glycine-serine flexible linker (GGGGSx3) between the C terminal domain of the V1/V2 loop and the N terminal domain of the V3 loops **(FIGURE 4-18).** The nucleotide and amino acid sequence of the resulting construct, UCSC 1209, is provided in **SUPPLEMENTAL TABLE 4-2**. The resulting V123 fragments with a 3X GGGGS linker are 199 amino acids in length and contain 12 predicted N-linked glycosylation sites (PNGS).

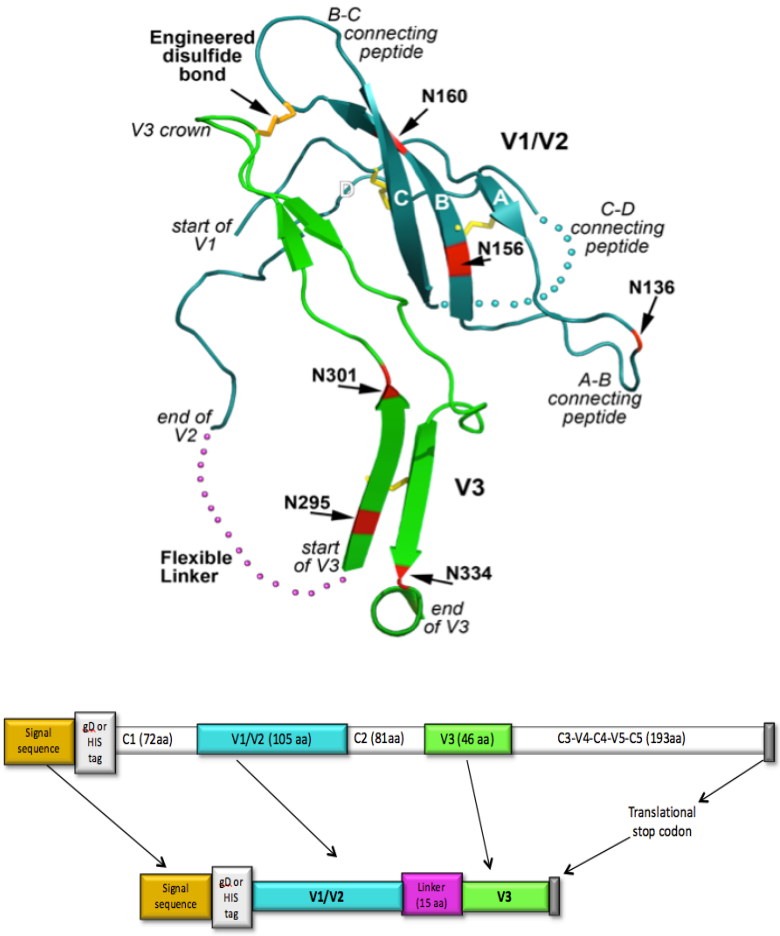

Figure 4-18. Diagram of the V1V2 and V3 domains. (A) Diagram of the 3-dimensional structure of the V1/V2 and V3 domains of gp120 based on the trimeric crystal structure of the BG505 SOSIP.664 complexed with PGT122[28]. Sequences from the V1/V2 domain form a 4-stranded β-sheet shown in teal. Sequences from the V3 domain are shown in bright green. The 81 amino acid C2 domain that normally connects the V1/V2 and V3 domains is replaced by a flexible 15 amino acid glycine-serine linker indicated by the pink dotted line. The intra-domain disulfide bonds within the V1/V2 or V3 domains are indicated in red. **(B)** Schematic of V1/V2/V3 fragment by deletion of the C1, C2, C3, V5, V5, and C5 domains and insertion of a signal sequence, purification tag, and flexible linker. A diagram shows the fusion of the V1/V2 (teal) and V3 domains (green) of gp120 with a 15 AA flexible linker (GGGGSx3) (magenta). To optimize the expression of the fragment, the signal sequence from the herpes simplex virus glycoprotein D (gD) was appended to the N terminus of the fragment (orange). A 27 AA HSV-1 gD tag (grey) was added adjacent to the signal sequence to facilitate purification.

When the V123 scaffolds are expressed purified by affinity chromatography, three peaks of different molecular weight eluted. A chromatograph of the affinity chromatography eluate of GNTI$^-$ expressed V123 fragment is shown in **FIGURE 4-19A**. The first two peaks that elute appear to have a higher molecular weight than the monomer when unreduced, running as a ~160kDa band, but run close the predicted size of the fragment monomer (~57kDa) when reduced with DTT (**FIGURE 4-19B**). Additionally, when assayed by ELISA, these two peaks displayed poor binding to the PG9, 10c10, and 34.1 antibodies (**FIGURE 4-19C**). The third distinct peak to elute ran as a somewhat smaller band (~53kDa) when unreduced. When reduced by DTT, a majority of the protein ran as a ~50kDa band, though a small portion ran as the ~160kDa oligomer. The third peak additionally showed improved binding to PG9 as compared to both the peak 1 and peak 2 fractions, as well as the large scale purified V123 batch (serial #512) used in assay.

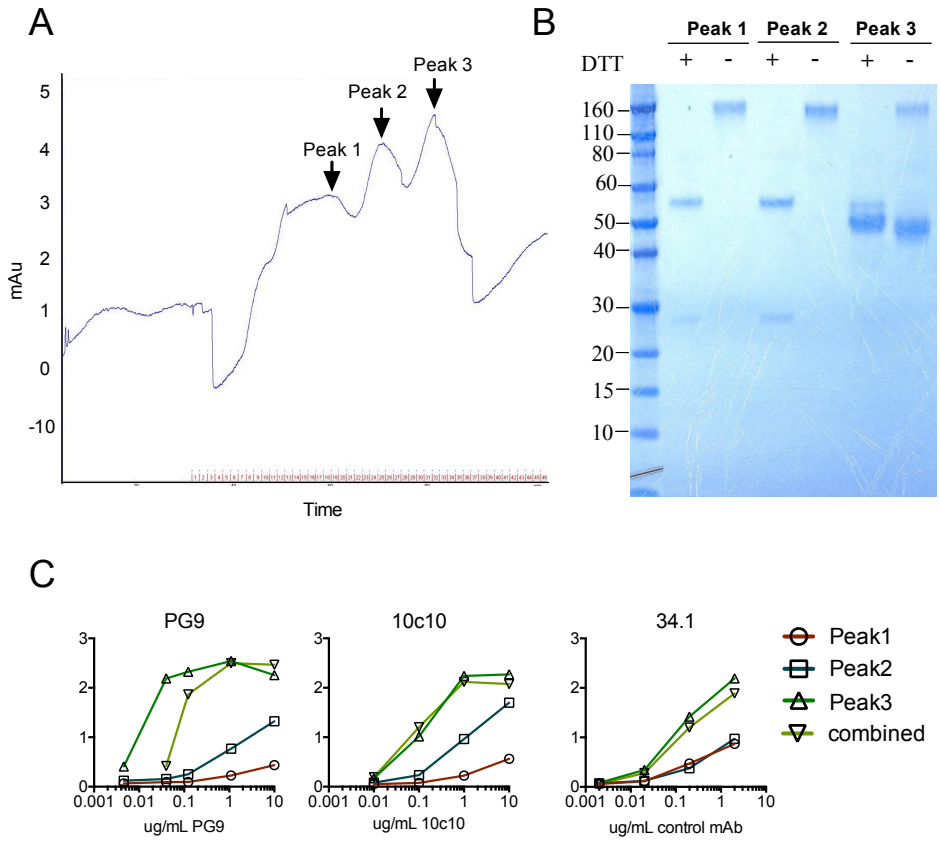

Figure 4-19. V123 fragment affinity chromatography purification peaks. (A)V123 fragments expressed in HEK 293 GNTI$^-$ cells were purified via affinity chromatography using a monoclonal antibody against the N-terminal gD tag. The chromatograph showing the eluent and collected peaks is shown. For analysis, the three major fragment containing peaks were collected separately and assayed as reduced and unreduced preparations by **(B)** SDS-PAGE for purity and size, and by **(C)** ELISA for antigenicity to the conformation and glycan dependent (PG9) and conformation independent (31.4 and 10c10) mAbs.

The V123 fragments were secreted, and their mobilities differed in a manner corresponding to their expected differences in presented glycoforms. When expressed in GNTI$^-$ cells and purified via affinity and size exclusion chromatography, the V123 fragments ran as a ~55kDa band. When expressed in kifunensine treated HEK 293 cells, the V123

fragments run as a ~60kDa band. Both GNTI$^-$ and kifunensine treated 293 expressed V123 fragments displayed similar mobility shifts from digest by PNGase F and Endo H glycosidase, indicating presence of predominantly oligomannose glycoforms (**FIGURE 4-20**). Both PNGase F and Endo H digested fragments, whether expressed in GNTI$^-$ or kifunensine treated 293 cells, ran as two distinct species with ~20kDa or 15kDa molecular weights. The presence of two distinct molecular weights of purified V123 preparations may be a result of heterogeneity of glycan occupancy.

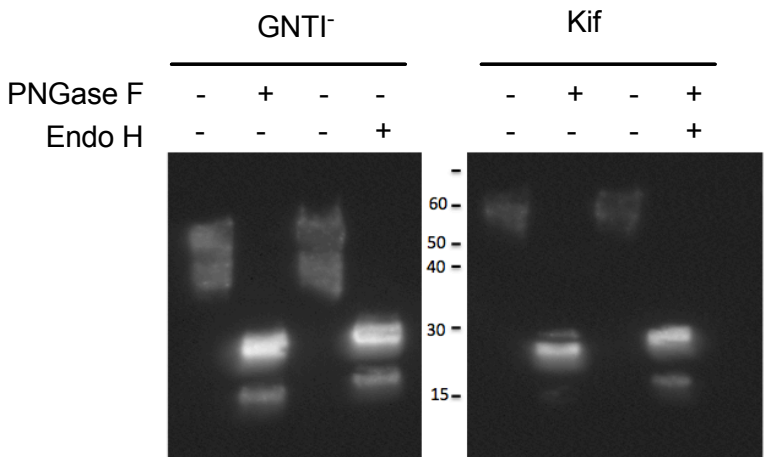

Figure 4-20 Glycosidase digests of the A244 V123 fragment grown in GNTI$^-$ or kifunensine treated 293 cells. The A244 V123 fragments grown in either GNTI$^-$ 293 or kifunensine-treated 293 cells were purified by affinity chromatography examined for sensitivity to digestion by the glycosidase enzymes PNGase F or Endo H. Mock digests were also performed in which the proteins were subjected to the digest conditions without the addition of the enzyme.

The protein preparations were assayed for binding to a panel of glycan and conformation dependent bNAbs that bind epitopes within the V1V2 or V3 domains.

Binding of V123 (3x GGGGS linker) fragments to bNAbs

While the V123 fragment grown in GNTI- cells showed similar binding to PG9 as the full length GNTI- expressed rgp120, the kifunnsine-expressed fragments displayed poor binding to PG9, while kifunensine-expressed rgp120 maintained PG9 binding. The expression-system dependence was also observed for PGT128 and PGT 126 binding to fragments; while full-length rgp120 bound to PGT128 regardless of cell expression system (with kifunensine-expressed rgp120 exhibiting slightly better binding), the V123 fragment only bound when expressed in the presence of kifunensine. Interestingly, the CHO1 and CH03 bNAbs bound similarly to V123 fragments and full length rgp120, regardless of cell expression system or glycoform. While PGT 121 and 122 bNAbs did not bind to any of the antigens, 10-1074, which binds a similar epitope, bound well to gp120 proteins, exhibiting poor but observable binding to the fragments (**FIGURE 4-21**).

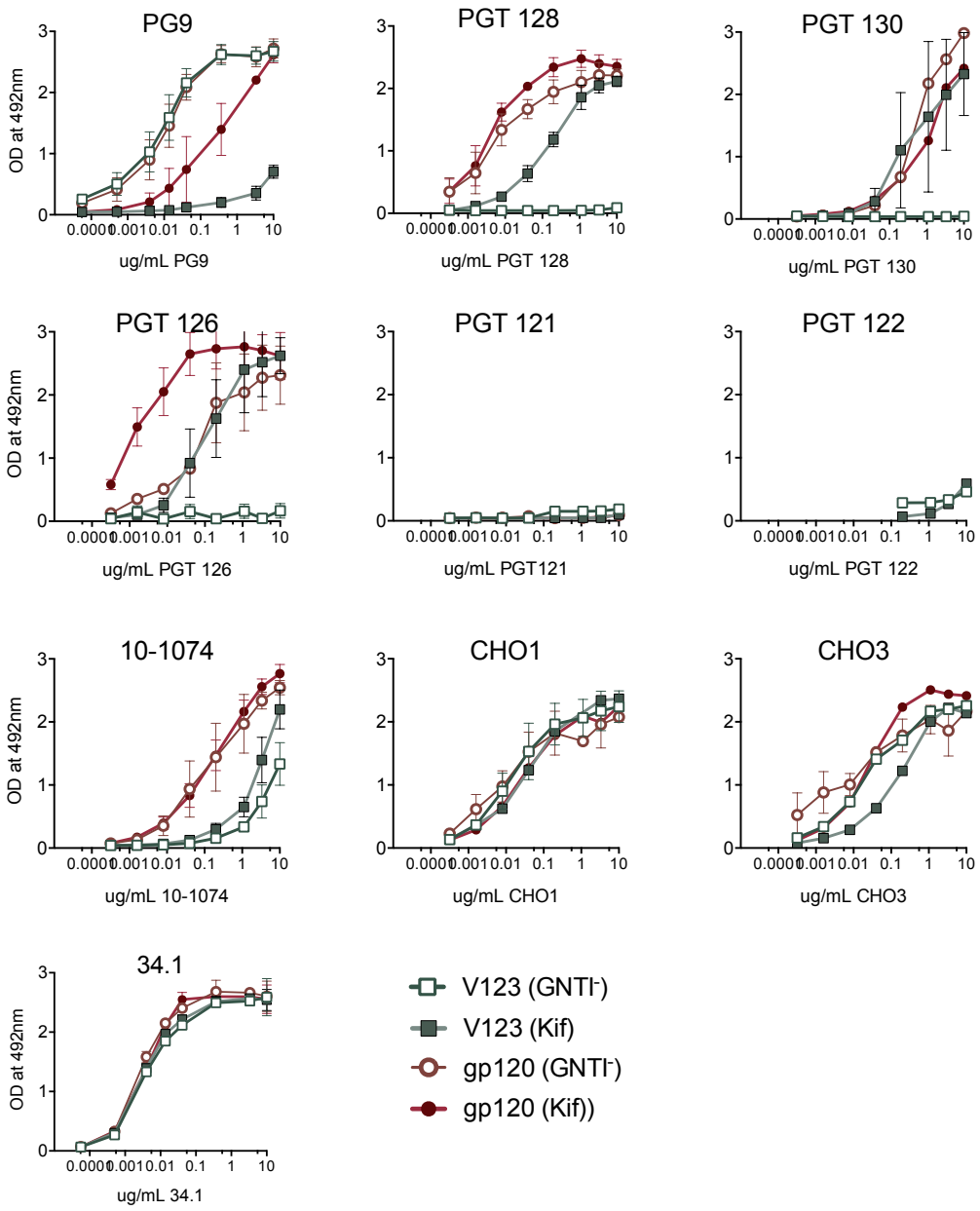

Figure 4-21 Binding of bNAbs to V123 fragment grown in GNTI$^-$ or kifunensine treated 293 cells. The V123 fragment grown in 293 GNTI$^-$ or kifunensine treated 293 cells was assayed for binding to multiple bNAbs by ELISA. Purified protein was assayed for antigenicity to an array of glycan depending broadly neutralizing antibodies by a direct coat ELISA. Assays were performed in at least duplicate, and error bars represent Standard Deviation.

V123 Immunogenicity experiments

The immunogenicity of the V123 fragments was tested in a preliminary immunogenicity experiment. The experiment (RI-01-15) used immunogens in which a mixed batch fermentation process was used to express a mixture of V123 immunogens in which kifunensine was added to GNTI$^-$ fermentation cultures in a manner that approximately half of the immunogens displayed mannose-5 glycoforms, and approximately half of the immunogens displayed mannose-9 glycoforms (**FIGURE 4-22**). V123 fragments expressed from the mixed batch fermentation process were purified via affinity chromatography to the N-terminal gD flag tag followed by size exclusion chromatography for removal of oligomeric species.

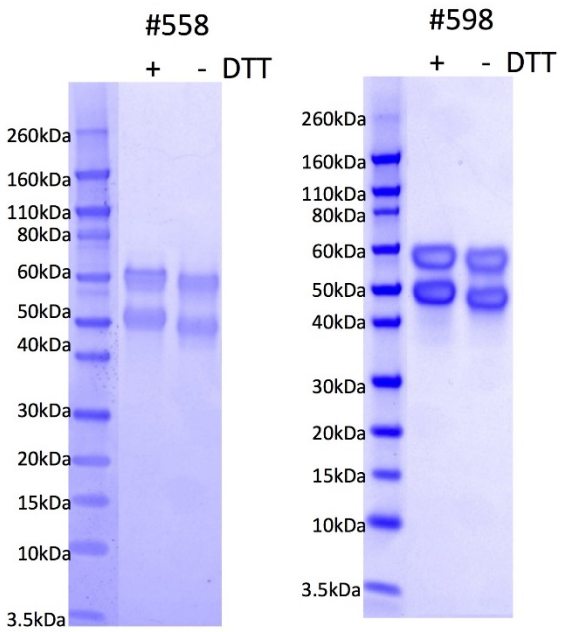

Serial #	Fragment ID	Description	recovered from supernatant volume	Final yield
558	UCSC 1209	A244 gd-V123 (Mixed-batch)	2.5 mg/1.5 mL	1.7 mg/L
598	UCSC 1209	A244 gd-V123 (Mixed-batch)	1.4 mg/3L	0.5 mg/L

Figure 4-22 Protein gels and purification yields for V123 proteins derived from mixed-batch fermentation culture. (A) A244 V123 protein (serial #558 and #598) were expressed via a mixed-batch GNTI$^-$/Kif fermentation protocol and purified via affinity chromatography batch production: The resulting proteins ran as two distinct bands, representative of two protein populations containing predominantly mannose-5 (~50kDa) or mannose-9 (~57kDa) glycoforms. The protein yields for V123 production lots #558 and #598 following affinity chromatography and size exclusion purification were calculated by BCA.

Sera from V123 (mixed batch)-immunized New Zealand White rabbits were compared with historical sera from New Zealand White rabbits immunized with; A244 V1V2 (GNTI$^-$) fragments, the clade B derived 108060 V3 (kifunensine) fragments, and/or full length

A244 gp120 ($GNTI^-$). The rabbit sera protocols used for comparison are included in **TABLE 4-7**

Sera collected two weeks after the third immunizations were tested for binding to relevant variable domain fragments from A244 and 108060 (A244 V1V2, 108060 V3), as well as peptide fragments spanning the V1V2 and V3 epitopes (A244 V2, A244 V2 (full), 108060 V3 stem, or A244 V3). The peptide sequences used in assay are provided in **TABLE 4-8**

Immunization protocol ID	Rabbit numbers	Immunization schedule	Immunogen
RI-01-15	476 and 477	Week 0, 2, 6	V123 (mixed batch)
RI-04-12	381, 382, 383	Week 0, 2, 4,8 ,12, 18	gD-A244 gp120/ gD-A244 V1V2 ($GNTI^-$)
RI-04-12	384, 385, 386	Week 0, 2, 4,8 ,12, 18	gD-A244 V1V2 ($GNTI^-$)
RI-04-12	378, 379, 380	Week 0, 2, 4,8 ,12, 18	gD-A244 gp120 ($GNTI^-$)
RI-04-12	375, 376, 377	Week 0, 2, 4,8 ,12, 18	gD-A244 gp120 (293)
RI-01-13	396, 397, 398	Weeks 0, 2, 8, 12, 20	gD-108060 V3 (Kif)

Table 4-7. Historical rabbit immunization protocols used for comparison in V123 mixed-batch immunization experiments.

Peptides used in scaffold immunogenicity studies:	
A244 V2	NMTTELRDKKQKVHA
A244 V2 (full)	MTTELRDKKQKVYALFYRL
108060 V3 stem	NCTRPGNNNTKTVLPVTPMSQLVFHATGDIIGNVSSTK
A244 V3	NCTRPSNNTRTSITIGPGQVFYRTGDIIGDIRKAYCNISGT

Table 4-8. Peptide sequence assayed in V123 immunogenicity experiments

Sera tested were from immunizations using A244 gp120 or gp120 fragments except the sera used from the RI-01-13 experiments, in which the V3 (kif) immunogen sequence was derived from a clade B strain (108060). Rabbit sera were pooled and assayed in quadruplicate by fluorescence immunoassay as described in Materials and Methods. Anti-V1V2 titers were measured using an A244 V1V2 fragment in which the gD flag tag had been

replaced by a polyhistidine tag (to avoid measurement of gD-specific antibodies (

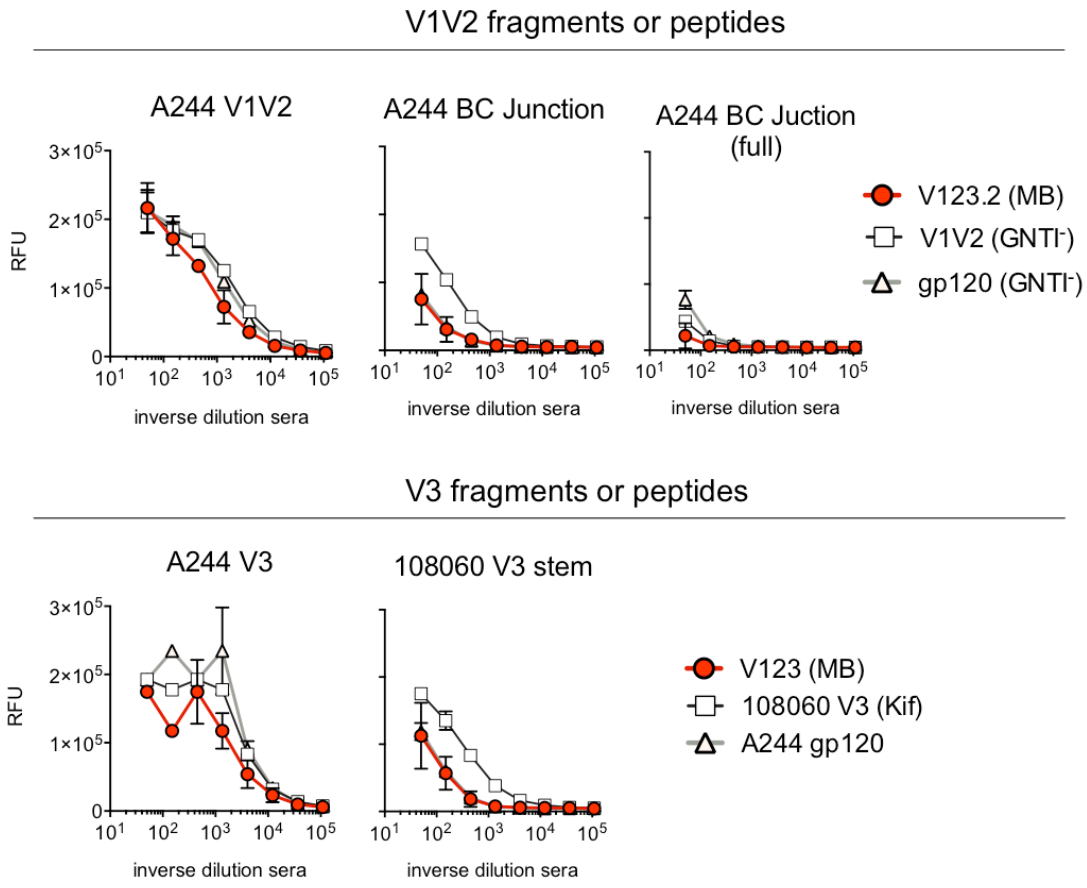

FIGURE 4-23). Area under the Curve (AUC) calculations performed using the GraphPad Prism software to quantitate antibody titer differences (**FIGURE 4-24**). Interestingly, no difference in titers to the A244 V1V2 fragment was observed amongst the different sera assayed. In general, the groups receiving a gp120 prime, V1V2 boost immunization protocol exhibited the highest antibody tiers for all V1V2 or V1V2 subunit antigens assayed. The groups that received the V1V2 fragment alone exhibited the second highest titers relative to the other groups tested, with the GNTI$^-$ gp120 immunized group displaying third highest titers, and the V123 (mixed-batch) immunized groups consistently exhibiting lowest titers.

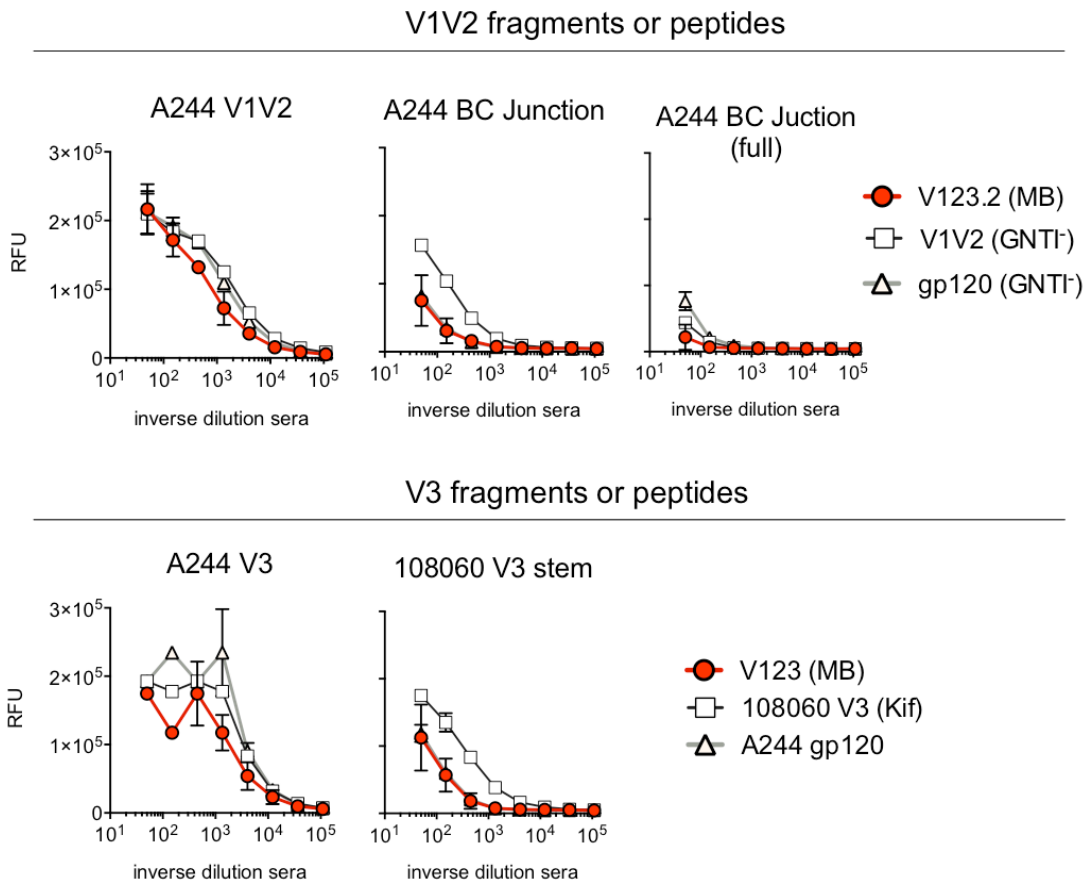

Figure 4-23 Antibody titers to regions in the V1V2 or V3 domains. Two New Zealand White rabbits were entered into an immunization experiment with A244 V123 scaffolds prepared using a mixed-batch expression protocol. Sera from the V123 immunized rabbits was compared to matched immunization bleeds from previous immunization experiments (detailed in **TABLE 4-7**Antibody binding titers to a streptavidin tagged A244 V1V2 fragment expressed in GNTI$^-$ cell line, or linear peptides to the V2 or V3 domain were assayed by fluorescence immunoassay. All assays were performed on pooled sera from two or more rabbits, and curves shown are the average of duplicate assays, and error bars represent standard error.

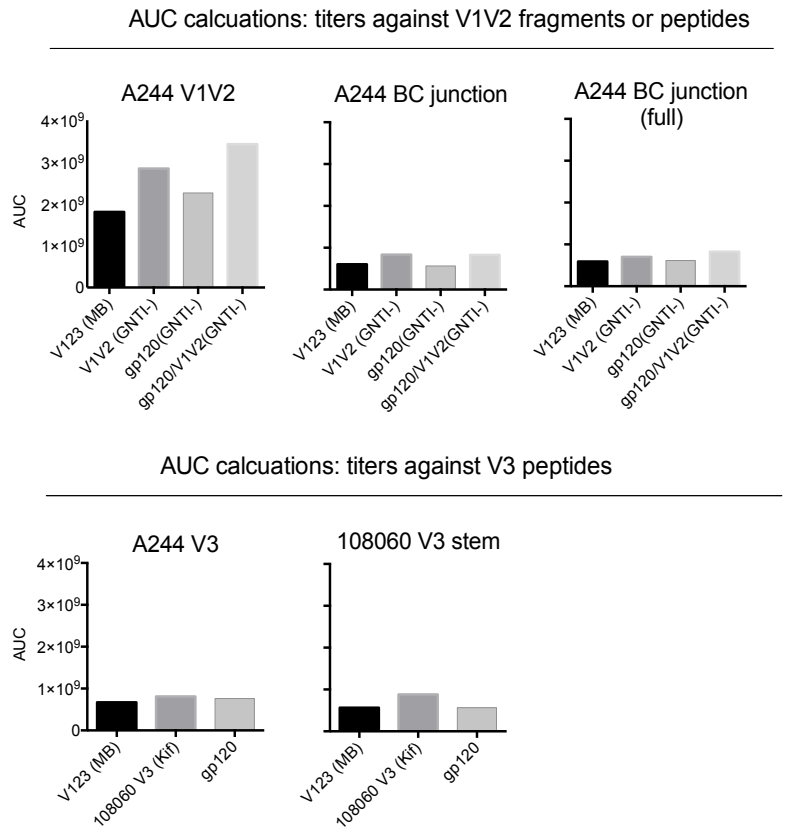

Figure 4-24 Area under the Curve (AUC) calculations of Antibody titers to regions in the V1V2 or V3 domains. Area under the Curve (AUC) calculations were performed to quantitate differences amongst FIA binding titers previously shown using the GraphPad Prism version 6.0 for Mac, GraphPad Software, La Jolla California USA, www.graphpad.com.

Expression of V123 fragments of different linker lengths

To understand how linker length may affect bNAb binding, we expressed the V123 fragments with different linker lengths in either HEK 293 GNTI$^-$, or kifunensine-treated HEK 293 cells. V123 fragment constructs were designed with either no GGGGS-linker (0x), one linker repeat (1x), two consecutive linker repeats (2x), or as the original 3 linker construct (3x). The nucleotide and amino acid sequences of the different constructs are detailed in **SUPPLEMENTAL TABLE 4-2.** We estimated levels of V123 protein expression in the different

cell expression systems with a quantitative SDS-PAGE and found that the HEK GNTI$^-$ expressed the V123 fragment at a level above20ng/mL (**FIGURE 4-25**). All 293 + kif expressed scaffolds expressed above 20 ng/mL, but the GNTI$^-$ expressed scaffolds expressed at lower levels, with all expressing at least above 5 ng/mL. There appeared to be a general trend of a lower number of linker repeats displaying higher expression levels, with the 0X linker construct displaying highest expression, and the 3X linker construct displaying amongst the lowest expression levels.

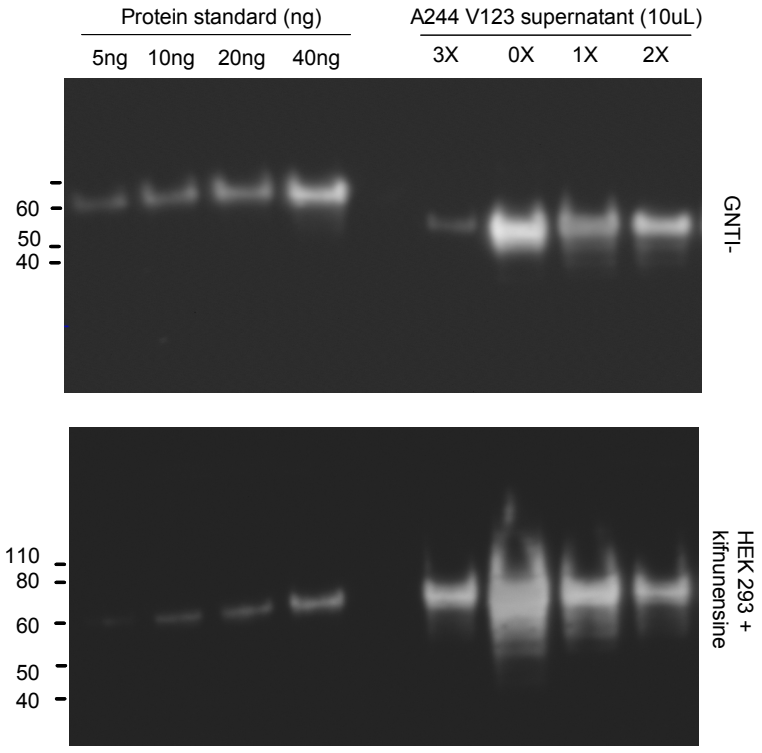

Figure 4-25 Estimation of V123 expression levels in cell culture supernatant by SDS-PAGE and western blot. Cell conditioned supernatant was harvested 5 days post-transfection, and 10 μL of protein were reduced and loaded analyzed by SDS-PAGE. Known concentrations of purified A244 V123 scaffold grown 293 GNTI$^-$ (top) or HEK 293 kifunensine treated cells were loaded as a standard. Gels were probed with anti-gD 34.2 and visualized with HRP-conjugated goat-anti-mouse polyclonal antibody.

When unpurified V123 fragments expressed in GNTI$^-$ cells were run as reduced or unreduced gels on SDS-PAGE, they ran as two distinct bands as seen in the affinity-purified V123 (GGGGSx3) protein preparations detailed previously. The major species exhibited the predicted molecular weight of a monomeric V123 scaffold displaying predominantly mannose-5 glycoforms. When run as unreduced samples, all the supernatants containing the different V123 GGGGS linker variants contained a minor a band at ~80kDa (**FIGURE 4-26**). A ~120kDa band could be found in the lane containing the unreduced 0X protein, indicating the presence of a higher weight V123 oligomer. This band may have been seen only in the 0X sample as the 0X linker protein displayed the highest expression. Thus, while undetectable by this assay, it is possible more species of unpurified V123 linker variants may additionally contain higher-level oligomers. However, overall, it appears that all the GGGGS linker length variants exhibit a degree of oligomerization upon expression.

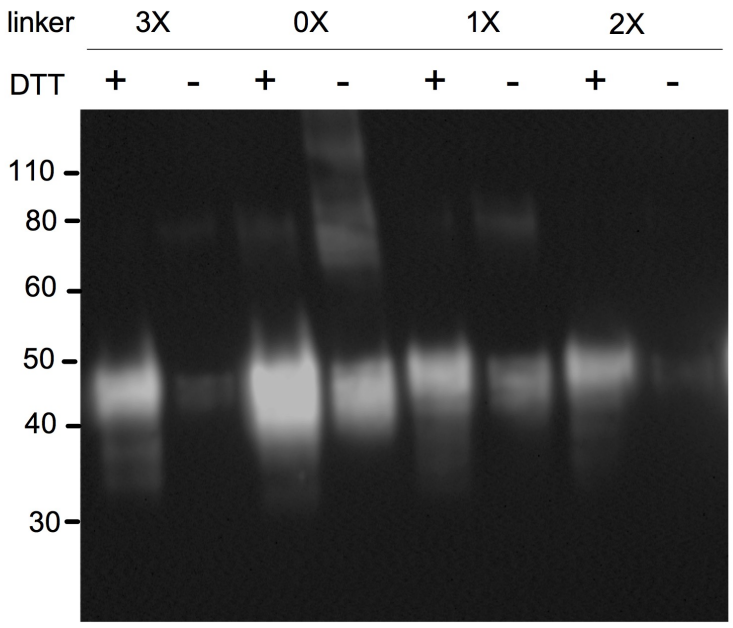

Figure 4-26 Reduced and unreduced gels of A244 V123 fragments with variation in linker length. Cell conditioned supernatant was harvested 5 days post-transfection, and cell culture supernatants were concentrated ~10x for V123 fragments. V123 fragments were run as DTT reduced or non-reduced preparations on SDS-PAGE, probed with anti-gD 34.2 and visualized using HRP-conjugated goat-anti-mouse polyclonal antibody.

bNAb binding to V123 linker variants

The A244 V123 fragments expressing the 0x, 1x, 2x, or 3x GGGS linkers were assessed for binding to various conformation- and non-conformation- dependent antibodies that target glycan-dependent epitopes within the V2 domain (PG9, CHO1 and CHO3), and glycan-dependent epitopes based in the V3 domain (PGT121, 125, 126, 128, and 130). Interestingly, the number of linker motifs incorporated (0, 1, 2 or 3) did not affect binding to the PG9 or PGT128 bNAbs when expressed in the GNTI$^-$ or kifunensine treated 293 cells, respectively (**FIGURE 4-27**).

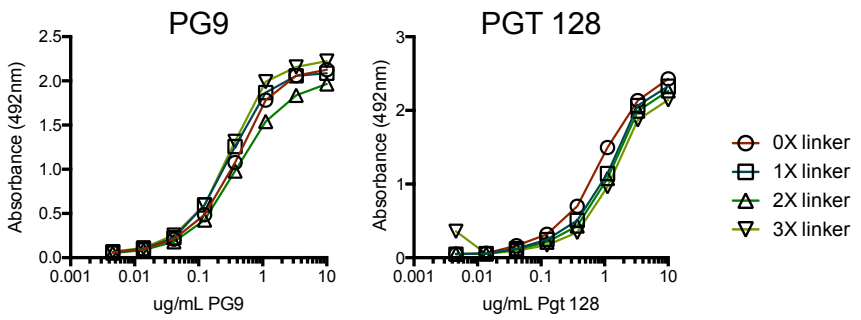

Figure 4-27 Binding of V123 fragments expressed in GNTI$^-$ or kifnuensine treated 293 cells to prototypic bNAbs. Four different A244 V123 fragments were engineered to contain 0, 1, 2, or 3 repeats of the GGGS linker sequence and assayed for antigenicity to bNAbs by a capture ELISA. Fragment binding to the V1V2 and V3 directed glycan dependent bNabs (PG9 and PGT 128, respectively) was used to identify whether linker length affected gross structure and antigenicity. Fragment linker variants were expressed in either 293 GNTI$^-$ cells were assayed against the PG9 bNab (**left)** and fragments expressed in kifunensine treated 293 cells were assessed for binding to the PGT 128 bNAb (**right**). Cell culture supernatant containing either Kif produced material, or GNTI$^-$ produced material, was normalized for A244 V123 content, and captured onto 34.1 coated plates via a gD tag and incubated with serial dilutions of bNAb. Antibody:antigen complexes were probed with of Fc specific peroxidase-conjugated goat anti-human IgG and developed with OPD substrate.

4.4 Discussion

Overall, the MGAT-expressed rgp120 displayed some differences in overall immunogenicity after three immunizations. Robust titers were seen in both groups against full-length rgp120 as well as to gp120 fragments within the V1V2 and V3 domain that were associated with protection in RV144. Interestingly, animals immunized with CHO-expressed rgp120 did appear to have a more consistent titer, while MGAT rgp120-immunized guinea pigs displayed a broad range of titers to antigens assayed. In spite of the major changes in charge and size of glycoforms presented (highly charged, large sialic acid glycoforms on the CHO derived rgp120, as opposed to the smaller, uncharged oligomannose glycoforms of MGAT derived rgp120), there appeared to be no major change to the overall immunogenicity

of the V1V2 and V3 epitopes assayed. Immunization with CHO rgp120 appeared to elicit a higher titer of antibodies that compete with PG9 binding, though it is not known if this population of antibodies would contribute to protection against infection.

As the AIDSVAX B/E, in conjunction with the VCP1521 canarypox vector, established a baseline of vaccine efficacy, building upon this immunization protocol offers a logical approach to optimizing a safe and effective vaccine. We propose that evaluating the efficacy of the immunogens described herein represents a systematic, stepwise modification in structure to improve vaccine efficacy. The immunogens using the glycan optimization strategies outlined in this report can be used in follow up studies in conjunction, or in parallel with RV144 follow-up studies investigating the role of A244, MN, or other gp120 immunogens in the elicitation of a protective immune response.

Following the results of the gp20 immunogenicity experiments, we aimed to create gp120 fragments that could be used to increase the magnitude of the antibody response against epitopes that correlated with protection in the RV144 trials. We were able to express V3 fragments of multiple clades that could bind to the prototypic V3 glycan dependent bNAb PGT128 in a glycoform-dependent manner. V3 fragments grown in kifunensine, and therefore displaying oligomannose glycoforms susceptible to Endo H digest, can be recognized by the PGT128 bNAb in a manner similar to previously described V3 fragments (163). However, immunization with these fragments failed to significantly improve titers to V3 peptides assayed in most cases. Interestingly, immunization protocols in which V3 fragments were used (immunization groups 3, 4, and 5) resulted in a slight increase in titers to the C terminus of the V3 stem peptide that contains amino acid epitopes bound by the PGT128 bNAb (132). However, minor improvements in titer to V3 epitopes did not reflect as improvements in neutralization titers to same or cross-clade viruses in TZM/bl neutralization assays. Despite this, such data is preliminary evidence that that the use of V3 fragments changes the

immunodominance of the V3 domain. In the face of the long-observed immunodominance of the V3 crown epitope (222), strategies to improve the immunogenicity of the V3 stem loop may be relevant to inducing bNAb-like antibodies. Thus, V3 fragment immunogens may have relevance in future immunization protocols.

We additionally explored the development of a minimal fragment containing the V1V2 and V3 domains of gp120. We found that V123 fragment could be designed with varying flexible (GGGGS) linkers that bind a broad family of broadly neutralizing antibodies in a glycoform-dependent manner. The V123 fragments could additionally be expressed in a mixed-batch fermentation process, which allowed the expression of a population of V123 fragments in which approximately 50% of the product contained predominantly mannose-5 glycoforms, and 50% of the product contained mannose-9 glycoforms. When compared to similar immunization protocols of gp120 or V1V2 of V3 immunization, the V123 fragment produced in mixed-batch culture did not significantly increase titers to peptides within the V1V2 or V3 domains. While varying the number of GGGGS linker repeats did not affect binding to bNAbs, it appeared to affect expression, with a general trend of increasing number of linkers correlating in decreased expression. This fragment might be further improved upon, either by linkage to nanoparticles or alone to increase the quality and magnitude of an immune response to highly neutralization-relevant regions of the virus envelope protein

Construct	Sequence
UCSC 907 MN 468 V3 fragment	Nucleotide: GCACGAGAATTCATGGGCGGAGCCGCCGCTAGACTGGGAGCCG TGATTCTGTTCGTCGTGATCGTGGGCCTGCATGGCGTGCGGGGC AAATATGCCCTGGCCGATGCCAGCCTGAAGATGGCCGACCCCAA CCGGTTCAGAGGCAAGGACCTGCCCGTGCTGGATCAGCTGCTG GAGGTACCAAGAAGCGAGGACTTCACCGACAACGCCAAGACCAT CATCGTGCACCTGAACGAGAGCGTGCAGATCAACTGCACCCGGC CCAACAACAACACCCGGAAGCGGATCCACATCGGCCCTGGCAGA GCCTTCTACACCACCAAGAACATCAAGGGCACCATCAGACAGGC CCACTGCAACATCAGCCGGGCCAAGTGGAACGACTGAGCGGCC GCAAAAGGAAAA Amino Acid: GAAARLGAVILFVVIVGLHGVRGKYALADASLKMADPNRFRGKDLPV LDQLLEVPRSEDFTDNAKTIIVHLNESVQINCTRPNNNTRKRIHIGPG RAFYTTKNIKGTIRQAHCNISRAKWND*
UCSC 908 CN97001 V3 fragment	Nucleotide: GCACGAGAATTCATGGGCGGAGCCGCCGCTAGACTGGGAGCCG TGATTCTGTTCGTCGTGATCGTGGGCCTGCATGGCGTGCGGGGC AAATATGCCCTGGCCGATGCCAGCCTGAAGATGGCCGACCCCAA CCGGTTCAGAGGCAAGGACCTGCCCGTGCTGGATCAGCTGCTG GAGGTACCAAGAAGCGAGAACCTGACCAACAACGTGAAAACCAT CATCGTGCACCTGAACCAGAGCGTGGAAATCGTGTGCACCAGAC CCGGCAACAACACCAGAAAGAGCATCCGGATCGGCCCTGGCCA GACCTTTTACGCCACCGGCGACATCATCGGCGATATCAGACAGG CCCACTGCAACATCAGCGAGGACAAGTGGAACGAATGAGCGGC CGCAAAAGGAAAA Amino Acid: MGGAAARLGAVILFVVIVGLHGVRGKYALADASLKMADPNRFRGKD LPVLDQLLEVPRSENLTNNVKTIIVHLNQSVEIVCTRPGNNTRKSIRIG PGQTFYATGDIIGDIRQAHCNISEDKWNE*
UCSC 909 TZ97008 V3 fragment	Nucleotide: GCACGAGAATTCATGGGCGGAGCCGCCGCTAGACTGGGAGCCG TGATTCTGTTCGTCGTGATCGTGGGCCTGCATGGCGTGCGGGGC AAATATGCCCTGGCCGATGCCAGCCTGAAGATGGCCGACCCCAA CCGGTTCAGAGGCAAGGACCTGCCCGTGCTGGATCAGCTGCTG GAGGTACCAAGAAGCAAGAACCTGACCGACAACGTGAAAACCAT CATCGTGCACCTGAACGAGAGCGTGGAAATCACCTGTATCAGAC CCGGCAACAACACCAGAAAGAGCATCCGGATCGGCCCAGGCCA GGCCTTTTATGCCACCGGCGACATCATCGGCAACATCAGACAGG CCCACTGCAACATCTCCGAGGACAAGTGGAACAAATGAGCGGCC GCAAAAGGAAAA Amino Acid: AREFMGGAAARLGAVILFVVIVGLHGVRGKYALADASLKMADPNRFR

	GKDLPVLDQLLEVPRSKNLTDNVKTIIVHLNESVEITCIRPGNNTRKSI RIGPGQAFYATGDIIGNIRQAHCNISEDKWNK*AAAKGK
UCSC 910 Bal V3 fragment	Nucleotide: GCACGAGAATTCATGGGCGGAGCCGCCGCTAGACTGGGAGCCG TGATTCTGTTCGTCGTGATCGTGGGCCTGCATGGCGTGCGGGGC AAATATGCCCTGGCCGATGCCAGCCTGAAGATGGCCGACCCCAA CCGGTTCAGAGGCAAGGACCTGCCCGTGCTGGATCAGCTGCTG GAGGTACCAAGAAGCGAGAACTTCACCAACAACGCCAAGACCAT CATCGTGCAGCTGAACGAGAGCGTGGAAATCAACTGCACCCGGC CCAACAACAACACCAGAAAGAGCATCAACATCGGCCCTGGCAGA GCCTTCTACACCACCGGCGAGATCATCGGCGACATCAGACAGGC CCACTGCAACCTGAGCCGGGCCAAGTGGAACGACTGAGCGGCC GCAAAAGGAAAA Amino Acid: MGGAAARLGAVILFVVIVGLHGVRGKYALADASLKMADPNRFRGKD LPVLDQLLEVPRSENFTNNAKTIIVQLNESVEINCTRPNNNTRKSINIG PGRAFYTTGEIIGDIRQAHCNLSRAKWND*
UCSC 703 108060 V3 fragment	Nucleotide: NNNNNNNNNNNNNNNTCGGTTCTATCGATTGAATTCCACTGCCTT CCACCAAGCTCTGCAGGATCCCAGAGTCAGGGGTCTGTATCTTC CTGCTGGTGGCTCCAGTTCAGGAACAGTAAACCCTGCTCCGAAT ATTGCCTCTCACATCTCGTCAATCTCCGCGAGGACTGGGGACCC TGTGACCTCAAGCTTCAGCGCGAACGACCAACTACCCCGATCAT CAGTTATCCTTAAGGTCTCTTTTGTGTGGTGCGTTCCGGTATGGG GGGGGCTGCCGCCAGGTTGGGGGCCGTGATTTTGTTTGTCGTCA TAGTGGGCCTCCATGGGGTCCGCGGCAAATATGCCTTGGCGGAT GCCTCTCTCAAGATGGCCGACCCCAATCGATTTCGCGGCAAAGA CCTTCCGGTCCTGGACCAGCTGCTCGAGGTACCAAGATCAGACA ATTTCTCGCAAAATGCCAAAATCATAATAGTACAGCTAAATGAAGC TGTAGTAATTAATTGTACAAGACCCGGCAACAATACAAGGAAAAG TATACCTATAGGACCAGGGAGAGCATTTTATGCAACAGGAGACAT AATAGGAAATATAAGACAAGCACATTGTAACGTTAGTAGTACAAA ATGGAATAATTAGCGGCCGCTCTAGAACTAGTGGATCCCCCGGG CTGCAGGAATTCGA Amino Acid: MGGAAARLGAVILFVVIVGLHGVRGKYALADASLKMADPNRFRGKD LPVLDQLLEVPRSDNFSQNAKIIIVQLNEAVVINCTRPGNNTRKSIPIG PGRAFYATGDIIGNIRQAHCNVSSTKWNN*

Supplemental Table 4-1 Summary of V3 constructs. Nucleotide and amino acid sequences of sequences of V3 fragments from diverse clades that were expressed as gp120 protein fragments.

A244_N332_W338A_V123_C119A_C205A_NtermgD_3xGGGGS (UCSC1209)	
>UCSC1209 ATGGGCGGAGCCGCCGCTAGACTGGGAGCCGTGATTCTGTTCGTCGTGATCGTGGG CCTGCATGGCGTGCGGGGCAAATATGCCCTGGCCGATGCCAGCCTGAAGATGGCCG ACCCCAACCGGTTCAGAGGCAAGGACCTGCCCGTGCTGGATCAGCTGCTGGAGGTA CCACTGAAGCCCGCCGTGAAGCTGACCCCTCCTTGTGTGACCCTGCACTGCACCAA CGCCAACCTGACCAAGGCCAATCTGACAAACGTGAACAACCGGACCAACGTGTCCAA CATCATCGGCAACATCACCGACGAAGTGCGGAACTGCAGCTTCAACATGACCACCGA GCTGCGGGACAAGAAACAGAAGGTGCACGCCCTGTTCTACAAGCTGGACATCGTGC CCATCGAGGACAACAACGACAGCAGCGAGTACCGGCTGATCAACTGCAACACCAGC GTGATCAAGCAGGCCGCTCCCAAGATCAGCTTCGACCCTGGCGGCGGAGGATCTGG CGGAGGCGGAAGTGGCGGAGGGGGCTCTGTGATCAATTGCACCCGGCCCAGCAAC AACACCAGAACCAGCATCACCATCGGCCCAGGCCAGGTGTTCTACCGGACCGGCGA TATCATCGGAGACATCCGGAAGGCCTACTGCAACATCAGCGGCACCGAGTGGAACT GA	
>UCSC1209 MGGAAARLGAVILFVVIVGLHGVRGKYALADASLKMADPNRFRGKDLPVLDQLLEVPLKP AVKLTPPCVTLHCTNANLTKANLTNVNNRTNVSNIIGNITDEVRNCSFNMTTELRDKKQKV HALFYKLDIVPIEDNNDSSEYRLINCNTSVIKQAAPKISFDPGGGGSGGGGSGGGGSVINC TRPSNNTRTSITIGPGQVFYRTGDIIGDIRKAYCNISGTEWN**	
I.	gD-1 ss MGGAAARLGAVILFVVIVGLHGVRG
II.	gD-1 flag KYALADASLKMADPNRFRGKDLPVLDQ
IV.	V123, C3 regions MGGAAARLGAVILFVVIVGLHGVRGKYALADASLKMADPNRFRGKDLPVLDQLLEVP LKPAVKLTPPCVTLHCTNANLTKANLTNVNNRTNVSNIIGNITDEVRNCSFNMTTELR DKKQKVHALFYKLDIVPIEDNNDSSEYRLINCNTSVIKQAAPKISFDP, and VINCTRPSNNTRTSITIGPGQVFYRTGDIIGDIRKAYCNISGTEWN *
A244_N332_W338A_V123_C119A_C205A_NtermgD_3xGGGGS (UCSC1242)	
>UCSC1242 ATGGGCGGAGCCGCTGCTAGACTGGGAGCCGTGATCCTGTTCGTCGTGATCGTGGG ACTGCATGGCGTGCGGGGCAAATACGCCCTGGCCGATGCCTCTCTGAAGATGGCCG ACCCCAACCGGTTCCGGGGCAAGGATCTGCCTGTGCTGGATCAGCTGCTGGAGGTA CCACTGAAGCCCGCCGTGAAGCTGACCCCTCCTTGTGTGACCCTGCACTGCACCAA CGCCAACCTGACCAAGGCCAATCTGACAAACGTGAACAACCGGACCAACGTGTCCAA CATCATCGGCAACATCACCGACGAAGTGCGGAACTGCAGCTTCAACATGACCACCGA GCTGCGGGACAAGAAACAGAAGGTGCACGCCCTGTTCTACAAGCTGGACATCGTGC CCATCGAGGACAACAACGACAGCAGCGAGTACCGGCTGATCAACTGCAACACCAGC GTGATCAAGCAGGCCGCTCCCAAGATCAGCTTCGACCCTGGCGGCGGAGGATCTGG CGGAGGCGGAAGTGGCGGAGGGGGCTCTGTGATCAATTGCACCCGGCCCAGCAAC AACACCAGAACCAGCATCACCATCGGCCCAGGCCAGGTGTTCTACCGGACCGGCGA TATCATCGGAGACATCCGGAAGGCCTACTGCAACATCTCCGGCACCGAGGCCAACTA G	
>UCSC1242 EFHCLPPSSAGSQSQGSVSSCWWLQFRNSKPCSEYCLSHLVNLREDWGPCDLKLQRE RPTTPIISYP*GLFCVVRSGMGGAAARLGAVILFVVIVGLHGVRGKYALADASLKMADPNR FRGKDLPVLDQLLEVPLKPAVKLTPPCVTLHCTNANLTKANLTNVNNRTNVSNIIGNITDEV RNCSFNMTTELRDKKQKVHALFYKLDIVPIEDNNDSSEYRLINCNTSVIKQAAPKISFDPG GGGSGGGGSGGGGSVINCTRPSNNTRTSITIGPGQVFYRTGDIIGDIRKAYCNISGTEAN*	
I.	gD-1 ss MGGAAARLGAVILFVVIVGLHGVRG

II.	gD-1 flag KYALADASLKMADPNRFRGKDLPVLDQ
IV.	V123, C3 regions LKPAVKLTPPCVTLHCTNANLTKANLTNVNNRTNVSNIIGNITDEVRNCSFNMTTELR DKKQKVHALFYKLDIVPIEDNNDSSEYRLINCNTSVIKQAAPKISFDP, and VINCTRPSNNTRTSITIGPGQVFYRTGDIIGDIRKAYCNISGTEAN*
A244_N332_W338A_V123_C119A_C205A_V123_NtermgD_1xGGGGS (UCSC1244)	
>UCSC1244 ATGGGCGGAGCCGCTGCTAGACTGGGAGCCGTGATCCTGTTCGTCGTGATCGTGGG ACTGCATGGCGTGCGGGGCAAATACGCCCTGGCCGATGCCTCTCTGAAGATGGCCG ACCCCAACCGGTTCCGGGGCAAGGATCTGCCTGTGCTGGATCAGCTGCTGGAGGTA CCACTGAAGCCCGCCGTGAAGCTGACCCCTCCTTGTGTGACCCTGCACTGCACCAA CGCCAACCTGACCAAGGCCAATCTGACAAACGTGAACAACCGGACCAACGTGTCCAA CATCATCGGCAACATCACCGACGAAGTGCGGAACTGCAGCTTCAACATGACCACCGA GCTGCGGGACAAGAAACAGAAGGTGCACGCCCTGTTCTACAAGCTGGACATCGTGC CCATCGAGGACAACAACGACAGCAGCGAGTACCGGCTGATCAACTGCAACACCAGC GTGATCAAGCAGGCCGCTCCCAAGATCAGCTTCGACCCTGGCGGCGGAGGCAGCG GATCCGTGATCAATTGCACCCGGCCCAGCAACAACACCAGAACCAGCATCACCATCG GCCCAGGCCAGGTGTTCTACCGGACCGGCGATATCATCGGAGACATCCGGAAGGCC TACTGCAACATCTCCGGCACCGAGGCCAACTAG	
>UCSC1244 EFHCLPPSSAGSQSQGSVSSCWWLQFRNSKPCSEYCLSHLVNLREDWGPCDLKLQRE RPTTPIISYP*GLFCVVRSGMGGAAARLGAVILFVVIVGLHGVRGKYALADASLKMADPNR FRGKDLPVLDQLLEVPLKPAVKLTPPCVTLHCTNANLTKANLTNVNNRTNVSNIIGNITDEV RNCSFNMTTELRDKKQKVHALFYKLDIVPIEDNNDSSEYRLINCNTSVIKQAAPKISFDPG GGGSGSVINCTRPSNNTRTSITIGPGQVFYRTGDIIGDIRKAYCNISGTEAN*	
I.	gD-1 ss MGGAAARLGAVILFVVIVGLHGVRG
II.	gD-1 flag KYALADASLKMADPNRFRGKDLPVLDQ
III.	Linkers LLEVP, GGGGSGS
A244_N332_W338A_V123_C119A_C205A_NtermgD_2xGGGGS (UCSC1245)	
>UCSC1245 ATGGGCGGAGCCGCTGCTAGACTGGGAGCCGTGATCCTGTTCGTCGTGATCGTGGG ACTGCATGGCGTGCGGGGCAAATACGCCCTGGCCGATGCCTCTCTGAAGATGGCCG ACCCCAACCGGTTCCGGGGCAAGGATCTGCCTGTGCTGGATCAGCTGCTGGAGGTA CCACTGAAGCCCGCCGTGAAGCTGACCCCTCCTTGTGTGACCCTGCACTGCACCAA CGCCAACCTGACCAAGGCCAATCTGACAAACGTGAACAACCGGACCAACGTGTCCAA CATCATCGGCAACATCACCGACGAAGTGCGGAACTGCAGCTTCAACATGACCACCGA GCTGCGGGACAAGAAACAGAAGGTGCACGCCCTGTTCTACAAGCTGGACATCGTGC CCATCGAGGACAACAACGACAGCAGCGAGTACCGGCTGATCAACTGCAACACCAGC GTGATCAAGCAGGCCGCTCCCAAGATCAGCTTCGACCCTGGCGGCGGAGGATCTGG CGGAGGCGGCTCTGTGATCAATTGCACCCGGCCCAGCAACAACACCAGAACCAGCA TCACCATCGGCCCAGGCCAGGTGTTCTACCGGACCGGCGATATCATCGGAGACATC CGGAAGGCCTACTGCAACATCTCCGGCACCGAGGCCAACTAG	
>UCSC1245 EFHCLPPSSAGSQSQGSVSSCWWLQFRNSKPCSEYCLSHLVNLREDWGPCDLKLQRE RPTTPIISYP*GLFCVVRSGMGGAAARLGAVILFVVIVGLHGVRGKYALADASLKMADPNR FRGKDLPVLDQLLEVPLKPAVKLTPPCVTLHCTNANLTKANLTNVNNRTNVSNIIGNITDEV	

RNCSFNMTTELRDKKQKVHALFYKLDIVPIEDNNDSSEYRLINCNTSVIKQAAPKISFDPG GGGSGGGGSVINCTRPSNNTRTSITIGPGQVFYRTGDIIGDIRKAYCNISGTEAN*	
I.	gD-1 ss MGGAAARLGAVILFVVIVGLHGVRG
II.	gD-1 flag KYALADASLKMADPNRFRGKDLPVLDQ
III.	Linkers LLEVP, GGGGSGGGGS
IV.	V123 and V3 regions LKPAVKLTPPCVTLHCTNANLTKANLTNVNNRTNVSNIIGNITDEVRNCSFNMTTELR DKKQKVHALFYKLDIVPIEDNNDSSEYRLINCNTSVIKQAAPKISFDP, and VINCTRPSNNTRTSITIGPGQVFYRTGDIIGDIRKAYCNISGTEAN*

Supplemental Table 4-2 Nucleotide and Amino acid sequences of expressed A244 V123 constructs. Sequence characteristics, such as the appended N-terminal gD signal sequence (ss), gD flag tag, and linkers, are included.

Conclusion

The development of a safe, effective vaccine for HIV continues to be a challenge. The diversity and biology of HIV make it a formidable target in the context of both natural infection and vaccine design. Additionally, historical challenges in HIV vaccine immunogen production and purification have presented additional hurdles to vaccine development. The data presented here contribute rationale, techniques, and potential immunogens to the field of gp120 based vaccine design. Firstly, the isolation of the monoclonal antibody 4B6 from a clade B gp140 immunogen showed a glycan epitope within the V1V2 domain can be immunogenic, and that antibodies can be raised to such epitopes under short immunization protocols. The addition of two or fewer conserved glycans, and modification of glycoform on the A244 and MN gp120 described a method to improve gp120 immunogens. Such methods can be applied to gp120 proteins of different strains to create gp120 proteins that better emulate the virion associated gp120 seen in the context of infection and recognized by bNAbs. Finally, the rapid development of the TZ97008 clade C gp120 expressing MGAT^{-} CHO cell line employed glycan modifications to produce a gp120 immunogen. The process used to make the TZ97008 immunogen is both scalable and amenable to cGMP production and can therefore be applied to other gp120 proteins for use in research or clinical trials.

The antibody-based correlates of protection identified in the RV144 trial provided impetuous to further pursue gp120 based HIV vaccine immunogens. However, a gp120 based vaccine will likely not be successful alone. Unfortunately, gp120-based vaccines have historically failed to elicit long lived anti-gp120 antibody-titers. Vaccine components designed to elicit a robust T-cell response against HIV, such as the canarypox vector or DNA priming immunogens, are currently being investigated for their potential to improve the magnitude and duration of the anti-gp120 antibody response (153, 154, 223). Thus, such components or

adjuvants may provide additional methods to improve upon the potential of the glycan-modified gp120 immunogens described here.

The studies described in this dissertation show that the antigenic structure of gp120 can be substantially improved with respect to the binding of broadly neutralizing antibodies. The discovery of glycan dependent epitopes on the HIV envelope protein was surprising and little is known about the best method to optimize antibody responses to these types of epitopes, which may be relevant not only for HIV, but also for other, heavily glycosylated viruses, such as cytomegalovirus. It is likely that immunogenicity studies in humans will be required to investigate this aspect of virus immunology. The novel cell lines and molecules described in this thesis were designed to enable studies in humans and further advance this area of research. We hope that ultimately, the stable, defined gp120 preparations described here can be used in immunogenicity experiments investigating protocols designed to elicit antibody responses to glycan dependent epitopes.

References

1. Jenner E. An Inquiry Into the Causes and Effects of the Variolæ Vaccinæ, Or Cow-Pox. In: Low, editor. iv, 116 p., [4] leaves of plates ed. London1798. p. 4.

2. Pasteur L. Mèthode pour prévenir la rage apres morsure. C R Acad Sci Paris. 1885;101:765–72.

3. Theiler M, Smith HH. The Effect of Prolonged Cultivation in vitro Upon the Pathogenicity of Yellow Fever Virus. 1937.

4. Sabin AB, Hennessen WA, Wincer J. Studies on Varients of Poliomyletis Virus. 1954.

5. Katz SL, Kempe CH, Black FL, Lepow ML, Krugman S, Haggerty RJ, et al. Studies on an attenuated measles-virus vaccine. VIII. General summary and evaluation of the results of vaccination. Am J Dis Child. 1960;100:942-6.

6. Hilleman MR, Buynak EB, Weibel RE, Stokes JJ. Live, Attenuated Mumps-Virus Vaccine. New England Journal of Medicine. 1968;278(5):227-32.

7. Plotkin SA, Farquhar JD, Katz M, Buser F. Attenuation of RA 27-3 rubella virus in WI-38 human diploid cells. Am J Dis Child. 1969;118(2):178-85.

8. Takahashi M, Okuno Y, Otsuka T, Osame J, Takamizawa A. Development of a live attenuated varicella vaccine. Biken J. 1975;18(1):25-33.

9. Pfeffer R, Kolle W. Experimentelle Untersuchungen zur Frage der Schutzimpfung des Menschen gegen Typhus

abdominalis. Deutsche Medizinische Wochenschrift. 1896;22:735-7.

10. Madsen T. Vaccination Against Whooping Cough. Journal of the American Medical Association. 1933;101(3):187-8.

11. Glenny AT, Hopkins BE. Diphtheria Toxoid as an Immunising Agent. Br J Exp Pathol. 1923;4(5):283-8.

12. Salk JE, Krech U, Youngner JS, Bennett BL, Lewis LJ, Bazeley PL. Formaldehyde treatment and safety testing of experimental poliomyelitis vaccines. Am J Public Health Nations Health. 1954;44(5):563-70.

13. Provost PJ, Hughes JV, Miller WJ, Giesa PA, Banker FS, Emini EA. An inactivated hepatitis A viral vaccine of cell culture origin. J Med Virol. 1986;19(1):23-31.

14. Nicholson KG, Tyrrell DA, Harrison P, Potter CW, Jennings R, Clark A, et al. Clinical studies of monovalent inactivated whole virus and subunit A/USSR/77 (H1N1) vaccine: serological responses and clinical reactions. J Biol Stand. 1979;7(2):123-36.

15. Wright PF, Thompson J, Vaughn WK, Folland DS, Sell SH, Karzon DT. Trials of influenza A/New Jersey/76 virus vaccine in normal children: an overview of age-related antigenicity and reactogenicity. J Infect Dis. 1977;136 Suppl:S731-41.

16. Gupta RK, Relyveld EH, Lindblad EB, Bizzini B, Ben-Efraim S, Gupta CK. Adjuvants--a balance between toxicity and adjuvanticity. Vaccine. 1993;11(3):293-306.

17. Sato Y, Sato H. Development of acellular pertussis vaccines. Biologicals. 1999;27(2):61-9.

18. Geeraedts F, Goutagny N, Hornung V, Severa M, de Haan A, Pool J, et al. Superior Immunogenicity of Inactivated Whole Virus H5N1 Influenza Vaccine is Primarily Controlled by Toll-like Receptor Signalling. PLoS Pathog. 42008.

19. Valenzuela P, Medina A, Rutter WJ, Ammerer G, Hall BD. Synthesis and assembly of hepatitis B virus surface antigen particles in yeast. Nature. 1982;298(5872):347.

20. Giuliani MM, Adu-Bobie J, Comanducci M, Aricò B, Savino S, Santini L, et al. A universal vaccine for serogroup B meningococcus. Proc Natl Acad Sci U S A. 1032006. p. 10834-9.

21. O'Ryan M, Stoddard J, Toneatto D, Wassil J, Dull PM. A multi-component meningococcal serogroup B vaccine (4CMenB): the clinical development program. Drugs. 2014;74(1):15-30.

22. Govan VA. A novel vaccine for cervical cancer: quadrivalent human papillomavirus (types 6, 11, 16 and 18) recombinant vaccine (Gardasil). Ther Clin Risk Manag. 2008;4(1):65-70.

23. Cuevas JM, Geller R, Garijo R, Lopez-Aldeguer J, Sanjuan R. Extremely High Mutation Rate of HIV-1 In Vivo. PLoS Biol. 2015;13(9):e1002251.

24. Learmont JC, Geczy AF, Mills J, Ashton LJ, Raynes-Greenow CH, Garsia RJ, et al. Immunologic and Virologic Status after 14 to 18 Years of Infection with an Attenuated Strain of HIV-1 — A Report from the Sydney Blood Bank Cohort. http://dxdoiorg/101056/NEJM199906033402203. 2008.

25. Korber B, Gaschen B, Yusim K, Thakallapally R, Kesmir C, Detours V. Evolutionary and immunological implications of contemporary HIV-1 variation. Br Med Bull. 2001;58:19-42.

26. Hughes SH, Coffin JM. What Integration Sites Tell Us about HIV Persistence. Cell Host Microbe. 2016;19(5):588-98.

27. Zhu P, Liu J, Bess J, Jr., Chertova E, Lifson JD, Grise H, et al. Distribution and three-dimensional structure of AIDS virus envelope spikes. Nature. 2006;441(7095):847-52.

28. Hatziioannou T, Evans DT. Animal models for HIV/AIDS research. Nat Rev Microbiol. 2012;10(12):852-67.

29. Morrow WJ, Wharton M, Lau D, Levy JA. Small animals are not susceptible to human immunodeficiency virus infection. J Gen Virol. 1987;68 (Pt 8):2253-7.

30. O'Neil SP, Novembre FJ, Hill AB, Suwyn C, Hart CE, Evans-Strickfaden T, et al. Progressive infection in a subset of HIV-1-positive chimpanzees. J Infect Dis. 2000;182(4):1051-62.

31. Chahroudi A, Bosinger SE, Vanderford TH, Paiardini M, Silvestri G. Natural SIV Hosts: Showing AIDS the Door. Science. 2012;335(6073).

32. Doores KJ, Bonomelli C, Harvey DJ, Vasiljevic S, Dwek RA, Burton DR, et al. Envelope glycans of immunodeficiency virions are almost entirely oligomannose antigens. Proc Natl Acad Sci U S A. 2010;107(31):13800-5.

33. Back NK, Smit L, De Jong JJ, Keulen W, Schutten M, Goudsmit J, et al. An N-glycan within the human immunodeficiency virus type 1 gp120 V3 loop affects virus neutralization. Virology. 1994;199(2):431-8.

34. McCaffrey RA, Saunders C, Hensel M, Stamatatos L. N-linked glycosylation of the V3 loop and the immunologically silent face of gp120 protects human immunodeficiency virus type 1 SF162 from neutralization by anti-gp120 and anti-gp41 antibodies. J Virol. 2004;78(7):3279-95.

35. Reitter JN, Means RE, Desrosiers RC. A role for carbohydrates in immune evasion in AIDS. Nat Med. 1998;4(6):679-84.

36. Wu Z, Kayman SC, Honnen W, Revesz K, Chen H, Vijh-Warrier S, et al. Characterization of neutralization epitopes in the V2 region of human

immunodeficiency virus type 1 gp120: role of glycosylation in the correct folding of the V1/V2 domain. J Virol. 1995;69(4):2271-8.

37. Kang SM, Quan FS, Huang C, Guo L, Ye L, Yang C, et al. Modified HIV envelope proteins with enhanced binding to neutralizing monoclonal antibodies. Virology. 2005;331(1):20-32.

38. Sagar M, Wu X, Lee S, Overbaugh J. Human immunodeficiency virus type 1 V1-V2 envelope loop sequences expand and add glycosylation sites over the course of infection, and these modifications affect antibody neutralization sensitivity. J Virol. 2006;80(19):9586-98.

39. Go EP, Liao HX, Alam SM, Hua D, Haynes BF, Desaire H. Characterization of Host-Cell Line Specific Glycosylation Profiles of Early Transmitted/Founder HIV-1 gp120 Envelope Proteins. J Proteome Res. 2013;12(3):1223-34.

40. Yu B, Morales JF, O'Rourke SM, Tatsuno GP, Berman PW. Glycoform and net charge heterogeneity in gp120 immunogens used in HIV vaccine trials. PLoS One. 2012;7(8):e43903.

41. Berman PW, Huang W, Riddle L, Gray AM, Wrin T, Vennari J, et al. Development of bivalent (B/E) vaccines able to neutralize CCR5-dependent viruses from the United States and Thailand. Virology. 1999;265(1):1-9.

42. Frey BF, Jiang J, Sui Y, Boyd LF, Yu B, Tatsuno G, et al. Effects of cross-presentation, antigen processing, and peptide binding in HIV evasion of T cell immunity*. J Immunol. 2018;200(5):1853-64.

43. Yu B, Fonseca DP, O'Rourke SM, Berman PW. Protease cleavage sites in HIV-1 gp120 recognized by antigen processing enzymes are conserved and located at receptor binding sites. J Virol. 2010;84(3):1513-26.

44. Rerks-Ngarm S, Pitisuttithum P, Nitayaphan S, Kaewkungwal J, Chiu J, Paris R, et al. Vaccination with ALVAC and AIDSVAX to prevent HIV-1 infection in Thailand. N Engl J Med. 2009;361(23):2209-20.

45. Cooney EL, McElrath MJ, Corey L, Hu SL, Collier AC, Arditti D, et al. Enhanced immunity to human immunodeficiency virus (HIV) envelope elicited by a combined vaccine regimen consisting of priming with a vaccinia recombinant expressing HIV envelope and boosting with gp160 protein. Proc Natl Acad Sci U S A. 1993;90(5):1882-6.

46. Haynes BF, Gilbert PB, McElrath MJ, Zolla-Pazner S, Tomaras GD, Alam SM, et al. Immune-correlates analysis of an HIV-1 vaccine efficacy trial. N Engl J Med. 2012;366(14):1275-86.

47. Liao HX, Bonsignori M, Alam SM, McLellan JS, Tomaras GD, Moody MA, et al. Vaccine induction of antibodies against a structurally heterogeneous site of

immune pressure within HIV-1 envelope protein variable regions 1 and 2. Immunity. 2013;38(1):176-86.

48. Zolla-Pazner S, deCamp A, Gilbert PB, Williams C, Yates NL, Williams WT, et al. Vaccine-induced IgG antibodies to V1V2 regions of multiple HIV-1 subtypes correlate with decreased risk of HIV-1 infection. PLoS One. 2014;9(2):e87572.

49. Gottardo R, Bailer RT, Korber BT, Gnanakaran S, Phillips J, Shen X, et al. Plasma IgG to linear epitopes in the V2 and V3 regions of HIV-1 gp120 correlate with a reduced risk of infection in the RV144 vaccine efficacy trial. PLoS One. 2013;8(9):e75665.

50. Plotkin SA. Correlates of protection induced by vaccination. Clin Vaccine Immunol. 17. United States2010. p. 1055-65.

51. Permar SR, Klumpp SA, Mansfield KG, Kim WK, Gorgone DA, Lifton MA, et al. Role of CD8(+) lymphocytes in control and clearance of measles virus infection of rhesus monkeys. J Virol. 2003;77(7):4396-400.

52. Bonsignori M, Pollara J, Moody MA, Alpert MD, Chen X, Hwang KK, et al. Antibody-dependent cellular cytotoxicity-mediating antibodies from an HIV-1 vaccine efficacy trial target multiple epitopes and preferentially use the VH1 gene family. J Virol. 2012;86(21):11521-32.

53. Baum LL, Cassutt KJ, Knigge K, Khattri R, Margolick J, Rinaldo C, et al. HIV-1 gp120-specific antibody-dependent cell-mediated cytotoxicity correlates with rate of disease progression. J Immunol. 1996;157(5):2168-73.

54. Chung AW, Ghebremichael M, Robinson H, Brown E, Choi I, Lane S, et al. Polyfunctional Fc-effector profiles mediated by IgG subclass selection distinguish RV144 and VAX003 vaccines. Sci Transl Med. 2014;6(228):228ra38.

55. Jefferis R. Isotype and glycoform selection for antibody therapeutics. Arch Biochem Biophys. 2012;526(2):159-66.

56. Saag M, University of Alabama at Birmingham B, Alabama, Deeks SG, San Francisco General Hospital UoC, San Francisco, California. How Do HIV Elite Controllers Do What They Do? Clinical Infectious Diseases. 2018;51(2):239-41.

57. Fellay J, Shianna KV, Ge D, Colombo S, Ledergerber B, Weale M, et al. A Whole-Genome Association Study of Major Determinants for Host Control of HIV-1. Science. 2007;317(5840):944-7.

58. Poropatich K, Sullivan DJ, Jr. Human immunodeficiency virus type 1 long-term non-progressors: the viral, genetic and immunological basis for disease non-progression. J Gen Virol. 2011;92(Pt 2):247-68.

59. Simek MD, Rida W, Priddy FH, Pung P, Carrow E, Laufer DS, et al. Human immunodeficiency virus type 1 elite neutralizers: individuals with broad and potent neutralizing activity identified by using a high-throughput neutralization

assay together with an analytical selection algorithm. J Virol. 83. United States2009. p. 7337-48.

60. Wibmer CK, Bhiman JN, Gray ES, Tumba N, Abdool Karim SS, Williamson C, et al. Viral escape from HIV-1 neutralizing antibodies drives increased plasma neutralization breadth through sequential recognition of multiple epitopes and immunotypes. PLoS Pathog. 2013;9(10):e1003738.

61. Moore PL, Gray ES, Wibmer CK, Bhiman JN, Nonyane M, Sheward DJ, et al. Evolution of an HIV glycan-dependent broadly neutralizing antibody epitope through immune escape. Nat Med. 2012;18(11):1688-92.

62. Klein F, Gaebler C, Mouquet H, Sather DN, Lehmann C, Scheid JF, et al. Broad neutralization by a combination of antibodies recognizing the CD4 binding site and a new conformational epitope on the HIV-1 envelope protein. J Exp Med. 2012;209(8):1469-79.

63. Scheid JF, Mouquet H, Feldhahn N, Seaman MS, Velinzon K, Pietzsch J, et al. Broad diversity of neutralizing antibodies isolated from memory B cells in HIV-infected individuals. Nature. 2009;458(7238):636-40.

64. Walker LM, Simek MD, Priddy F, Gach JS, Wagner D, Zwick MB, et al. A limited number of antibody specificities mediate broad and potent serum neutralization in selected HIV-1 infected individuals. PLoS Pathog. 2010;6(8):e1001028.

65. Walker LM, Huber M, Doores KJ, Falkowska E, Pejchal R, Julien JP, et al. Broad neutralization coverage of HIV by multiple highly potent antibodies. Nature. 2011;477(7365):466-70.

66. Bonsignori M, Hwang KK, Chen X, Tsao CY, Morris L, Gray E, et al. Analysis of a clonal lineage of HIV-1 envelope V2/V3 conformational epitope-specific broadly neutralizing antibodies and their inferred unmutated common ancestors. J Virol. 85. United States2011. p. 9998-10009.

67. Mouquet H, Scharf L, Euler Z, Liu Y, Eden C, Scheid JF, et al. Complex-type N-glycan recognition by potent broadly neutralizing HIV antibodies. Proc Natl Acad Sci U S A. 2012;109(47):E3268-77.

68. Burton DR, Hangartner L. Broadly Neutralizing Antibodies to HIV and Their Role in Vaccine Design. Annu Rev Immunol. 2016;34:635-59.

69. Moldt B, Rakasz EG, Schultz N, Chan-Hui PY, Swiderek K, Weisgrau KL, et al. Highly potent HIV-specific antibody neutralization in vitro translates into effective protection against mucosal SHIV challenge in vivo. Proc Natl Acad Sci U S A. 2012;109(46):18921-5.

70. Shingai M, Nishimura Y, Klein F, Mouquet H, Donau OK, Plishka R, et al. Antibody-mediated immunotherapy of macaques chronically infected with SHIV suppresses viraemia. Nature. 2013;503(7475):277-80.

71. Xiao X, Chen W, Feng Y, Zhu Z, Prabakaran P, Wang Y, et al. Germline-like predecessors of broadly neutralizing antibodies lack measurable binding to HIV-1 envelope glycoproteins: implications for evasion of immune responses and design of vaccine immunogens. Biochem Biophys Res Commun. 2009;390(3):404-9.

72. Hoot S, McGuire AT, Cohen KW, Strong RK, Hangartner L, Klein F, et al. Recombinant HIV envelope proteins fail to engage germline versions of anti-CD4bs bNAbs. PLoS Pathog. 2013;9(1):e1003106.

73. Klein F, Diskin R, Scheid JF, Gaebler C, Mouquet H, Georgiev IS, et al. Somatic mutations of the immunoglobulin framework are generally required for broad and potent HIV-1 neutralization. Cell. 2013;153(1):126-38.

74. Sok D, Laserson U, Laserson J, Liu Y, Vigneault F, Julien JP, et al. The effects of somatic hypermutation on neutralization and binding in the PGT121 family of broadly neutralizing HIV antibodies. PLoS Pathog. 2013;9(11):e1003754.

75. Chen W, Streaker ED, Russ DE, Feng Y, Prabakaran P, Dimitrov DS. Characterization of germline antibody libraries from human umbilical cord blood and selection of monoclonal antibodies to viral envelope glycoproteins: implications for mechanisms of immune evasion and design of vaccine immunogens. Biochem Biophys Res Commun. 2012;417(4):1164-9.

76. Liao HX, Lynch R, Zhou T, Gao F, Alam SM, Boyd SD, et al. Co-evolution of a broadly neutralizing HIV-1 antibody and founder virus. Nature. 2013;496(7446):469-76.

77. Doria-Rose NA, Schramm CA, Gorman J, Moore PL, Bhiman JN, DeKosky BJ, et al. Developmental pathway for potent V1V2-directed HIV-neutralizing antibodies. Nature. 2014;509(7498):55-62.

78. Jardine J, Julien JP, Menis S, Ota T, Kalyuzhniy O, McGuire A, et al. Rational HIV immunogen design to target specific germline B cell receptors. Science. 2013;340(6133):711-6.

79. Sok D, Laserson U, Laserson J, Liu Y, Vigneault F, Julien JP, et al. The Effects of Somatic Hypermutation on Neutralization and Binding in the PGT121 Family of Broadly Neutralizing HIV Antibodies. PLoS Pathog. 2013;9(11).

80. Klein F, Halper-Stromberg A, Horwitz JA, Gruell H, Scheid JF, Bournazos S, et al. HIV therapy by a combination of broadly neutralizing antibodies in humanized mice. Nature. 2012;492(7427):118-22.

81. Julg B, Liu P-T, Wagh K, Fischer WM, Abbink P, Mercado NB, et al. Protection against a mixed SHIV challenge by a broadly neutralizing antibody cocktail. 2017.

82. Yates NL, Liao HX, Fong Y, deCamp A, Vandergrift NA, Williams WT, et al. Vaccine-induced Env V1-V2 IgG3 correlates with lower HIV-1 infection risk and declines soon after vaccination. Sci Transl Med. 2014;6(228):228ra39.

83. Robb ML, Rerks-Ngarm S, Nitayaphan S, Pitisuttithum P, Kaewkungwal J, Kunasol P, et al. Risk behaviour and time as covariates for efficacy of the HIV vaccine regimen ALVAC-HIV (vCP1521) and AIDSVAX B/E: a post-hoc analysis of the Thai phase 3 efficacy trial RV 144. Lancet Infect Dis. 2012;12(7):531-7.

84. Lewis G, L D, R.C G. Antibody persistence and T-cell balance: Two key factors confronting HIV vaccine development. 2014.

85. Lasky LA, Groopman JE, Fennie CW, Benz PM, Capon DJ, Dowbenko DJ, et al. Neutralization of the AIDS retrovirus by antibodies to a recombinant envelope glycoprotein. Science. 1986;233(4760):209-12.

86. Berman PW, Gregory TJ, Riddle L, Nakamura GR, Champe MA, Porter JP, et al. Protection of chimpanzees from infection by HIV-1 after vaccination with recombinant glycoprotein gp120 but not gp160. Nature. 1990;345(6276):622-5.

87. Walker LM, Huber M, Doores KJ, Falkowska E, Pejchal R, Julien JP, et al. Broad neutralization coverage of HIV by multiple highly potent antibodies. Nature. 2011;477(7365):466-70.

88. Walker LM, Phogat SK, Chan-Hui PY, Wagner D, Phung P, Goss JL, et al. Broad and potent neutralizing antibodies from an African donor reveal a new HIV-1 vaccine target. Science. 326. United States2009. p. 285-9.

89. McLellan JS, Pancera M, Carrico C, Gorman J, Julien JP, Khayat R, et al. Structure of HIV-1 gp120 V1/V2 domain with broadly neutralizing antibody PG9. Nature. 2011;480(7377):336-43.

90. Pejchal R, Doores KJ, Walker LM, Khayat R, Huang PS, Wang SK, et al. A potent and broad neutralizing antibody recognizes and penetrates the HIV glycan shield. Science. 2011;334(6059):1097-103.

91. Kondo H, Yumoto K, Alwood JS, Mojarrab R, Wang A, Almeida EA, et al. Oxidative stress and gamma radiation-induced cancellous bone loss with musculoskeletal disuse. J Appl Physiol. 2010;108(1):152-61.

92. Leonard CK, Spellman MW, Riddle L, Harris RJ, Thomas JN, Gregory TJ. Assignment of intrachain disulfide bonds and characterization of potential glycosylation sites of the type 1 recombinant human immunodeficiency virus envelope glycoprotein (gp120) expressed in Chinese hamster ovary cells. J Biol Chem. 1990;265(18):10373-82.

93. Zolla-Pazner S, Cardozo T. Structure-function relationships of HIV-1 envelope sequence-variable regions refocus vaccine design. Nat Rev Immunol. 2010;10(7):527-35.

94. Go EP, Hewawasam G, Liao HX, Chen H, Ping LH, Anderson JA, et al. Characterization of glycosylation profiles of HIV-1 transmitted/founder envelopes by mass spectrometry. J Virol. 2011;85(16):8270-84.

95. Wei X, Decker JM, Wang S, Hui H, Kappes JC, Wu X, et al. Antibody neutralization and escape by HIV-1. Nature. 2003;422(6929):307-12.

96. Wyatt R, Moore J, Accola M, Desjardin E, Robinson J, Sodroski J. Involvement of the V1/V2 variable loop structure in the exposure of human immunodeficiency virus type 1 gp120 epitopes induced by receptor binding. J Virol. 1995;69(9):5723-33.

97. Bunnik EM, Pisas L, van Nuenen AC, Schuitemaker H. Autologous neutralizing humoral immunity and evolution of the viral envelope in the course of subtype B human immunodeficiency virus type 1 infection. J Virol. 2008;82(16):7932-41.

98. Rong R, Bibollet-Ruche F, Mulenga J, Allen S, Blackwell JL, Derdeyn CA. Role of V1V2 and other human immunodeficiency virus type 1 envelope domains in resistance to autologous neutralization during clade C infection. J Virol. 2007;81(3):1350-9.

99. van Gils MJ, Bunnik EM, Boeser-Nunnink BD, Burger JA, Terlouw-Klein M, Verwer N, et al. Longer V1V2 region with increased number of potential N-linked

glycosylation sites in the HIV-1 envelope glycoprotein protects against HIV-specific neutralizing antibodies. J Virol. 2011;85(14):6986-95.

100. van Gils MJ, Bunnik EM, Burger JA, Jacob Y, Schweighardt B, Wrin T, et al. Rapid escape from preserved cross-reactive neutralizing humoral immunity without loss of viral fitness in HIV-1-infected progressors and long-term nonprogressors. J Virol. 2010;84(7):3576-85.

101. Sanders RW, Venturi M, Schiffner L, Kalyanaraman R, Katinger H, Lloyd KO, et al. The mannose-dependent epitope for neutralizing antibody 2G12 on human immunodeficiency virus type 1 glycoprotein gp120. J Virol. 2002;76(14):7293-305.

102. Trkola A, Purtscher M, Muster T, Ballaun C, Buchacher A, Sullivan N, et al. Human monoclonal antibody 2G12 defines a distinctive neutralization epitope on the gp120 glycoprotein of human immunodeficiency virus type 1. J Virol. 1996;70(2):1100-8.

103. Berman PW. Development of bivalent rgp120 vaccines to prevent HIV type 1 infection. AIDS Res Hum Retroviruses. 1998;14 Suppl 3:S277-89.

104. Liu P, Yates NL, Shen X, Bonsignori M, Moody MA, Liao HX, et al. Infectious virion capture by HIV-1 gp120-specific IgG from RV144 vaccinees. J Virol. 2013;87(14):7828-36.

105. Berman PW, Riddle L, Nakamura G, Haffar OK, Nunes WM, Skehel P, et al. Expression and immunogenicity of the extracellular domain of the human immunodeficiency virus type 1 envelope glycoprotein, gp160. J Virol. 1989;63(8):3489-98.

106. O'Rourke SM, Schweighardt B, Scott WG, Wrin T, Fonseca DP, Sinangil F, et al. Novel ring structure in the gp41 trimer of human immunodeficiency virus type 1 that modulates sensitivity and resistance to broadly neutralizing antibodies. J Virol. 2009;83(15):7728-38.

107. Nakamura GR, Fonseca DP, O'Rourke SM, Vollrath AL, Berman PW. Monoclonal Antibodies to the V2 Domain of MN-rgp120: Fine Mapping of Epitopes and Inhibition of alpha4beta7 Binding. PLoS One. 2012;7(6):e39045.

108. Berman PW, Nunes WM, Haffar OK. Expression of membrane-associated and secreted variants of gp160 of human immunodeficiency virus type 1 in vitro and in continuous cell lines. J Virol. 1988;62(9):3135-42.

109. Kohler G, Milstein C. Continuous cultures of fused cells secreting antibody of predefined specificity. Nature. 1975;256(5517):495-7.

110. Smith DH, Winters-Digiacinto P, Mitiku M, O'Rourke S, Sinangil F, Wrin T, et al. Comparative immunogenicity of HIV-1 clade C envelope proteins for prime/boost studies. PLoS One. 2010;5(8):e12076.

111. Montefiori DC. Evaluating neutralizing antibodies against HIV, SIV, and SHIV in luciferase reporter gene assays. Curr Protoc Immunol. 2005;64:12.1.1-.1.7.

112. Katoh K, Toh H. Recent developments in the MAFFT multiple sequence alignment program. Brief Bioinform. 2008;9(4):286-98.

113. Nakamura GR, Byrn R, Wilkes DM, Fox JA, Hobbs MR, Hastings R, et al. Strain specificity and binding affinity requirements of neutralizing monoclonal antibodies to the C4 domain of gp120 from human immunodeficiency virus type 1. J Virol. 1993;67(10):6179-91.

114. Seaman MS, Janes H, Hawkins N, Grandpre LE, Devoy C, Giri A, et al. Tiered categorization of a diverse panel of HIV-1 Env pseudoviruses for assessment of neutralizing antibodies. J Virol. 2010;84(3):1439-52.

115. Robbins PW, Trimble RB, Wirth DF, Hering C, Maley F, Maley GF, et al. Primary structure of the Streptomyces enzyme endo-beta-N-acetylglucosaminidase H. J Biol Chem. 1984;259(12):7577-83.

116. Wong-Madden ST, Landry D. Purification and characterization of novel glycosidases from the bacterial genus Xanthomonas. Glycobiology. 1995;5(1):19-28.

117. Julien JP, Cupo A, Sok D, Stanfield RL, Lyumkis D, Deller MC, et al. Crystal structure of a soluble cleaved HIV-1 envelope trimer. Science. 2013;342(6165):1477-83.

118. Trkola A, Pomales AB, Yuan H, Korber B, Maddon PJ, Allaway GP, et al. Cross-clade neutralization of primary isolates of human immunodeficiency virus type 1 by human monoclonal antibodies and tetrameric CD4-IgG. J Virol. 1995;69(11):6609-17.

119. Vijh-Warrier S, Pinter A, Honnen WJ, Tilley SA. Synergistic neutralization of human immunodeficiency virus type 1 by a chimpanzee monoclonal antibody against the V2 domain of gp120 in combination with monoclonal antibodies against the V3 loop and the CD4-binding site. J Virol. 1996;70(7):4466-73.

120. Moore PL, Gray ES, Wibmer CK, Bhiman JN, Nonyane M, Sheward DJ, et al. Evolution of an HIV glycan-dependent broadly neutralizing antibody epitope through immune escape. Nat Med. 2012;18:1688–92.

121. Kwong PD, Mascola JR. Human antibodies that neutralize HIV-1: identification, structures, and B cell ontogenies. Immunity. 2012;37(3):412-25.

122. Julien JP, Cupo A, Sok D, Stanfield RL, Lyumkis D, Deller MC, et al. Crystal Structure of a Soluble Cleaved HIV-1 Envelope Trimer. Science. 2013.

123. Bonsignori M, Alam SM, Liao HX, Verkoczy L, Tomaras GD, Haynes BF, et al. HIV-1 antibodies from infection and vaccination: insights for guiding vaccine design. Trends in microbiology. 2012;20(11):532-9.

124. Klein F, Mouquet H, Dosenovic P, Scheid JF, Scharf L, Nussenzweig MC. Antibodies in HIV-1 vaccine development and therapy. Science. 2013;341(6151):1199-204.

125. Kong L, Julien J-P, Calarese D, Scanlan CN, Lee H-K, Rudd P, et al. Toward a Carbohydrate-Based HIV Vaccine. In: Klyosov A, editor. Glycobiology and Drug Design. 2012. Washington, D.C.: American Chemical Society; 2012. p. 187-215.

126. Britt WJ, Vugler LG. Processing of the gp55-116 envelope glycoprotein complex (gB) of human cytomegalovirus. J Virol. 1989;63(1):403-10.

127. Vigerust DJ, Shepherd VL. Virus glycosylation: role in virulence and immune interactions. Trends in microbiology. 2007;15(5):211-8.

128. de Bruyn G, Rossini AJ, Chiu YL, Holman D, Elizaga ML, Frey SE, et al. Safety profile of recombinant canarypox HIV vaccines. Vaccine. 2004;22(5-6):704-13.

129. Pitisuttithum P, Berman PW, Phonrat B, Suntharasamai P, Raktham S, Srisuwanvilai LO, et al. Phase I/II study of a candidate vaccine designed against the B and E subtypes of HIV-1. J Acquir Immune Defic Syndr. 2004;37(1):1160-5.

130. Rolland M, Edlefsen PT, Larsen BB, Tovanabutra S, Sanders-Buell E, Hertz T, et al. Increased HIV-1 vaccine efficacy against viruses with genetic signatures in Env V2. Nature. 2012;490(7420):417-20.

131. Pancera M, Yang Y, Louder MK, Gorman J, Lu G, McLellan JS, et al. N332-Directed broadly neutralizing antibodies use diverse modes of HIV-1 recognition: inferences from heavy-light chain complementation of function. PLoS One. 2013;8(2):e55701.

132. Pejchal R, Doores KJ, Walker LM, Khayat R, Huang PS, Wang SK, et al. A potent and broad neutralizing antibody recognizes and penetrates the HIV glycan. Science. 2011;334(6059):1097-103.

133. Kong L, Lee JH, Doores KJ, Murin CD, Julien JP, McBride R, et al. Supersite of immune vulnerability on the glycosylated face of HIV-1 envelope glycoprotein gp120. Nat Struct Mol Biol. 2013;20(7):796-803.

134. Julien JP, Sok D, Khayat R, Lee JH, Doores KJ, Walker LM, et al. Broadly neutralizing antibody PGT121 allosterically modulates CD4 binding via recognition of the HIV-1 gp120 V3 base and multiple surrounding glycans. PLoS Pathog. 2013;9(5):e1003342.

135. Sok D, Doores KJ, Briney B, Le KM, Saye-Francisco KL, Ramos A, et al. Promiscuous glycan site recognition by antibodies to the high-mannose patch of gp120 broadens neutralization of HIV. Sci Transl Med. 2014;6(236):236ra63.

136. Pritchard LK, Spencer DI, Royle L, Bonomelli C, Seabright GE, Behrens AJ, et al. Glycan clustering stabilizes the mannose patch of HIV-1 and preserves vulnerability to broadly neutralizing antibodies. Nat Commun. 2015;6:7479.

137. Crooks ET, Tong T, Osawa K, Binley JM. Enzyme digests eliminate nonfunctional Env from HIV-1 particle surfaces, leaving native Env trimers intact and viral infectivity unaffected. J Virol. 2011;85(12):5825-39.

138. Pritchard LK, Vasiljevic S, Ozorowski G, Seabright GE, Cupo A, Ringe R, et al. Structural Constraints Determine the Glycosylation of HIV-1 Envelope Trimers. Cell Rep. 2015;11(10):1604-13.

139. Morell AG, Irvine RA, Sternlieb I, Scheinberg IH, Ashwell G. Physical and chemical studies on ceruloplasmin. V. Metabolic studies on sialic acid-free ceruloplasmin in vivo. J Biol Chem. 1968;243(1):155-9.

140. Morell AG, Gregoriadis G, Scheinberg IH, Hickman J, Ashwell G. The role of sialic acid in determining the survival of glycoproteins in the circulation. J Biol Chem. 1971;246(5):1461-7.

141. Kong L, Sheppard NC, Stewart-Jones GB, Robson CL, Chen H, Xu X, et al. Expression-system-dependent modulation of HIV-1 envelope glycoprotein antigenicity and immunogenicity. J Mol Biol. 2010;403(1):131-47.

142. Raska M, Takahashi K, Czernekova L, Zachova K, Hall S, Moldoveanu Z, et al. Glycosylation patterns of HIV-1 gp120 depend on the type of expressing cells and affect antibody recognition. J Biol Chem. 2010;285(27):20860-9.

143. Halper-Stromberg A, Lu CL, Klein F, Horwitz JA, Bournazos S, Nogueira L, et al. Broadly neutralizing antibodies and viral inducers decrease rebound from HIV-1 latent reservoirs in humanized mice. Cell. 2014;158(5):989-99.

144. Gurgo C, Guo HG, Franchini G, Aldovini A, Collalti E, Farrell K, et al. Envelope sequences of two new United States HIV-1 isolates. Virology. 1988;164(2):531-6.

145. McCutchan FE, Hegerich PA, Brennan TP, Phanuphak P, Singharaj P, Jugsudee A, et al. Genetic variants of HIV-1 in Thailand. AIDS Res Hum Retroviruses. 1992;8(11):1887-95.

146. Kearse M. Geneious Basic: an integrated and extendable desktop software platform for the organization and analysis of sequence data. In: Moir R, Wilson, A., Stones-Havas, S., Cheung, M.,, Sturrock S, Buxton, S., Cooper, A., Markowitz, S., Duran, C., Thierer,, T. A, B., Mentjies, P., & Drummond, A., editors. Bioinformatics: *28* (12), 1647-1649. p. 1647-9.

147. Gibbs J. Selecting the detection system – colorimetric, fluorescent, luminescent methods. 5 ed. Corning Incorporated Life Sciences Corning, New York: Corning Life Sciences; 2001.

148. Huang J, Kang BH, Pancera M, Lee JH, Tong T, Feng Y, et al. Broad and potent HIV-1 neutralization by a human antibody that binds the gp41-gp120 interface. Nature. 2014;515(7525):138-42.

149. Wu X, Yang ZY, Li Y, Hogerkorp CM, Schief WR, Seaman MS, et al. Rational design of envelope identifies broadly neutralizing human monoclonal antibodies to HIV-1. Science. 2010;329(5993):856-61.

150. Morales JF, Morin TJ, Yu B, Tatsuno GP, O'Rourke SM, Theolis R, Jr., et al. HIV-1 envelope proteins and V1/V2 domain scaffolds with mannose-5 to improve the magnitude and quality of protective antibody responses to HIV-1. J Biol Chem. 2014;289(30):20526-42.

151. Krumm SA, Mohammed H, Le KM, Crispin M, Wrin T, Poignard P, et al. Mechanisms of escape from the PGT128 family of anti-HIV broadly neutralizing antibodies. Retrovirology. 2016;13:8.

152. Clements GJ, Price-Jones MJ, Stephens PE, Sutton C, Schulz TF, Clapham PR, et al. The V3 loops of the HIV-1 and HIV-2 surface glycoproteins contain proteolytic cleavage sites: a possible function in viral fusion? AIDS Res Hum Retroviruses. 1991;7(1):3-16.

153. Barouch DH, Picker LJ. Novel vaccine vectors for HIV-1. Nat Rev Microbiol. 12. England2014. p. 765-71.

154. Stephenson KE, D'Couto HT, Barouch DH. New concepts in HIV-1 vaccine development. Curr Opin Immunol. 2016;41:39-46.

155. Medlock J, Pandey A, Parpia AS, Tang A, Skrip LA, Galvani AP. Effectiveness of UNAIDS targets and HIV vaccination across 127 countries. Proceedings of the National Academy of Sciences. 2017;114(15):4017-22.

156. Gorman J, Soto C, Yang MM, Davenport TM, Guttman M, Bailer RT, et al. Structures of HIV-1 Env V1V2 with broadly neutralizing antibodies reveal commonalities that enable vaccine design. Nat Struct Mol Biol. 2016;23(1):81-90.

157. Zhou T, Georgiev I, Wu X, Yang ZY, Dai K, Finzi A, et al. Structural basis for broad and potent neutralization of HIV-1 by antibody VRC01. Science. 2010;329(5993):811-7.

158. Conley AJ, Kessler JA, 2nd, Boots LJ, Tung JS, Arnold BA, Keller PM, et al. Neutralization of divergent human immunodeficiency virus type 1 variants and primary isolates by IAM-41-2F5, an anti-gp41 human monoclonal antibody. Proc Natl Acad Sci U S A. 1994;91(8):3348-52.

159. Huang J, Ofek G, Laub L, Louder MK, Doria-Rose NA, Longo NS, et al. Broad and potent neutralization of HIV-1 by a gp41-specific human antibody. Nature. 2012;491(7424):406-12.

160. Cardoso RM, Zwick MB, Stanfield RL, Kunert R, Binley JM, Katinger H, et al. Broadly neutralizing anti-HIV antibody 4E10 recognizes a helical conformation of a highly conserved fusion-associated motif in gp41. Immunity. 2005;22(2):163-73.

161. Scharf L, Scheid JF, Lee JH, West AP, Jr., Chen C, Gao H, et al. Antibody 8ANC195 reveals a site of broad vulnerability on the HIV-1 envelope spike. Cell Rep. 2014;7(3):785-95.

162. Correia BE, Bates JT, Loomis RJ, Baneyx G, Carrico C, Jardine JG, et al. Proof of principle for epitope-focused vaccine design. Nature. 2014;507(7491):201-6.

163. Zhou T, Zhu J, Yang Y, Gorman J, Ofek G, Srivatsan S, et al. Transplanting supersites of HIV-1 vulnerability. PLoS One. 2014;9(7):e99881.

164. de Taeye SW, Moore JP, Sanders RW. HIV-1 Envelope Trimer Design and Immunization Strategies To Induce Broadly Neutralizing Antibodies. Trends Immunol. 2016;37(3):221-32.

165. Wang S, Arthos J, Lawrence JM, Van Ryk D, Mboudjeka I, Shen S, et al. Enhanced Immunogenicity of gp120 Protein When Combined with Recombinant DNA Priming To Generate Antibodies That Neutralize the JR-FL Primary Isolate of Human Immunodeficiency Virus Type 1. J Virol. 792005. p. 7933-7.

166. Approaches to the development of broadly protective HIV vaccines: challenges posed by the genetic, biological and antigenic variability of HIV-1: Report from a meeting of the WHO-UNAIDS Vaccine Advisory Committee Geneva, 21-23 February 2000. Aids. 2001;15(6):W1-w25.

167. Doores KJ, Burton DR. Variable loop glycan dependency of the broad and potent HIV-1-neutralizing antibodies PG9 and PG16. J Virol. 84. United States2010. p. 10510-21.

168. Byrne G, O'Rourke M. S, L. Alexander D, Yu B, Doran R, Wright M, et al. CRISPR/Cas9 gene editing for the creation of an MGAT1 deficient CHO cell line to control HIV-1 vaccine glycosylation [IN PRESS]. 2018.

169. Flynn NM, Forthal DN, Harro CD, Judson FN, Mayer KH, Para MF. Placebo-controlled phase 3 trial of a recombinant glycoprotein 120 vaccine to prevent HIV-1 infection. J Infect Dis. 191. United States2005. p. 654-65.

170. Zambonelli C, Dey AK, Hilt S, Stephenson S, Go EP, Clark DF, et al. Generation and Characterization of a Bivalent HIV-1 Subtype C gp120 Protein Boost for Proof-of-Concept HIV Vaccine Efficacy Trials in Southern Africa. PLoS One. 2016;11(7):e0157391.

171. Liao HX, Tsao CY, Alam SM, Muldoon M, Vandergrift N, Ma BJ, et al. Antigenicity and immunogenicity of transmitted/founder, consensus, and

chronic envelope glycoproteins of human immunodeficiency virus type 1. J Virol. 2013;87(8):4185-201.

172. Stamatakis A. RAxML version 8: a tool for phylogenetic analysis and post-analysis of large phylogenies. Bioinformatics. 2014;30(9):1312-3.

173. Larkin MA, Blackshields G, Brown NP, Chenna R, McGettigan PA, McWilliam H, et al. Clustal W and Clustal X version 2.0. Bioinformatics. 2007;23(21):2947-8.

174. Paradis E, Claude J, Strimmer K. APE: Analyses of Phylogenetics and Evolution in R language. Bioinformatics. 2004;20(2):289-90.

175. Moritz B, Becker PB, Gopfert U. CMV promoter mutants with a reduced propensity to productivity loss in CHO cells. Sci Rep. 2015;5:16952.

176. Doran RC, Tatsuno GP, O'Rourke SM, Yu B, Alexander DL, Mesa KA, et al. Glycan modifications to the gp120 immunogens used in the RV144 vaccine trial improve binding to broadly neutralizing antibodies. PLoS One. 2018;13(4).

177. Doran RC, Morales JF, To B, Morin TJ, Theolis R, Jr., O'Rourke SM, et al. Characterization of a monoclonal antibody to a novel glycan-dependent epitope in the V1/V2 domain of the HIV-1 envelope protein, gp120. Mol Immunol. 2014;62(1):219-26.

178. Mouquet H. Antibody B cell responses in HIV-1 infection. Trends Immunol. 2014;35(11):549-61.

179. Morales JF, Yu B, Perez G, Mesa KA, Alexander DL, Berman PW. Fragments of the V1/V2 domain of HIV-1 glycoprotein 120 engineered for improved binding to the broadly neutralizing PG9 antibody. Mol Immunol. 2016;77:14-25.

180. Wang Z, Lorin C, Koutsoukos M, Franco D, Bayat B, Zhang Y, et al. Comprehensive Characterization of Reference Standard Lots of HIV-1 Subtype C Gp120 Proteins for Clinical Trials in Southern African Regions. Vaccines (Basel). 2016;4(2).

181. O'Rourke SM, Byrne G, Gwen T, Meredith W, Yu B, Mesa KA, et al. Robotic selection for the rapid development of stable CHO cell lines for HIV vaccine for production. 2018.

182. Jones DH, McBride BW, Roff MA, Farrar GH. Efficient purification and rigorous characterisation of a recombinant gp120 for HIV vaccine studies. Vaccine. 1995;13(11):991-9.

183. Dowd CS, Leavitt S, Babcock G, Godillot AP, Van Ryk D, Canziani GA, et al. Beta-turn Phe in HIV-1 Env binding site of CD4 and CD4 mimetic miniprotein enhances Env binding affinity but is not required for activation of co-receptor/17b site. Biochemistry. 2002;41(22):7038-46.

184. Srivastava IK, Stamatatos L, Legg H, Kan E, Fong A, Coates SR, et al. Purification and characterization of oligomeric envelope glycoprotein from a

primary R5 subtype B human immunodeficiency virus. J Virol. 2002;76(6):2835-47.

185. Wang S, Chou TH, Hackett A, Efros V, Wang Y, Han D, et al. Screening of primary gp120 immunogens to formulate the next generation polyvalent DNA prime-protein boost HIV-1 vaccines. Hum Vaccin Immunother. 2017;13(12):2996-3009.

186. Go EP, Herschhorn A, Gu C, Castillo-Menendez L, Zhang S, Mao Y, et al. Comparative Analysis of the Glycosylation Profiles of Membrane-Anchored HIV-1 Envelope Glycoprotein Trimers and Soluble gp140. J Virol. 2015;89(16):8245-57.

187. Scandella CJ, Kilpatrick J, Lidster W, Parker C, Moore JP, Moore GK, et al. Nonaffinity purification of recombinant gp120 for use in AIDS vaccine development. AIDS Res Hum Retroviruses. 1993;9(12):1233-44.

188. PW B, editor Strategies for Improving the AIDSVAX Vaccines. NIAID HIV Env Manufacturing Workshop; 2015; Rockville, MD.

189. Bekker LG ea. Subtype C ALVAC-HIV and bivalent subtype C gp120/MF59 HIV-1 vaccine in low-risk, HIV-uninfected, South African adults: a phase 1/2 trial. - PubMed - NCBI. 2018.

190. HVTN Studies 2018 Available from: https://www.hvtn.org/en/science/HVTN-studies.html.

191. Wu X, Zhou T, Zhu J, Zhang B, Georgiev I, Wang C, et al. Focused evolution of HIV-1 neutralizing antibodies revealed by structures and deep sequencing. Science. 2011;333(6049):1593-602.

192. Sanders RW, Derking R, Cupo A, Julien JP, Yasmeen A, de Val N, et al. A next-generation cleaved, soluble HIV-1 Env Trimer, BG505 SOSIP.664 gp140, expresses multiple epitopes for broadly neutralizing but not non-neutralizing antibodies. PLoS Pathog. 2013;9(9):e1003618.

193. Steichen JM, Kulp DW, Tokatlian T, Escolano A, Dosenovic P, Stanfield RL, et al. HIV Vaccine Design to Target Germline Precursors of Glycan-Dependent Broadly Neutralizing Antibodies. Immunity. 2016;45(3):483-96.

194. Shen X, Basu R, Sawant S, Beaumont D, Kwa SF, LaBranche C, et al. HIV-1 gp120 and Modified Vaccinia Virus Ankara (MVA) gp140 Boost Immunogens Increase Immunogenicity of a DNA/MVA HIV-1 Vaccine. J Virol. 2017;91(24).

195. Jiang X, Totrov M, Li W, Sampson JM, Williams C, Lu H, et al. Rationally Designed Immunogens Targeting HIV-1 gp120 V1V2 Induce Distinct Conformation-Specific Antibody Responses in Rabbits. J Virol. 2016;90(24):11007-19.

196. Rolland M, Gilbert P. Evaluating Immune Correlates in HIV Type 1 Vaccine Efficacy Trials: What RV144 May Provide. AIDS Res Hum Retroviruses. 2012;28(4):400-4.

197. Cormier EG, Dragic T. The Crown and Stem of the V3 Loop Play Distinct Roles in Human Immunodeficiency Virus Type 1 Envelope Glycoprotein Interactions with the CCR5 Coreceptor. Journal of Virology. 2002;76(17):8953-7.

198. Jiang X, Burke V, Totrov M, Williams C, Cardozo T, Gorny MK, et al. Conserved structural elements in the V3 crown of HIV-1 gp120. Nat Struct Mol Biol. 2010;17(8):955-61.

199. Cormier EG, Tran DN, Yukhayeva L, Olson WC, Dragic T. Mapping the determinants of the CCR5 amino-terminal sulfopeptide interaction with soluble human immunodeficiency virus type 1 gp120-CD4 complexes. J Virol. 2001;75(12):5541-9.

200. Edlefsen PT, Gilbert PB, Rolland M. Sieve analysis in HIV-1 vaccine efficacy trials. Curr Opin HIV AIDS. 2013;8(5):432-6.

201. Zolla-Pazner S, Edlefsen PT, Rolland M, Kong XP, deCamp A, Gottardo R, et al. Vaccine-induced Human Antibodies Specific for the Third Variable Region of HIV-1 gp120 Impose Immune Pressure on Infecting Viruses. EBioMedicine. 2014;1(1):37-45.

202. Permar SR, Fong Y, Vandergrift N, Fouda GG, Gilbert P, Parks R, et al. Maternal HIV-1 envelope-specific antibody responses and reduced risk of perinatal transmission. J Clin Invest. 2015;125(7):2702-6.

203. Balasubramanian P, Williams C, Shapiro MB, Sinangil F, Higgins K, Nádas A, et al. Functional Antibody Response Against V1V2 and V3 of HIV gp120 in the VAX003 and VAX004 Vaccine Trials.

204. Forthal DN, Gilbert PB, Landucci G, Phan T. Recombinant gp120 vaccine-induced antibodies inhibit clinical strains of HIV-1 in the presence of Fc receptor-bearing effector cells and correlate inversely with HIV infection rate. J Immunol. 2007;178(10):6596-603.

205. Wang Q, Dai Y, Sun Z, Su X, Yu Y, Hua C, et al. HIV-1 Env DNA prime plus gp120 and gp70-V1V2 boosts induce high level of V1V2-specific IgG and ADCC responses and low level of Env-specific IgA response: implication for improving RV144 vaccine regimen. Emerg Microbes Infect. 2017;6(11):e102.

206. Garrity RR, Rimmelzwaan G, Minassian A, Tsai WP, Lin G, de Jong JJ, et al. Refocusing neutralizing antibody response by targeted dampening of an immunodominant epitope. J Immunol. 1997;159(1):279-89.

207. Musich T, Peters PJ, Duenas-Decamp MJ, Gonzalez-Perez MP, Robinson J, Zolla-Pazner S, et al. A conserved determinant in the V1 loop of HIV-1 modulates the V3 loop to prime low CD4 use and macrophage infection. J Virol. 2011;85(5):2397-405.

208. Pastore C, Nedellec R, Ramos A, Pontow S, Ratner L, Mosier DE. Human immunodeficiency virus type 1 coreceptor switching: V1/V2 gain-of-fitness

mutations compensate for V3 loss-of-fitness mutations. J Virol. 2006;80(2):750-8.

209. Cole KS, Steckbeck JD, Rowles JL, Desrosiers RC, Montelaro RC. Removal of N-linked glycosylation sites in the V1 region of simian immunodeficiency virus gp120 results in redirection of B-cell responses to V3. J Virol. 2004;78(3):1525-39.

210. Losman B, Bolmstedt A, Schonning K, Bjorndal A, Westin C, Fenyo EM, et al. Protection of neutralization epitopes in the V3 loop of oligomeric human immunodeficiency virus type 1 glycoprotein 120 by N-linked oligosaccharides in the V1 region. AIDS Res Hum Retroviruses. 2001;17(11):1067-76.

211. Shibata J, Yoshimura K, Honda A, Koito A, Murakami T, Matsushita S. Impact of V2 mutations on escape from a potent neutralizing anti-V3 monoclonal antibody during in vitro selection of a primary human immunodeficiency virus type 1 isolate. J Virol. 2007;81(8):3757-68.

212. Krachmarov CP, Honnen WJ, Kayman SC, Gorny MK, Zolla-Pazner S, Pinter A. Factors determining the breadth and potency of neutralization by V3-specific human monoclonal antibodies derived from subjects infected with clade A or clade B strains of human immunodeficiency virus type 1. J Virol. 2006;80(14):7127-35.

213. Pinter A, Honnen WJ, He Y, Gorny MK, Zolla-Pazner S, Kayman SC. The V1/V2 domain of gp120 is a global regulator of the sensitivity of primary human immunodeficiency virus type 1 isolates to neutralization by antibodies commonly induced upon infection. J Virol. 2004;78(10):5205-15.

214. Lyumkis D, Julien JP, de Val N, Cupo A, Potter CS, Klasse PJ, et al. Cryo-EM structure of a fully glycosylated soluble cleaved HIV-1 envelope trimer. Science. 2013;342(6165):1484-90.

215. Eggink D, Melchers M, Wuhrer M, van Montfort T, Dey AK, Naaijkens BA, et al. Lack of complex N-glycans on HIV-1 envelope glycoproteins preserves protein conformation and entry function. Virology. 2010;401(2):236-47.

216. Sarzotti-Kelsoe M, Bailer RT, Turk E, Lin CL, Bilska M, Greene KM, et al. Optimization and validation of the TZM-bl assay for standardized assessments of neutralizing antibodies against HIV-1. J Immunol Methods. 2014;409:131-46.

217. Rachel C. Doran GPT, Sara, M. O'Rourke BY, David L. Alexander,, Kathryn A. Mesa PWB. Glycan modifications to the gp120 immunogens used in the RV144 vaccine trial improve binding to broadly neutralizing antibodies. PlosOne; 2018.

218. Karasavvas N, Billings E, Rao M, Williams C, Zolla-Pazner S, Bailer RT, et al. The Thai Phase III HIV Type 1 Vaccine trial (RV144) regimen induces antibodies that target conserved regions within the V2 loop of gp120. AIDS Res Hum Retroviruses. 2012;28(11):1444-57.

219. Moseri A, Tantry S, Sagi Y, Arshava B, Naider F, Anglister J. An optimally constrained V3 peptide is a better immunogen than its linear homolog or HIV-1 gp120. Virology. 2010;401(2):293-304.

220. Elbein AD, Tropea JE, Mitchell M, Kaushal GP. Kifunensine, a potent inhibitor of the glycoprotein processing mannosidase I. J Biol Chem. 1990;265(26):15599-605.

221. Huston JS, Levinson D, Mudgett-Hunter M, Tai MS, Novotny J, Margolies MN, et al. Protein engineering of antibody binding sites: recovery of specific activity in an anti-digoxin single-chain Fv analogue produced in Escherichia coli. Proc Natl Acad Sci U S A. 1988;85(16):5879-83.

222. Gorny MK, Revesz K, Williams C, Volsky B, Louder MK, Anyangwe CA, et al. The v3 loop is accessible on the surface of most human immunodeficiency virus type 1 primary isolates and serves as a neutralization epitope. J Virol. 2004;78(5):2394-404.

223. Wang Q, Dai Y, Sun Z, Su X, Yu Y, Hua C, et al. HIV-1 Env DNA prime plus gp120 and gp70-V1V2 boosts induce high level of V1V2-specific IgG and ADCC responses and low level of Env-specific IgA response: implication for improving RV144 vaccine regimen. Emerg Microbes Infect. 2017;6(11):e102-.